e-ISSN 2667-9973
p-ISSN 1512-1127

საქართველოს გეოფიზიკური საზოგადოების ჟურნალი

მყარი დედამიწის, ატმოსფეროს, ოკეანისა და კოსმოსური პლაზმის ფიზიკა

ტომი 27 , № 1

JOURNAL
OF THE GEORGIAN GEOPHYSICAL SOCIETY

Physics of Solid Earth, Atmosphere, Ocean and Space Plasma

Vol. 27 , № 1

Tbilisi
2024

e-ISSN 2667-9973
p-ISSN 1512-1127

საქართველოს გეოფიზიკური საზოგადოების ჟურნალი

მყარი დედამიწის, ატმოსფეროს, ოკეანისა და კოსმოსური პლაზმის ფიზიკა

ტომი 27 , № 1

JOURNAL
OF THE GEORGIAN GEOPHYSICAL SOCIETY

Physics of Solid Earth, Atmosphere, Ocean and Space Plasma

Vol. 27 , № 1

Tbilisi
2024

საქართველოს გეოფიზიკური საზოგადოების ჟურნალი
მყარი დედამიწის, ატმოსფეროს, ოკეანისა და კოსმოსური პლაზმის ფიზიკა
მთავარი რედაქტორი: თ. ჭელიძე

ჟურნალის შინაარსი:

ჟურნალი მოიცავს მყარი დედამიწის, ატმოსფეროს, ოკეანისა და კოსმოსური პლაზმის ფიზიკის ყველა მიმართულებას. ჟურნალში ქვეყნდება: კვლევითი წერილები, მიმოხილვები, მოკლე ინფორმაციები, დისკუსიები, წიგნების მიმოხილვები, განცხადებები, კონფერენციების მოხსენებები.

JOURNAL OF THE GEORGIAN GEOPHYSICAL SOCIETY

Physics of Solid Earth, Atmosphere, Ocean and Space Plasma

Editor-in-chief: T. Chelidze

Scope of the Journal:

The Journal is devoted to all branches of the Physics of Solid Earth, Atmosphere, Ocean and Space Plasma. Types of contributions are: research papers, reviews, short communications, discussions, book reviews, announcements, conference reports.

ЖУРНАЛ ГРУЗИНСКОГО ГЕОФИЗИЧЕСКОГО ОБЩЕСТВА

Физика Твердой Земли, Атмосферы, Океана и Космической Плазмы

Главный редактор: Т. Челидзе

Содержание журнала:

Журнал Грузинского геофизического общества охватывает все направления физики твердой Земли, Атмосферы, Океана и Космической Плазмы. В журнале публикуются научные статьи, обзоры, краткие информации, дискуссии, обозрения книг, объявления, доклады конференций.

მისამართი:

საქართველო, 0160, თბილისი, ალექსიძის ქ. 1, მ. ნოდიას სახ. გეოფიზიკის ინსტიტუტი
ტელ.: 233-28-67; ფაქსი; (995 32 2332867); ელ. ფოეტა: tamaz.chelidze@gmail.com; avtandilamiranashvili@gmail.com;
geophysics.journal@tsu.ge

გამოქვეყნების განრიგი და ხელმოწერა:

გამოიცემა წელიწადში ორჯერ. მყარი ვერსიის წლიური ხელმოწერის ფასია: უცხოელი ხელმომწერისათვის - 30 დოლარი, საქართველოში - 10 ლარი. ხელმოწერის მოთხოვნა უნდა გაიგზავნოს რედაქციის მისამართით. შესაძლებელია უფასო ონლაინ წვდომა:
http://openjournals.gela.org.ge/index.php/GGS

ჟურნალი ინდექსირებულა Google Scholar-ში:
https://scholar.google.com/citations?hl=en&user=pdG-bMAAAAAJ

Address:

M. Nodia Institute of Geophysics, 1 Alexidze Str., 0160 Tbilisi, Georgia
Tel.: 233-28-67; Fax: (99532) 2332867; e-mail: tamaz.chelidze@gmail.com; avtandilamiranashvili@gmail.com;
geophysics.journal@tsu.ge

Publication schedule and subscription information:

The journal is issued twice a year. The subscription price for print version is 30 $ in year.
Subscription orders should be sent to editor's address. Free online access is possible:
http://openjournals.gela.org.ge/index.php/GGS

The journal is indexed in the Google Scholar:
https://scholar.google.com/citations?hl=en&user=pdG-bMAAAAAJ

Адрес:

Грузия, 0160, Тбилиси, ул. Алексидзе, 1. Институт геофизики им. М. З. Нодиа
Тел: 233-28-67; 294-35-91; Fax: (99532)2332867; e-mail: tamaz.chelidze@gmail.com; avtandilamiranashvili@gmail.com;
geophysics.journal@tsu.ge

Порядок издания и условия подписки:

Журнал издается дважды в год. Годовая подписная цена для печатной версии - 30 долларов США. Заявка о подписке высылается в адрес редакции. Имеется бесплатный онлайн доступ
http://openjournals.gela.org.ge/index.php/GGS

Журнал индексирован в Google Scholar:
https://scholar.google.com/citations?hl=en&user=pdG-bMAAAAAJ

This journal uses Open Journal Systems 2.4.8.3, which is open source journal management and publishing software developed, supported, and freely distributed by the Public Knowledge Project under the GNU General Public License.

(http://openjournals.gela.org.ge/index.php?journal=GGS&page=about&op=aboutThisPublishingSystem)

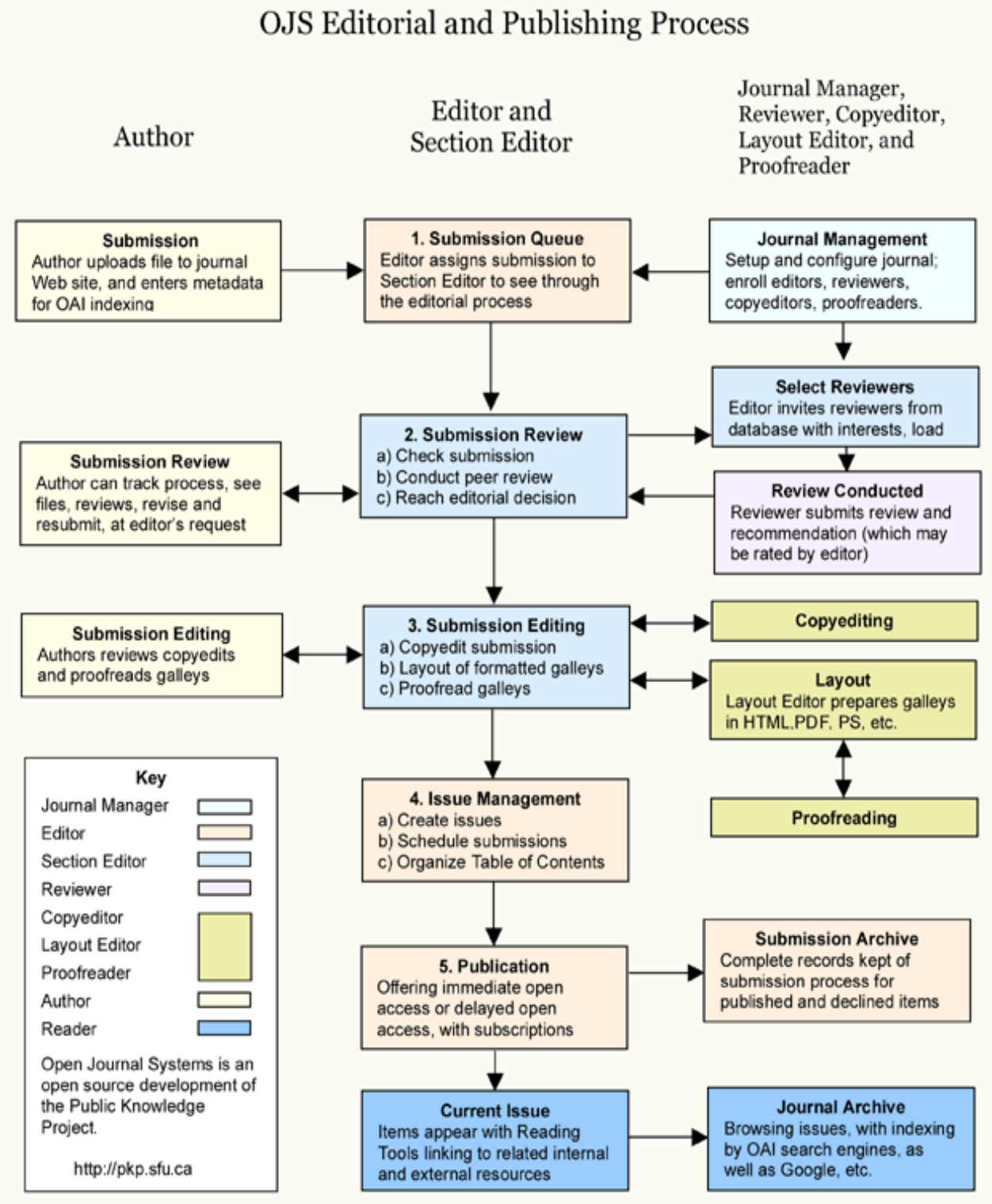

Journal of the Georgian Geophysical Society, e-ISSN: 2667-9973, p-ISSN: 1512-1127
Physics of Solid Earth, Atmosphere, Ocean and Space Plasma, v. 27(1), 2024, pp. 5 - 8

Phase Shift Sign Changes into Boreholes of Georgia

Genadi N. Kobzev, Giorgi I. Melikadze, Tamar J. Jimsheladze

M. Nodia Institute of Geophysics of the I. Javakhishvili Tbilisi State University, Georgia,
[1]e-mail: kobzev47@gmail.com

ABSTRACT

Using the example of a Georgian well, the possibility of regular changes in the sign of the phase shift between gravity and water level is shown.
Key words: *phase shift, water level, gravity, ellipse method.*

Introduction

In early articles on the topic of the phase shift between the water level in a well and gravity, was noted with surprise: in response to gravity, the water level should change its amplitude with a delay, but the water got ahead of it. Thus, when filtering near M2 (12.4206 h), there is an expected delay in the reaction of water, but when filtering in the region O1 (25.8193 h), water is ahead of gravity [1].

There are many articles and models that explain the phase shift in one direction or another. Various factors were taken into account: the water layer has the type confined, unconfined, leaky, etc. In particular, the presence of a negative skin effect was recognized as the reason for the advance of water [2]. By default, it is assumed that for the well the phase shift or its sign has a constant value.

Using the example of Georgian wells, we will show that the phase shift between the water level and gravity can regularly move from a state of lag to advance and vice versa. Therefore, depending on the time period for the well, both positive and negative phase shift values can be observed.

When studying the phase shift, we used the idea of an ellipse as presented in [3] and modified in [4].

To understand the issue, let's consider several comparisons. Let there be two functions: y=sin(*t*) and y1=sin(*t*-pi/6). Function y1 is obtained from the first by adding a negative number "-pi/6" to the argument and reacts "delayed" to an increase in *t*.

Example 1. If you build a motion trajectory, where X=sin(*t*); Y=sin(*t*-pi/6), then you get an ellipse, where the point with coordinate (X,Y) moves "counterclockwise" as *t* increases (Fig.1). If you specify sin(*t*+pi/6) as Y, then the point moves "clockwise".

Conclusion 1*:* by studying whether the point moves "counterclockwise" or "clockwise", you can find out whether there is a delay (phase shift <0) or advance (shift >0).

Note also: the greater the phase shift, the "thicker" the ellipse becomes. And vice versa, if the phase shift is 0, then we get a straight line on the graph.

Example 2. Let the reference function maintain its amplitude, and the function y1, maintaining the phase shift, reduces its amplitude (Fig.2). Let's depict both functions on one graph, where X=sin(*t*); Y=A*sin(*t*-pi/6), and coefficient A varies from 1 to 0.1. In this case, the ellipse graph will slope downward.

Example 3. Let the original functions simultaneously decrease their amplitude. The result is concentrically located ellipses that have changed their amplitude but retained their slope (Fig.3).

Conclusion 2: changing the slope of the ellipse allows you to determine whether the dependent function reacts consistently to a change in the reference one, or whether the proportion of their connection has changed.

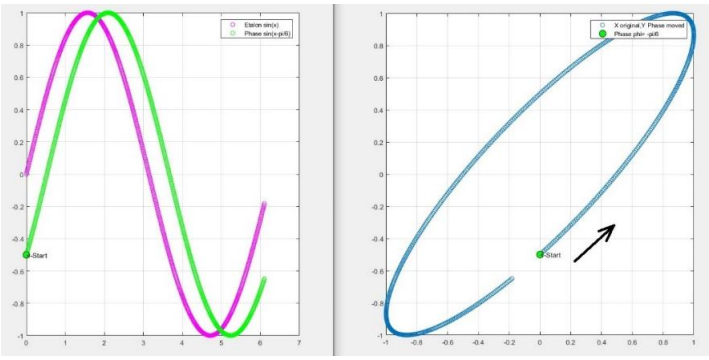

Fig.1. Red: y=sin(*t*);
green: y1=sin(*t*-pi/6)

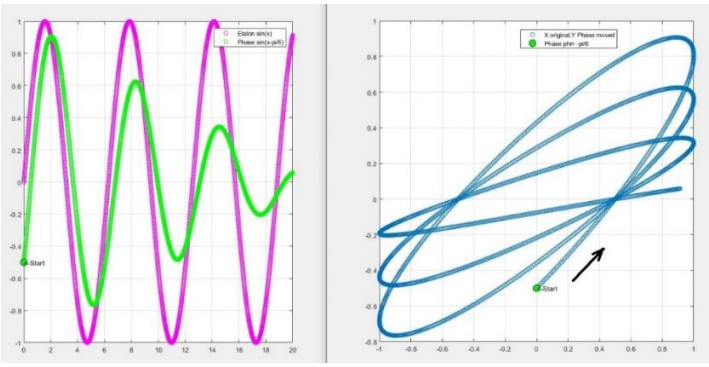

Fig.2. Red: y=sin(*t*);
green: y1=A*sin(*t*-pi/6),
A=1.0->0.1 for *t*=0:20

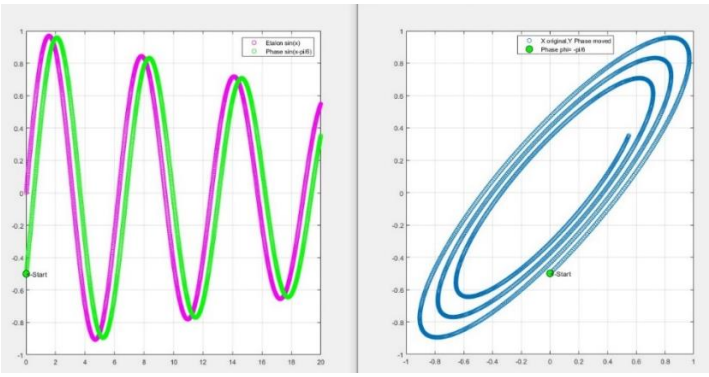

Fig.3. Red: y=A*sin(*t*);
green: y1=A*sin(*t*-pi/6),
A=1.0->0.1 for *t*=0:20

Results

A study of data from Lagodekhi and Kobuleti revealed a significant delay in the response of water levels to gravity. But for Marneuli and Nakalakevi there is both a delay and advance of gravity.

Let's consider the data obtained at the well Marneuli (January 5-February 17, 2024).

The variables are gravity y=tidalZ and water level in the form y1="-water" (in kPa). The influence of the atmosphere on water levels is removed. If the influence is retained, the results will be significantly different. Using the cwt and icwt functions (MatLab), these data are filtered in the region of M2 (12.42 h) and O1 (25.82 h). Next, we consider 2d or 3d graphs of these variables.

2d chart. We will place tidalZ on the OX axis, and "-water" along the OY axis. For clarity, in Fig.4 the influence of the atmosphere was not removed from the water level. The tilts of the ellipses are visible, therefore there are changes in the connection between the movement of water and gravity. There is also a change in the direction of movement "clockwise" or "counterclockwise", i.e. change in the sign of the phase shift.

3d graph. At X=*t* (time, minutes), Y=tidalZ, Z=-water, a 3d graph makes it possible to determine the direction of movement of a point in time and see the change in phase shift: "clockwise" or "counterclockwise" the point moves. Figures 5 and 6 show two-dimensional projections of 3D graphs, allowing you to see changes in the directions of movement over time.

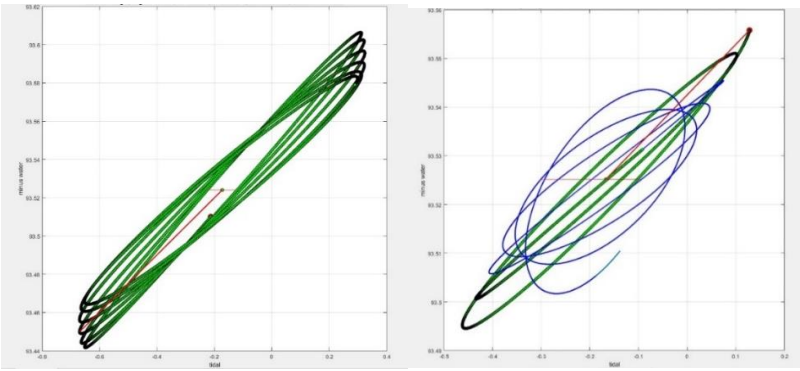

Fig.4a. Movement is only "clockwise". M2 filtration. The influence of the atmosphere was not removed.

Fig.4b. Movement "clockwise" (green) and "counterclockwise" (blue). M2 filtration. The influence of the atmosphere was not removed.

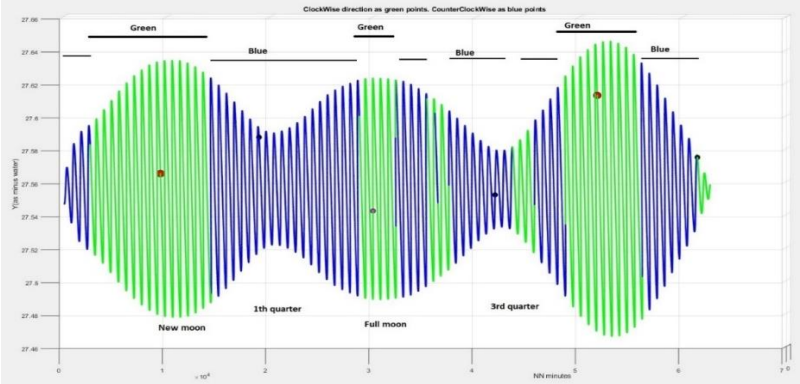

Fig.5. Marneuli 2024, M2, Y(minus water), the influence of the atmosphere is removed. Phase shift >0 (advanced, green). Phase shift <0 (delay, blue).

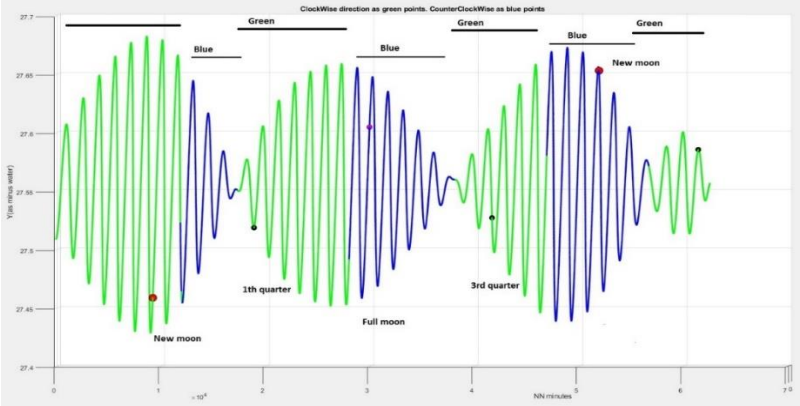

Fig.6. Marneuli 2024, O1, Y(minus water), the influence of the atmosphere is removed. Phase shift >0 (advanced, green). Phase shift <0 (delay, blue).

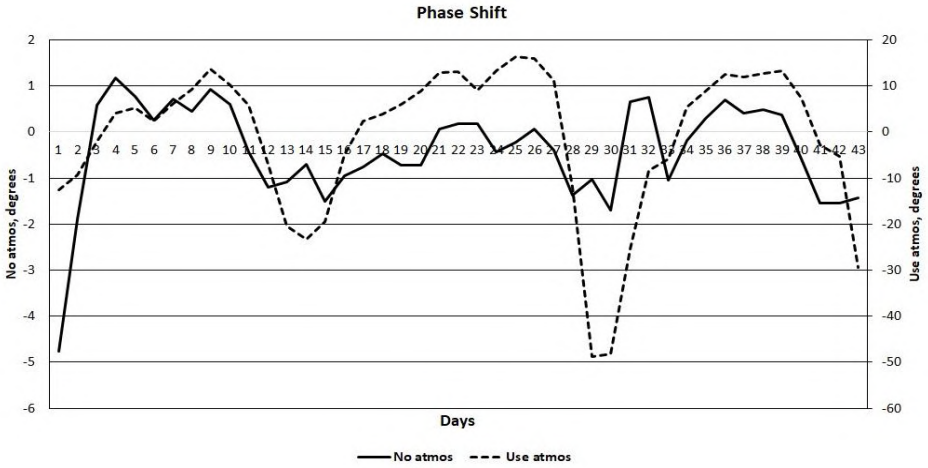

Fig.7. Phase shift, Marneuli, January 5-February 17, 2024, M2 filtration. The influence of the atmosphere is removed (no atmos, solid line) or saved (use atmos, dashed line).

Note that if the influence of the atmosphere was not removed from the water level, then the magnitude of the phase shift and the range of changes turn out to be significant. If the influence of the atmosphere is removed from the water level, then the scatter of the phase shift is an order of magnitude smaller (Fig.7).

In [1], when calculating the phase shift, time intervals of 30 days were used. From the above figures it can be seen that the choice of time interval can affect the average value of the phase shift and even its sign.

References

[1] Hsieh P.A., Bredehoeft J.D., Farr J.M. Determination of aquifer transmissivity from earth tide analysis, Water Resour. Res., 23, 1987, pp.1824–1832.

[2] Gao X., Sato K., Horne R. N. General solution for tidal behavior in confined and semiconfined aquifers considering skin and wellbore storage effects. Water Resour. Res, 56, 2020, e2020WR027195. https://doi.org/10.1029/2020WR027195.

[3] Vinogradov E., Gorbunova E., Besedina A., Kabychenko N. Earth tide analysis specifics in case of unstable aquifer regime. Pure Appl. Geophys. Springer International Publishing AG, 2017, DOI 10.1007/s00024-017- 1585-z.

[4] Kobzev G., Melikadze G., Jimsheladze T. Phase shift of water response to gravity in Georgian wells. Transactions of Mikheil Nodia Institute of Geophysics, ISSN 1512-1135, vol. LXXV, 2022, pp.31-39.

საქართველოს ჭაბურღილებში წყლის დონის ფაზური წანაცვლების ნიშნის ცვლილება

გ. კობზევი, გ. მელიქაძე, თ. ჯიმშელაძე

რეზიუმე

საქართველოს ტერიტორიაზე განლაგებული ჭაბურღილების მაგალითზე, ნაჩვენებია გრავიტაციასა და წყლის დონეს შორის ფაზურ წანაცვლების ნიშნის რეგულარული ცვლილების შესაძლებლობა.

საკვანძო სიტყვები: ფაზური წანაცვლება, წყლის დონე, გრავიტაცია, ელიფსის მეთოდი.

Изменения знака фазового сдвига уровня воды в скважинах Грузии

Г. Кобзев, Г. Меликадзе, Т. Джимшеладзе

Резюме

На примере скважины Грузии показывается возможность регулярного изменения знака в фазовом сдвиге между гравитацией и уровнем воды.

Ключевые слова: фазовый сдвиг, уровень воды, гравитация, метод эллипса.

Journal of the Georgian Geophysical Society, e-ISSN: 2667-9973, p-ISSN: 1512-1127
Physics of Solid Earth, Atmosphere, Ocean and Space Plasma, v. 27(1), 2024, pp. 9 - 18

Comparison of Satellite Remote Sensing and Field Ground Observation Data for the Large Glaciers Retreat Study in Georgia

[1]George I. Kordzakhia, [1]Larisa D. Shengelia, [2]Genadi A. Tvauri, [3]Murman Sh. Dzadzamia, [3]Giorgi N. Guliashvili, [3]Sopio T. Beridze

[1] Institute of Hydrometeorology of the Georgian Technical University, Georgia,
[2] E. Andronikashvili Institute of Physics of the I. Javakhishvili Tbilisi State University, Georgia,
[3] National Environmental Agency of the Ministry of Environmental Protection and Agriculture, Georgia
[1]e-mail: giakordzakhia@gmail.com

ABSTRACT

The results of the comparison of satellite remote sensing (SRS) data and ground-based observation (GBO) information on the large glaciers (Adishi, Shkhara and Gergeti) of Georgia are presented. From each satellite image, the location of the tip of the glacier's tongue was determined, a chronological order of the data was made, and the average rate of glacier retreat was calculated. Using SRS, the dynamics of the retreat of glaciers are studied based on the determination of individual places of movement of the tip of the glacier tongue. The dynamics of some large glaciers retreat based on the GBO data of the National Hydrometeorological Service (NEA) of Georgia is presented and is additionally used for quality assessment and quality control (QA/QC) of the results. The analyses show that based on SRS and GBO data the retreats of studied glaciers are nonlinear and by high confidence can be presented by a parabola curve. The comparison of SRS and GBO data shows that they are in good agreement with each other.

Keywords: *Georgian glaciers, satellite remote sensing, ground-based observations, climate change.*

Introduction

Over the last decades, global warming has led to a widespread shrinking of the cryosphere, with mass loss from ice sheets and glaciers (*very high confidence*) [1]. Projected physical changes include global glacier mass loss expected to continue in the near future (2031–2050) due to rising surface air temperatures (high confidence), with imminent consequences for river flows and local hazards (*high confidence*) [1].

To study the impact of climate change on glaciers, along with the SRS data the GBO data is needed. This is preconditioned by the fact that using high-resolution SRS allows the simultaneous study of the state of large glaciers with the required resolution and accuracy, under conditions of limited material resources and time [2,3]. The GBO data is needed for the QA/QC of the results.

Used satellite data that is available through Earth Resources Observation Systems (EROS). This archive, which is under the jurisdiction of the US Department of the Interior, preserves data obtained by Landsat satellites, as well as satellite images at the disposal of NASA. For the QA/QC of the results, complex use of historical glacier catalogue data, existing field material and expert knowledge is necessary.

Materials and methods

The impact of ongoing climate change on glacier degradation is one of the most visible when studying the retreat of large glaciers (area > 2 km^2). A methodology has been developed to study the dynamics of retreat of large glaciers.

Weather conditions have a significant impact on the use of SRS, in particular, in case of cloudiness, it is impossible to use satellite images. When observing glaciers, this limitation is added to the state of the surface of the glacier itself. The surface of the glacier should be as free as possible from snow cover, in particular, SRS should be carried out from the end of the ablation until the first snowfall. In the Earth, this period depends on the location of the glacier, altitude, climate and weather conditions. Under the conditions of the modern climate, this time interval for Georgia covers the period from the end of June to the beginning of October.

The contouring of glaciers is carried out by manual digitization, during which expert knowledge is taken into account. ASTER DEM digital terrain model and topographic maps of the USSR (1:50,000) of the 60s of the last century were used to identify the studied glaciers and specify their contours.

When studying the dynamics of the retreat of large glaciers, it is especially important to accurately determine the location of the end of the glacier tongue. The use of expert knowledge is essential when the glacier tongue is covered by moraines and/or debris.

Glaciers, whose tip of the tongue is formed, is outlined and is not covered by either broken material or cloud, have been selected for the study. The methodology for determining the dynamics and rate of retreat at the end of the glacier tongue for large glaciers is presented in [4, 5].

Results

Only nine large glaciers were selected from the large glaciers of Georgia, the condition of which was satisfactory for our purposes. Of these nine glaciers, only three glaciers could be compared with NEAs' GBO data. These glaciers are Adishi and Shkhara belonging to the R. Enguri glacia basin and Gerget glacier of the R. Tergi glacial basin.

For example, let's consider in detail the dynamics of the change in the location of the end of the tongue of the Adishi glacier based on the determination of individual places of the movement of the tip of the tongue. According to each satellite image, let's make a chronological order of the data and calculate the average speed of glacier retreat. For the QA/QC of the obtained results, NEAs' data is used.

Fig. 1 shows a schematic image of the retreat of the Adishi Glacier on the background of the August 25, 2022, Landsat 8 OLI TIRS satellite image, where the green pins show the results obtained by GBO data. In different years, the location of the glacier is shown with a different coloured outline. The length of glacier retreat can be calculated through the white dashed line crossing the contours. From September 13, 1977 to August 25, 2022, this figure was approximately 601 m.

Table 1 below summarizes the features of the Adishi Glacier retreat. The satellite image from 1977 is considered the starting point. 23 different satellite data files taken between 1977 and 2022 from satellite data are selected to study the retreat of the Adishi Glacier. To avoid overloading the image in Figure 1, only 8 contours of the location of the tip of the glacier tongue are plotted in different years. Table 1 summarizes the individual characteristics of these satellite data.

Tables 1 and 2 show the coordinates and retreat distances of the end of the Adishi glacier tongue according to satellite data (period 1977 and 2020) and correspondingly GBO data covering the period of 1985-2022.

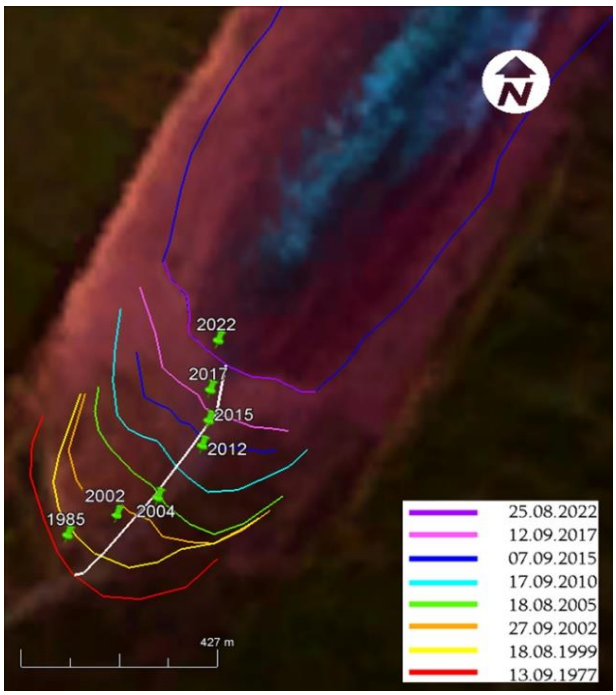

Fig. 1. Schematic picture of the retreat of the Adishi Glacier (r. Enguri Basin).

Table 1. According to SRS data, the location of the end of the Adishi glacier tongue and retreat distances.

№	Satellite Type	Date	Coordinates (Grad.)		Retreat (m)
			Latitude	Longitude	
1	Landsat 2 MSS	13.09.1977	42.989233°	42.984633°	0
2	Landsat 5 TM	09.10.1986	42.989254°	42.984746°	9.39
3	Landsat 5 TM	01.09.1987	42.989281°	42.984876°	20.2
4	Landsat 4 TM	23.09.1989	42.989486°	42.985144°	53
5	Landsat 5 TM	15.09.1998	42.989552°	42.985231°	62.3
6	Landsat 7 ETM+	18.08.1999	42.989630°	42.985334°	75.1
7	Landsat 7 ETM+	05.09.2000	42.990473°	42.986319°	91.2
8	Landsat 7 ETM+	27.09.2002	42.989572°	42.985452°	198
9	Landsat 5 TM	28.08.2003	42.990546°	42.986400°	209
10	Landsat 7 ETM+	08.15.2004	42.990784°	42.986682°	244
11	Landsat 7 ETM+	18.08.2005	42.990946°	42.986846°	266
12	Landsat 7 ETM+	08.10.2006	42.991070°	42.986972°	284
13	Landsat 5 TM	16.08.2007	42.991120°	42.987025°	290
14	Landsat 7 ETM+	29.08.2009	42.991328°	42.987225°	319
15	Landsat 7 ETM+	17.09.2010	42.991471°	42.987368°	338
16	Landsat 5 TM	27.08.2011	42.991630°	42.987524°	360
17	Landsat 8 OLI TIRS	23.08.2013	42.991732°	42.987623°	374
18	Landsat 8 OLI TIRS	26.08.2014	42.991891°	42.987775°	396
19	Landsat 8 OLI TIRS	07.09.2015	42.992109°	42.987981°	424
20	Landsat 8 OLI TIRS	24.08.2016	42.992361°	42.988220°	459
21	Landsat 8 OLI TIRS	12.09.2017	42.992570°	42.988423°	488
22	Landsat 8 OLI TIRS	11.09.2020	42.993209°	42.988620°	560
23	Landsat 8 OLI TIRS	25.08.2022	42.993568°	42.988683°	601

Table 2. Location of the end of Adishi glacier tongue and retreat distances according to GBO data.

№	Date	Coordinates (Grad.)		Retreat (m)
		Latitude	Longitude	
1	15.09.1985	42.989886	42.984383	0
2	20.08.2002	42.990296	42.985645	116
3	15.08.2004	42.990659	42.986799	220
4	10.08.2012	42.991733	42.987981	371
5	19.09.2015	42.992250	42.988157	432
6	05.07.2017	42.992881	42.988198	501
7	10.07.2022	42.993902	42.988410	614

Fig. 2.a presents the graph of the change in the location of the Adishi glacier tongue and the corresponding trend, constructed using SRS data. The initial condition corresponds to 1977. To detail the characterisation of the impact of the current climate change on the Adishi glacier, the graphs (Fig. 2. b) are constructed, where the observational period is divided into two sub-periods: 1977-1998 and 1999-2020.

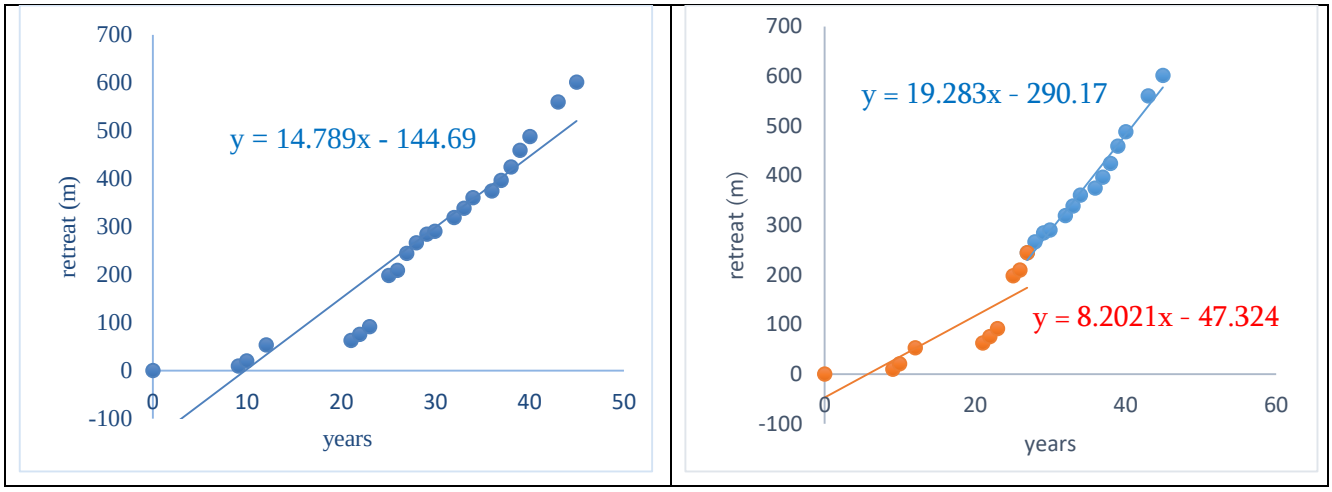

a b

Fig. 2. The dynamics of the retreat of the Adishi glacier according to SRS: a - for the full period of observation, b - for two sub-periods of observation.

The same actions for the GBA data give a graph of the retreat of the Adishi glacier (Fig. 3 a). The initial state corresponds to 1985. For more information, the observation period is divided into two sub-periods: 1985-2004 and 2004-2022. The corresponding graphs are given in Fig. 3 b.

The analysis shows that the rate of retreat of Addishi glacier according to SRS and GBO data are: during the whole period was about 14.8 and correspondingly 17.0 m/year. In the first subperiod, the velocity is approximately 8.2 and 9.5 m/year and in the second subperiod - about 19.3 and 22.2 m/year respectively. Both the SRS and GBO data show that the retreat in the second subperiod is significantly greater than the retreat in the first subperiod, that is, the retreat of the glacier is non-linear.

The analysis shows that the difference between SRS and GBO data for the entire period is about 2.9 m/year, while the difference for the first period is about 1.3 m/year and about 2.9 m/year for the second period. This difference is due to the differences between the periods of satellite and ground observations, as well as the differences in reference measurements.

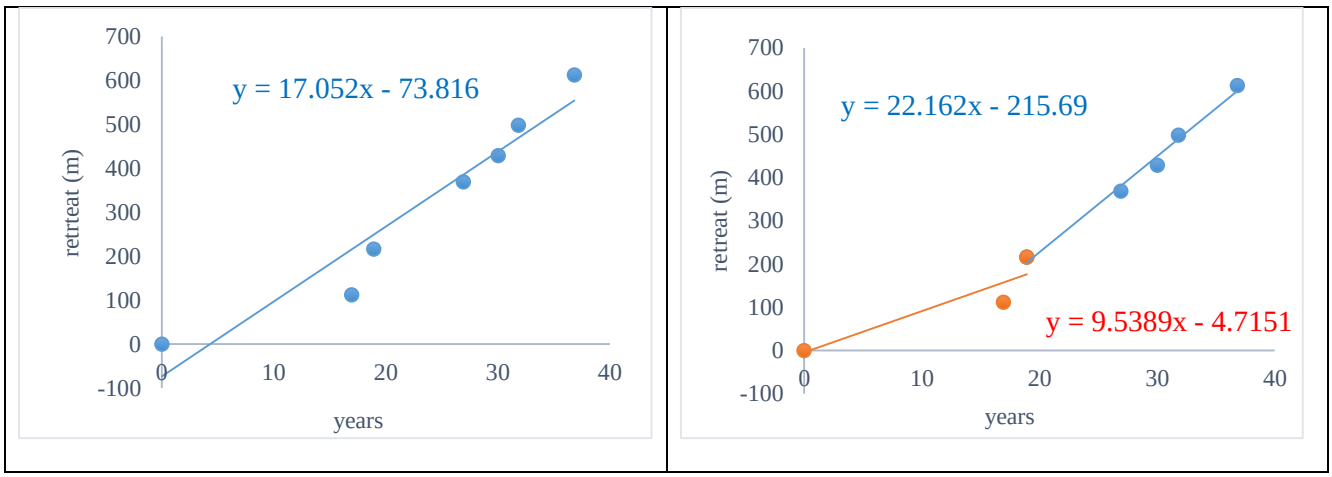

a b

Fig. 3. The dynamics of the retreat of the Adishо glacier according to GBO: a - for the full period of observation, b - for two sub-periods of observation.

These data confirm that the rapid degradation of the Adishi glacier is caused by modern climate change. On the other hand, glacier retreat data is an effective indicator of current climate change and its acceleration in time. The non-linear retreat of the Adishi glacier by SRS and GBO, as well as the retreat of other large glaciers of Georgia discussed by us [6-8] is described with high accuracy by a parabola curve.

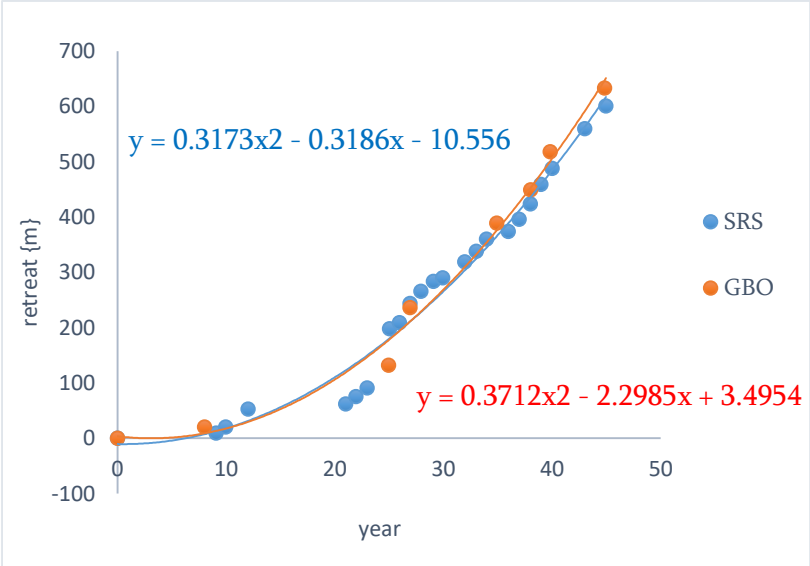

Fig. 4. Retreat graphs of Adishi Glacier based on SRS and GBO data

A comparison of the graphs in Fig. 4 shows that the graphs created based on SRS and GBO data are in satisfactory agreement with each other.

Fig. 5 shows a schematic image of the retreat of the Shkhara Glacier on the background of the September August 25, 2022, Landsat 8 OLI TIRS satellite image, where the green pins show the results obtained by the GBO data. In different years, the location of the glacier is shown with a different coloured outline. The same activities that were carried out for the Adishi glacier give for Shkhara glacier retreat the same picture i.e. the glacier retreat is nonlinear, it is well described by the parabola curve both for the SRS and GBO. A comparison of the graphs in Fig. 5 shows that the SRS and GBO graphs are in satisfactory agreement with each other.

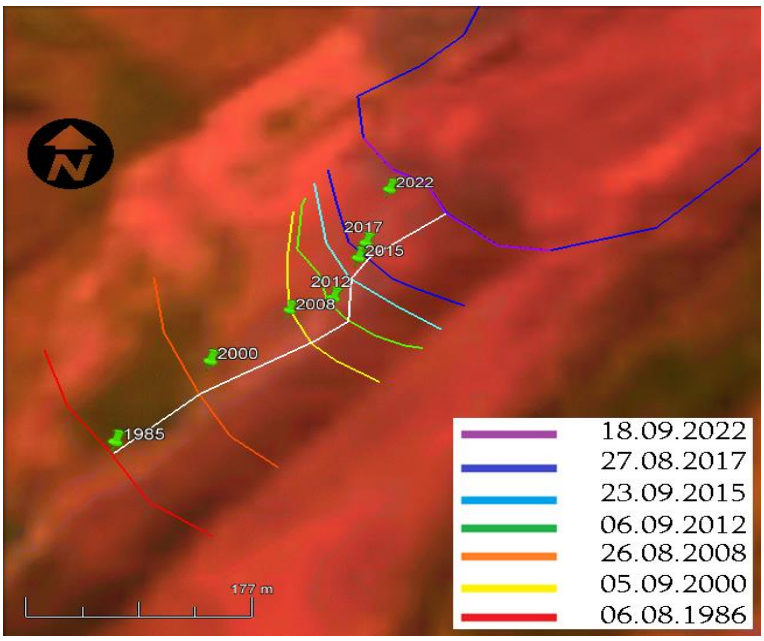

Fig. 5. Schematic image of Shkhara glacier retreat on the background of the September 18, 2022, Landsat 9 OLI TIRS sensor image. The green pins show the results obtained based on GBO data.

The retreat of the Shkhara glacier is discussed analogously as it was done for the Adishi glacier. It is received that 1. the retreat is non-linear, and 2. the retreat of the Shkhara glacier is described with high accuracy by a parabola curve (Fig. 6) based on SRS and SBO data. A comparison of the SRS and GBO graphs in Figure 6 shows that they are in good agreement with each other.

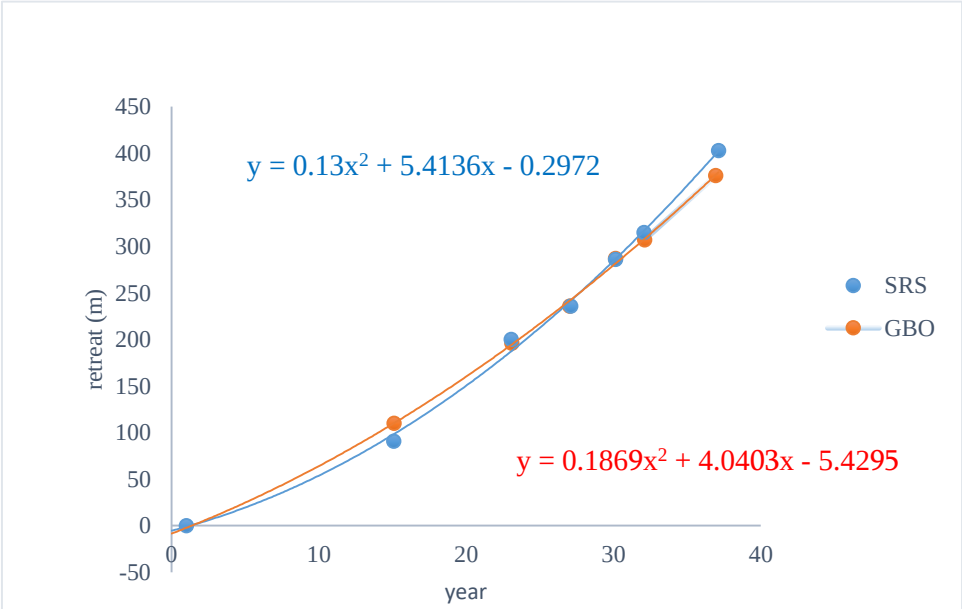

Fig. 6. Retreat graphs of Shkhara glacier based on SRS and GBO data

Among the large glaciers of Eastern Georgia, only the end of the Gergeti glacier is not covered with debris, which allows the use of multispectral sensors. To study the physical picture of the Gergeti Glacier retreat, Landsat satellite sensor data is used.

To study the retreat of the Gergeti glacier, 12 different satellite data files from 1977-2022 are selected. According to each satellite image, the location of the tip of the Gergeti glacier tongue was determined, and the data were chronologically ordered (Fig. 7).

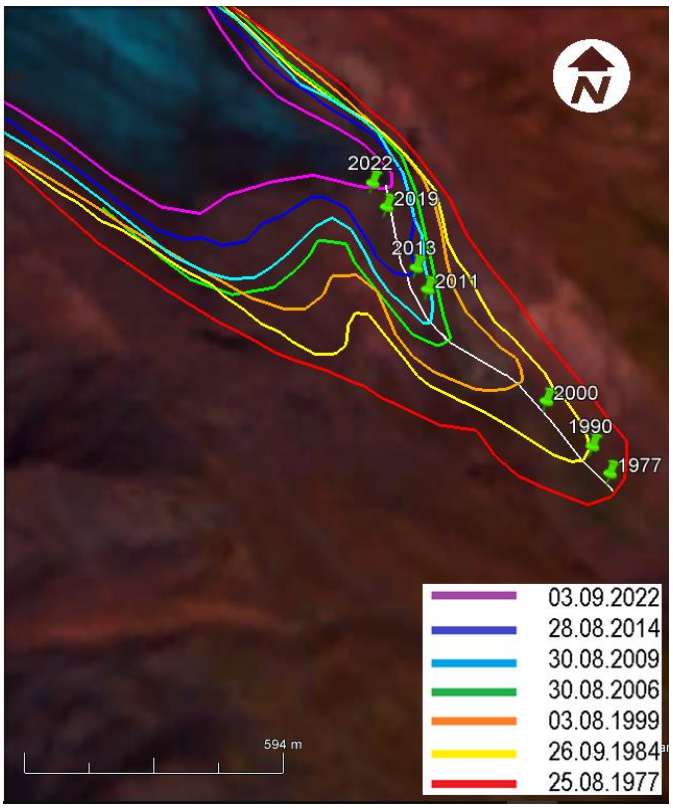

Fig. 7. Schematic image of Gergeti glacier retreat on the background of the September 3, 2022, Landsat 8 OLI TIRS sensor image. The green pins show the GBO data.

The steps to reveal the retreat dependence on time of the Gergeti glacier are the same steps that were carried out for the Adishi glacier. The same results are received i.e. the retreat of the Gergeti glacier is non-linear and is described with high accuracy by parabola curves correspondingly for SRS and GBO data (Fig. 8). A comparison of the SRS and GBO graphs in Figure 8 shows that they are in good agreement with each other.

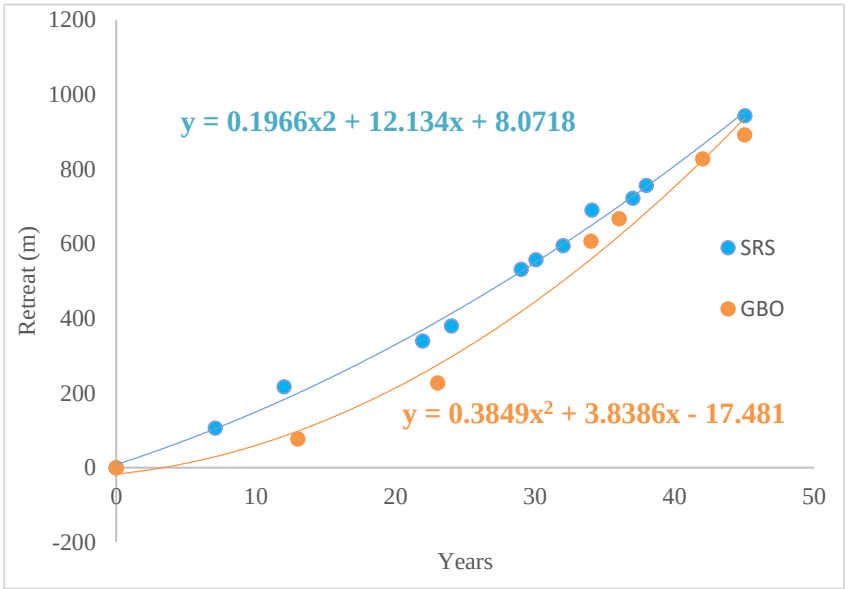

Fig. 8. Retreat graphs of Gergeti glacier based on SRS and GBO data.

Conclusion

Large glacier degradation under modern climate change poses a significant threat to the country's sustainable development and the study of their retreat is considered one of the priority activities. To obtain a scientifically based answer regarding the large glaciers' degradation issues, taking into account the impact of current climate change, it is necessary to use SRS and GBO data. If we analyse the graphs of SRS and GBO data for all three glaciers, it is evident that glacier retreat is nonlinear both for SRS and GBO data and is described with high confidence by parabola curves. A comparison of the SRS and GBO graphs shows that they are in good agreement with each other. The detail considering the corresponding graphs shows that the differences in the SRS and GBO data at the beginning of the graphs are bigger than in recent years. This is explained by the fact that earlier field ground observations were carried out using the geodetic planning method, and since 2004 - using a special field Global Positioning System (GPS), which also uses satellite information and has high accuracy. A comparison of SRS and GBO graphs that define good agreement with each other confirms the relevance of using GBO data for quality assessment and quality control (OA/OC) of SRS data.

The presentation was made at the international scientific conference "Geophysical processes in the Earth and its envelopes", Tbilisi, Georgia, November 16-17, 2023.

Acknowledgement

The research was performed with the support of the Shota Rustaveli National Science Foundation project FR-21-1996 "Research on the Degradation of Georgian Glaciers in Recent Decades and the Creation of an Electronic Atlas of Georgian Glaciers".

References

[1] IPCC (2018). A Special Report of the Intergovernmental Panel on Climate Change. The Ocean and Cryosphere in a Changing Climate. Edited by Melinda Tignor, Elvira Poloczanska, Katja Mintenbeck, Andrés Alegre, Maike Nicolai, Andrew Okem, Jan Petzold, Bardhyl Rama, Nora M. Weyer. Working Group II Technical Report. IPCC, Geneva, Switzerland, 2018, 755 p.

[2] Zemp M. et al. Historically unprecedented global glacier decline in the early 21st century. J. Glaciology, 61 (228), 2015, pp. 745-762, doi: 10. 3189/2015Jog15J017.

[3] Kordzakhia G., Shengelia L., Tvauri G., Dzadzamia M. Impact of Modern Climate Change on Glaciers in East Georgia. Bulletin of the Georgian National Academy of Sciences, Vol. 10, №4, 2016, pp. 56−63.

[4] Kordzakhia G., Shengelia L., Tvauri G., Dzadzamia M. Research of Glaciers Variation Dynamics in East Georgia Under the Impact of Modern Climate Change, Proceedings of the Fourth Plenary Conference and Field Trips of UNESCO−IUGS−IGCP 610 project „From the Caspian to Mediterranean: Environmental Change and Human Response during the Quaternary"(2013−2017), 2-9 October, 2016, pp. 96-100, Printed in Georgia, Georgian National Academy of Sciences, Georgia, Tb., 2016, pp. 96-100.

[5] Kordzakhia G. I., Shengelia L. D., Tvauri G. A., Dzadzamia M. Sh. The climate change impacton the glaciers of Georgia. In Journal-World Science, vol. 1, № 4(44), Warsaw, Poland, 2019, pp. 29-34.

[6] Шенгелия Л.Д., Кордзахия Г.И., Тваури Г.А., Дзадзамия М. Ш. Влияние текущего изменения климата на большие ледники Грузии. „География: развитие науки и образования" Коллективная монография по материалам Всероссийской, с международным участием, научно-практической конференции LXXII Герценовские чтения 18−21 апреля 2019 года. Изд-во РГПУ им. А.И. Герцена, т. I, Россия, С.-П., 2019, с. 218-226.

[7] Kordzakhia G., Shengelia L., Tvauri G., Dzadzamia M. Climate Change Impact on the Glaciers of the Rioni River Basin (Georgia). Acta Horticulturae et Regiotecturae – Special Issue Nitra, Slovaca Universitas Agriculturae Nitriae, 2021, pp. 27–30.
[8] Kordzakhia G. Fourth National Communication of Georgia, Under the United Nations Framework Convention on Climate Change. 4.4 Glaciers, Tbilisi, Georgia, 2021, pp. 241-250.

საქართველოს დიდი მყინვარების უკანდახევის კვლევისთვის თანამგზავრული დისტანციური ზონდირების და საველე მიწისპირა დაკვირვების მონაცემების შედარება

გ. კორძახია, ლ. შენგელია, გ. თვაური, მ. ძაძამია, გ. გულიაშვილი, ს. ბერიძე

რეზიუმე

წარმოდგენილია საქართველოს დიდ მყინვარებზე (ადიში, შხარა გერგეთი) თანამგზავრული დისტანციური დაკვირვების და საველე მიწისპირა დაკვირვების მონაცემების შედარების შედეგები. თითოეული თანამგზავრული სურათის მიხედვით დადგინდა მყინვარის ენის ბოლოს მდებარეობა, შედგა მონაცემთა ქრონოლოგიური რიგი და გამოთვლილ იქნა მყინვარის უკანდახევის საშუალო სიჩქარე. თდზ-ის გამოყენებით შესწავლილია მყინვარების უკანდახევის დინამიკა მყინვარის ენის წვერის მოძრაობის ცალკეული ადგილების განსაზღვრის საფუძველზე. შედეგების ხარისხის შეფასებისა და კონტროლისათვის გამოყენებულია გარემოს ეროვნული სააგენტოს საველე დაკვირვებების მიწისპირა მონაცემები. დადგინდა, რომ შესწავლილი მყინვარების უკანდახევა არაწრფივი ხასიათისაა და მაღალი სიზუსტით აღიწერება პარაბოლის მრუდით. ასევე დიდი სიზუსტით პარაბოლის მრუდით აღიწერება შედეგების ხარისხის შეფასებისა და კონტროლისათვის გამოყენებული საველე ექსპედიციის მონაცემების მიხედვით აგებული მყინვარების უკანდახევის გრაფიკი. თანამგზავრული დისტანციური დაკვირვების და საველე მიწისპირა დაკვირვების მონაცემების შედარება გვიჩვენებს, რომ შესწავლილი მყინვარების თდზ-ისა და საველე დაკვირვებების მიწისპირა მონაცემები ერთმანეთთან კარგ თანხვედრაშია.

საკვანძო სიტყვები: საქართველოს მყინვარები, სატელიტური დისტანციური ზონდირება, მიწისზედა დაკვირვებები, კლიმატის ცვლილება.

Сравнение данных спутникового дистанционного зондирования и полевых наземных наблюдений для исследования отступления Больших ледников Грузии

Г. Кордзахия, Л. Шенгелия, Г. Тваури, М. Дзадзамиа, Г. Гулиашвили, С. Беридзе

Резюме

Представлены результаты сравнения данных спутникового дистанционного зондирования (СДН) с данными полевых наземных наблюдений за большими ледниками Грузии (Адиши, Шхара Гергети). По каждому спутниковому снимку определялось положение вершины языка ледника, приводилась

хронологическая упорядоченность данных и рассчитывалась средняя скорость отступания ледника. С помощью СДН изучается динамика отступания ледников на основе определения местонахождения кончика языка ледника при движении. Для оценки и контроля качества результатов используются наземные данные полевых наблюдений Национального агентства по охране окружающей среды. Установлено, что отступление изученных ледников носит нелинейный характер и с высокой точностью описывается параболической кривой. Также график отступления ледников, построенный по данным полевой экспедиции, используемый для оценки качества и контроля результатов, с большой точностью описывается кривой параболы. Сравнение данных спутниковых дистанционных наблюдений и данных полевых наземных наблюдений показывает, что СДН изученных ледников и наземные данные полевых наблюдений хорошо согласуются друг с другом.

Ключевые слова: Ледники Грузии, спутниковое дистанционное зондирование, наземные наблюдения, изменение климата.

Journal of the Georgian Geophysical Society, e-ISSN: 2667-9973, p-ISSN: 1512-1127
Physics of Solid Earth, Atmosphere, Ocean and Space Plasma, v. 27(1), 2024, pp. 19 - 24

Study of Kutaisi City Atmospheric Air Pollution with PM10 Particles using Numerical Modeling. A Case of Fresh Western Background Breeze

[1,2]Aleksandre A. Surmava, [2]Vepkhia G. Kukhalashvili, [1]Natia G.Gigauri, [1]Liana N. Intskirveli

[1]Institute of Hydrometeorology of the Georgian Technical University, Georgia,
[2]M. Nodia Institute of Geophysics of the I. Javakhishvili Tbilisi State University, Georgia
[1]e-mail: l.inwkirveli@gtu.ge

ABSTRACT

Study of Kutaisi city atmospheric air pollution with PM10 particles has been conducted by means of combined integration of 3D regional model of atmospheric processes evolution and equation of admixtures transfer-diffusion. Patterns of PM10 concentration time chance and spatial distribution have been obtained. It has been shown that a formed field of wind velocity promotes PM10 particles transportation from the city and atmosphere "self-purification" process. It has been obtained by calculations that aerosol propagation process conventionally runs by four stages and depends on motor transport traffic intensity, trunk roads' location and city relief. Relatively high pollution zones have been identified. It has been established that thermal stability of the atmosphere in the surface layer of atmosphere plays crucial role in time change of microaerosols' concentration and high concentrations formation process.

Key words: *PM10 pollution of atmosphere, numerical modeling, concentration, fresh western breeze.*

Introduction

Protection of atmospheric air of urbanized environment from aerosol pollution is a topical problem of the modern ecology. It is of great medical and socioeconomic importance [1]. Among numerous substances polluting the atmospheric air a special place is held by the smallest particles, sizes of which don't exceed 2.5 and 10 μm (PM2.5 and PM10). They are originated as a result of both current natural processes taking place on the Earth (rock erosion, desert winds etc.), and agricultural, industrial and transport-related human activity. Due to small sizes, PM2.5 and PM10 easily penetrate human cardiovascular system, precipitate there and cause numerous diseases, and even death on frequent occasions [2-4].

Problem of atmospheric air protection from microparticles pollution is very important not only in large cities and industrial regions, but also in resort-recreation centers and separate small cities. Cities of Georgia aren't ranked among heavily polluted cities of the world [5], however in some cases microparticle concentrations there exceed maximum permissible concentrations [6-8] and have a negative impact on human health.

Some air-protection measures have been scheduled over the recent years for improvement of atmospheric air purity of Georgian cities [9, 10]. In order to enhance their efficiency, it is necessary to carry out these measures based on scientifically substantiated studies.

In the presented article, the problem of PM10 pollution of atmospheric air of Kutaisi – the second largest city of Georgia and its adjacent territories resulted from motor transport traffic has been studied theoretically, using the computer modeling of admixtures propagation in the atmosphere.

Research method

The atmosphere of Kutaisi city and its adjacent territory with an area of 13.4 x 13.4 km has been selected for studies (Fig. 1). This territory is of complex orography – terrain height varies from 80 to 450 m. The orography is confined by ranges and separate mountains from north and east, while the western and southern parts of city and its surroundings are located at the Kolkheti lowland.

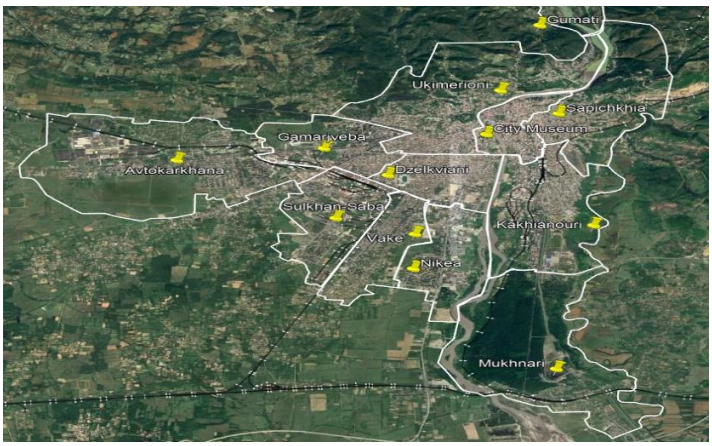

Fig. 1. Urbanized relief of Kutaisi and adjacent territories, and administration units (AU).

This work studies spatial distribution and time change of concentration of microparticles discharged into surface layer of the atmosphere over the mentioned territory, using numerical modeling. Regional model of atmospheric processes development at the Caucasus territory and the method of numerical integration of equation of admixtures transfer-diffusion in the atmosphere are used for modeling [13-15]. Integration is made at the numerical grid composed of 67×67×31 points. Numerical grid steps along meridian and parallel are equal to 200 m. A vertical dimensionless step in free atmosphere equals to 1/31, that approximately corresponds to 300 m. A vertical step in 100 m thick surface layer of the atmosphere varies from 0.5 to 15 m. Time step is 1 sec. Calculations are made for 3-day period. A case of background fresh western breeze under dry weather conditions of June is considered. Wind velocity at surface layer height (100 m) is 11 m/sec. Above the surface layer wind velocity linearly increases and reaches 20 m/sec at 9 km altitude. Relative atmospheric humidity is 50%.

It is assumed that PM10 pollution of the atmosphere is caused by motor transport traffic in the city and its adjacent territory. Emissions occur at 0.5 m height from the earth surface in 5 types of areas: trunk roads, central streets of the city, residential areas, industrial zones and unpopulated territories of surrounding villages. Emission rate is different depending on the area, is of 24 hour-periodic nature and proportional to motor transport traffic intensity. It is minimal in the interval from 0 to 4AM, then linearly increases from 4AM to 10AM and remains constant from 10AM to 6PM. From 6PM to midnight a discharge rate linearly reduces and becomes equal to emission rate of 0 AM.

Numerical modeling results

Spatial concentration and time change of PM10 concentration discharged by motor transport into atmosphere of Kutaisi obtained using numerical modeling in case of fresh western breeze are given in Fig. 2.

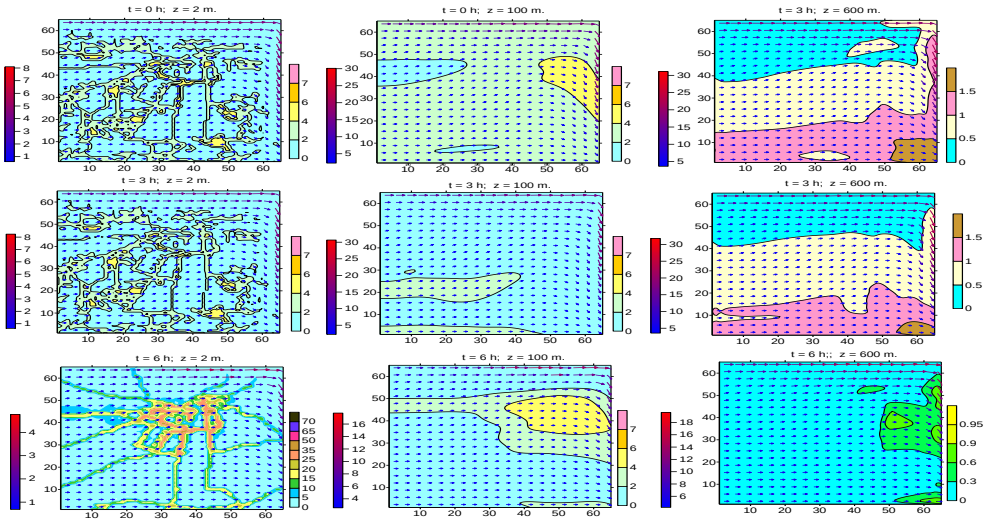

Fig. 2. Spatial concentration of PM10 concentration (μg/m^3) and wind velocity vector (m/sec), obtained using numerical modeling, when t = 0, 3 and 6 h.

As is seen from Fig. 2, a terrain effect on background fresh western breeze doesn't cause significant change of wind velocity in the surface layer and the lower part of boundary layer of the atmosphere. Terrain effect is manifested in wind velocity reduction at the city territory and emergence of a component directed north-eastward. In a whole, in the modeling area, wind velocity at 2 m height from earth surface increases from south to north and from west to east from 0.8 to 8 m/sec. With the distance from the Earth ground a terrain effect gradually weakens, wind keeps its western direction, while a wind velocity values at 600 m height vary within a range of 4-30 m/sec.

The analysis of time change of microaerosol concentration field, obtained by calculations, shows that concentration values are minimal within an interval of t = 0-3 h. At 2 m height when t = 0 h, PM10 concentration value is within 0-2 μg/m^3 at the major part of the city. Concentration equal to 2-4 μg/m^3 is obtained in the surroundings of main city streets. Maximum concentrations, 4-6 μg/m^3, are registered at the territories of administration units (Gamarjveba, Dzelkviani, City-Museum) located in the city center, as well as in suburban areas (Kakhianouri and Avtokarkhana AUs, Baloji village) and territories situated south-westward and south-eastward of the city.

At 100 m height from the earth surface, when t = 0 h, PM10 concentration value is 2-4 μg/m^3 in the major part of the modeling area, and 0-2 and 4-6 μg/m^3 in two areas of small size. Concentration value at 600 m height doesn't exceed 2 μg/m^3. By t = 3h, a pattern of spatial concentration of the surface concentration at 100 and 600 m height doesn't experience qualitative change, and small reduction of concentration takes place in quantitative terms. Rise of atmospheric air pollution level starts in parallel with increase of motor transport traffic intensity. When t = 6h, concentration values are within limits of 15-20 μg/m^3 at 2 m height from the earth surface at urbanized territories and in the close proximity of central streets. In the mentioned period of time, a weak substance transfer from surface layer of the atmosphere to its upper parts occurs. As a result, by t = 6 h, at 100 and 600 m from the earth surface, maximum concentration values reach 6 and 1 μg/m^3, respectively. Increase of atmospheric concentration lasts until 10-11AM. This increase is especially intense in the city center and its north-eastern part (Ukimerioni, Gamarjveba, Sapichkhia, Dzelkviani and City-Museum) (Fig. 3). Concentration value at this territory reaches 35 μg/m^3. Concentration increase also takes place at the highways connecting Kutaisi with Khoni, Tskaltubo resort, Samtredia and at the Kutaisi by-pass road.

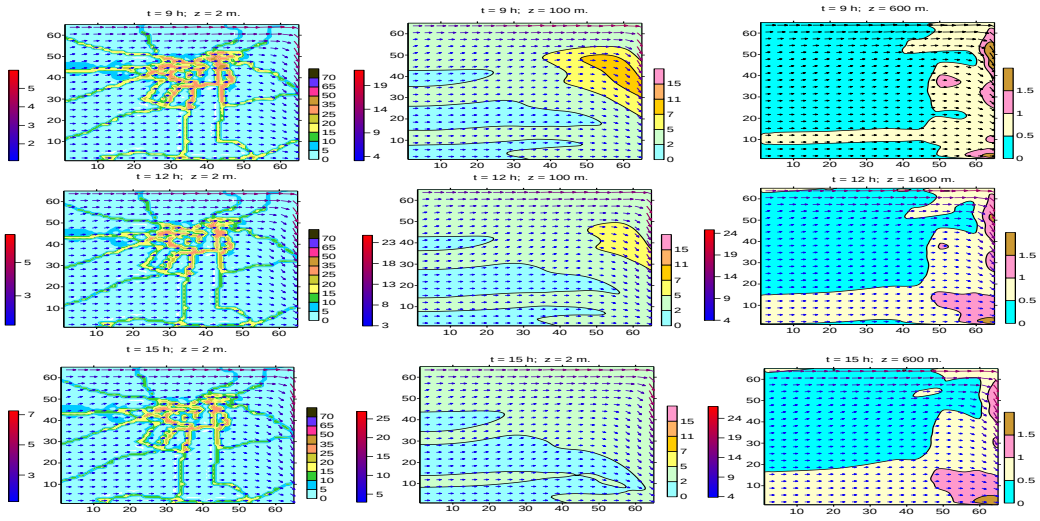

Fig. 3. Spatial distribution of PM10 concentration (μg/m^3) and wind velocity vector (m/sec), obtained by numerical modeling, when t = 9, 12 and 15 h.

After 11 AM, concentration starts to reduce throughout the modeling area. This reduction lasts until 3 PM. A uniform increase of concentration takes place after 3PM, as well. Maximum concentration 30-35 μg/m^3 is registered at 6-7PM in the surroundings of main avenues of the city (Fig. 4). In the ensuing points of time concentration quickly reduces until the midnight, and afterwards the pollution change process lasts on a quasi-periodical basis.

At 100 and 600 m level from the surface, concentration value is mainly within the limits of 2-7 μg/m^3 and a time of achievement of its maximum values (7-11 μg/m^3) by 2-3 hours lags behind a time of achievement of maximum surface concentration.

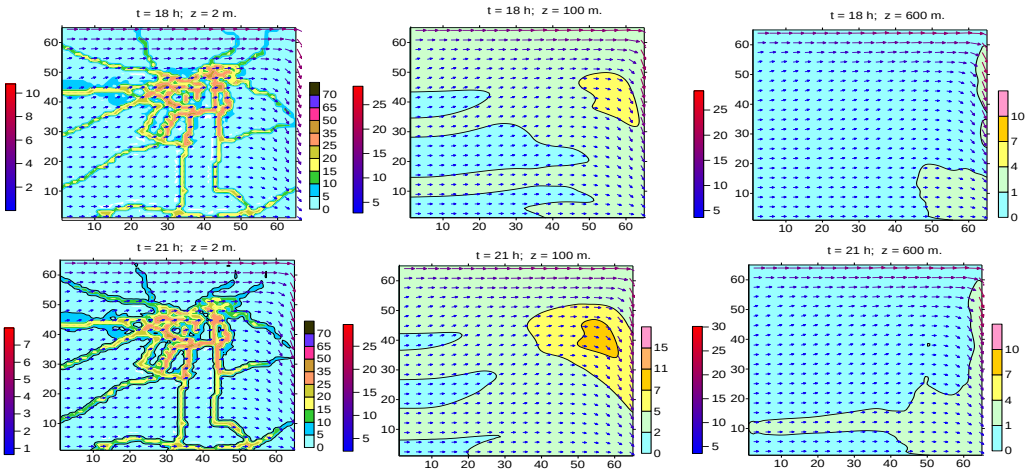

Fig. 4. Spatial distribution of PM10 concentration (μg/m^3) and wind velocity vector (m/sec), obtained by numerical modeling, when t =18 and 21 h.

In Fig. 5 there is shown the diagram of PM10 concentration time change obtained via calculations for main types of observation points. It is seen from Fig. 5 that time change of concentration at trunk roads, main city streets and urbanized territories is characterized by presence of 2 maximums (when t = 8-9 h and 19-21 h) and 2 minimums (when t = 4 and 14-15 h) of concentration. The more is PM10 emission rate, the more apparent are mentioned extremums. It is worth noticing the presence of local concentration maximums by 6AM.

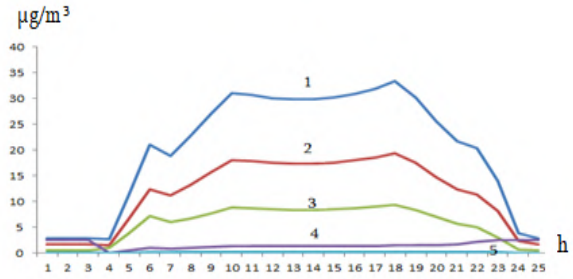

Fig. 5. Time change of PM10 concentration at trunk roads (1), central city streets (2), along industrial (3) and rural (4) zones and in unpopulated points at 2 m height from the earth surface.

As for rural-type settled and unpopulated territories, concentrations values in their surroundings don't exceed 5 μg/m^3 and their time change is not clearly expressed.

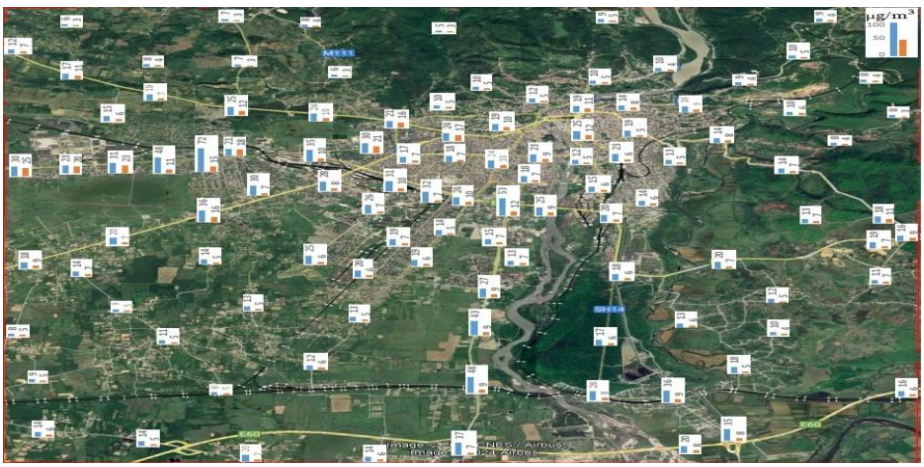

Fig. 6. Column diagrams and numerical values of PM2.5 (red) and PM10 (blue) concentrations (μg/m^3) obtained by experimental measurements.

Numerical modeling results have been compared with the results of carried-out special expedition measurements (Fig. 6). As the comparison showed, the results of theoretical and experimental measurements are close to each other. The mentioned fact points at the great importance of motor transport traffic in the process of microaerosol pollution of Kutaisi atmosphere.

Conclusions

Peculiarities of spatial distribution and time change of PM10 concentrations generated by motor transport at the territory of Kutaisi city in case of background fresh breeze in June have been studied by means of numerical modeling. It has been shown that the values of calculated concentrations are within the values observed. Patterns of spatial distribution of concentration in the city and its adjacent territories have been established at different parts of a day. It has been shown that spatial distribution of concentration significantly depends on both motor transport intensity and kinematics of surface layer of the atmosphere and local circulation system formed by diurnal change of thermal regime on the underlying surface.

Acknowledgments. The scientific research has been funded and performed with financial support of the Shota Rustaveli National Science Foundation within the grant project FR-22-4765.

ლიტერატურა - REFERENCES - ЛИТЕРАТУРА

[1] Integrated Science Assessment for Particulate Matter. EPA. United States Environmental Protector Agency, 2019, p.1967. EPA/600/R-19/188. www.epa.gov.isa.

[2] Pope C.A., Burnett R.T., Thun M.J., Calle E.E, Krewski D., et al. Lung cancer, cardiopulmonary mortality, and long-term exposure to fine particulate air pollution. J. Am. Med. Assoc, 287, 2002, pp. 1132–1141.

[3] World Health Organization. Regional Office for Europe. Review of evidence on health aspects of air–REVIHAAP Project. First result.

[4] Mortality and burden of disease from ambient air pollution-WHO. https://www.who.int/gho/phe/outdoor_air_pollution/burden/en/

[5] World's most polluted cities (historical data 2017-2022). https://www.iqair.com/world-most-polluted-cities.

[6] Kobza J., Geremek M., Dul L. Characteristics of air quality and sources affecting high levels of PM10 and PM2.5 in Poland, Upper Silesia urban area Environmental Monitoring and Assessment. 190, Article number 515, 2018.

[7] Girish Agrawal, Dinesh Mohan, Hifzur Rahman. Ambient air pollution in selected small cities in India: Observed trends and future challenges. IATSS Research. Volume 45, Issue 1, April 2021, pp 19-30. https://doi.org/10.1016/j.iatssr.2021.03.004.

[8] Air quality in Tbilisi. IQ Air. https://www.iqair.com/georgia/t-bilisi/tbilisi

[9] National Environment and Health Action Plan of Georgia 2018-2022 (NEHAP-2) https://test.ncdc.ge/Handlers/GetFile.ashx?ID=951a795c-ab20-4bdd-8f32-57959e3e1728

[10] ქ. რუსთავის ატმოსფერული ჰაერის ხარისხის გაუმჯობესების სამოქმედო გეგმა 2020-2022. https://mepa.gov.ge/Ge/PublicInformation/27987

[11] Amiranashvili A. G., Kirkitadze D. D., Kekenadze E. N. Pandemic of Coronavirus COVID-19 and Air Pollution in Tbilisi in Spring 2020. Journal of Georgian Geophysical Society, 23(1), 2020. https://doi.org/10.48614/ggs2320202654

[12] Surmava A.A., Kukhalashvili V.G., Gigauri N.G., Intskirveli L. N. PM2.5 and PM10 in the Atmosphere of Kutaisi City. Journal of Georgian Geophysical Society, 26(2), 2023. https://doi.org/10.60131/ggs.2.2023.7445

[13] Surmava A., Intskirveli L., Kukhalashvili V. Numerical Modeling of the Transborder, Regional and Local Diffusion of the Dust in Georgian Atmosphere, p.139, Publishing House, Technical University", ISBN 978-9941-28-810-4, Tbilisi, Georgia, 2021. http//www.gtu.ge (in Georgian).

[14] Kazakov A. L., Lazriev G. L. On Parametrization of Atmospheric Boundary Layer and Active Soil Layer. Izvestiya, Atmospheric and Oceanic Physics, 15, 1978, pp. 257-265.

[15] Marchuk G.I. Mathematical modeling in the problem of the environment. Moscow, Science, 1982, 320 p. (in Russian).

ქ. ქუთაისის ატმოსფერული ჰაერის PM10–ით დაბინძურების გამოკვლევა რიცხვითი მოდელირებით. ფონური დასავლეთის ძლიერი ქარის შემთხვევა

ა. სურმავა, ვ. კუხალაშვილი, ნ. გიგაური, ლ. ინწკირველი

რეზიუმე

ქ.ქუთაისის ატმოსფერული ჰაერის PM10–ით დაბინძურების კვლევა განხორციელებულია ატმოსფერული პროცესების ევოლუციის 3D რეგიონალური მოდელისა და მინარევების გადატანა - დიფუზიის განტოლების ერთობლივი ინტეგრირებით. მიღებულია PM10–ის კონცენტრაციის დროში ცვლილებისა და სივრცული განაწილების სურათები. ნაჩვენებია, რომ ფორმირებული ქარის სიჩქარის ველი ხელს უწყობს PM10–ის ქალაქიდან გატანა და ატმოსფეროს ,,თვითგასუფთავების“ პროცესს. გამოთვლებით მიღებულია, რომ აეროზოლის გავრცელების პროცესი პირობითად მიმდინარეობს ოთხ ეტაპად და დამოკიდებულია ავტოტრანსპორტის მოძრაობის ინტენსივობაზე, მაგისტრალების მდებარეობაზე და ქალაქის რელიეფზე. განსაზღვრულია შედარებით მაღალი დაბინძურების არეები. მიღებულია, რომ ატმოსფეროს მიწისპირა ფენაში ატმოსფეროს თერმული მდგრადობა თამაშობს მნიშვნელოვან როლს მიკროაეროზოლის კონცენტრაციის დროში ცვლილებისა და მაღალი კონცენტრაციების ფორმირების პროცესში.

საკვანძო სიტყვები: ატმოსფეროს PM10–ით დაბინძურება, რიცხვითი მოდელირება, კონცენტრაცია, ფონური დასავლეთის ძლიერი ქარი.

Исследование загрязнения атмосферного воздуха г. Кутаиси частицами PM10 численным моделированием. Случай сильного фонового западного ветра

А. Сурмава, В. Кухалашвили, Н. Гигаури, Л. Инцкирвели

Резюме

Путем численного моделирования исследованы особенности пространственного распространения и изменения во времени частиц PM10, образованных автотранспортом на территории г. Кутаиси в случае сильного фонового западного ветра в июне. Показано, что значения вычисленных концентраций находятся в пределах наблюдаемых величин. Установлены картины поверхностного распределения концентраций в городе и на прилегающих к нему территориях в разное время дня. Показано, что пространственное распределение концентрации в значительной степени зависит как от интенсивности движения автотранспорта, так и от кинематики приземного слоя атмосферы и локальной циркуляционной системы, сформированной суточным изменением термального режима на подстилающей поверхности.

Ключевые слова: загрязнение атмосферы частицами PM10, численное моделирование, концентрация, сильный фоновый западный ветер.

Journal of the Georgian Geophysical Society, e-ISSN: 2667-9973, p-ISSN: 1512-1127
Physics of Solid Earth, Atmosphere, Ocean and Space Plasma, v. 27(1), 2024, pp. 25 - 32

Hydrochemical Study of Artesian and Spring Waters of Racha-Lechkhumi and Kvemo Svaneti Region in 2022-2024

Lali U. Shavliashvili, Gulchina P. Kuchava, Ekaterina Sh.Shubladze, Mariam Sh. Tabatadze

Institute of Hydrometeorology of the Georgian Technical University, Tbilisi, Georgia

ABSTRACT

Hydrochemical characteristic of artesian and spring (drinking) waters available at the territory adjacent to arsenic processing enterprises of Racha-Lechkhumi and Kvemo Svaneti region in 2022-2024 has been considered in the work. There have been identified artesian and spring waters polluted with different ingredients.
The following conclusions have been made based on the carried-out studies:

- *in some cases, among ingredients polluting artesian and spring waters there has been registered increase of some components (mineral forms of nitrogen, water hardness, sulfates, mineralization, microbiological indicators) compared to respective MPCs; these waters belong to the category of medium-salt (average mineralization) waters, while an acid water of the spring located below Lentekhi is ranked among highly mineralized waters;*
- *total arsenic content in the spring waters flowing towards Tsana in 2022-2024 has surpassed the MPC and arsenic hazard quotient HQ_{Dw} >1, so these waters are at risk;*
- *arsenic concentration in other spring waters is within the norm.*

Key words: *artesian waters, spring waters, hydrochemistry, arsenic, pollution.*

Introduction

Arsenic ore extraction, processing and arsenic-containing compounds production took place for several decades in Tsana and Uravi villages of Racha-Lechkhumi and Kvemo Svaneti region. As of today, both deposits are temporarily closed down and there is no more arsenic production there. But a large amount of toxic waste remained due to arsenic production (more than 130 000 ton of waste containing 4-9% of white arsenic) is still stored at the territory of mining and chemical plant and is not safely disposed there [1; 2]. For years, the basic mechanism of arsenic waste propagation is related to washing-out of toxic waste by atmospheric precipitations and waters of overflowing rivers and their transfer that leads to high risk of ecological catastrophe for artesian waters and soils [3-5].

Arsenic is a natural component of the Earth crust and is spread in any ecosystem. It is represented in the nature by organic and inorganic forms, and the latter is very toxic [6]. Despite the fact that generally arsenic may penetrate the human organism through skin, respiratory passages, it mainly hit the organism from food and drinking water. Organic arsenic varieties are most common in sea products, while in the land products they are basically represented by inorganic forms of 3-5-valent arsenic. Based on this fact, arsenic mainly enters the food chain from polluted soil and water.

Materials and methods

Physical-chemical and hydrochemical characteristic of artesian and spring waters available at the territory adjacent to arsenic processing enterprises of Racha-Lechkhumi and Kvemo Svaneti region in 2022-2024 is given in the work. With the purpose of solution of assigned tasks, sampling points for artesian and

spring waters have been selected from background and contaminated places of the Racha-Lechkhumi and Kvemo Svaneti region.

The following indicators have been identified in the water samples taken: physical-chemical and hydrochemical parameters, in particular: pH, electric conductivity; biogenic substances: NO_2^-, NO_3^-, NH_4^+, PO_4^{3-}, principal ions, mineralization, general total forms of arsenic [7], total Coliforms, E-coli and fecal streptococci [8].

The following formula has been used for calculation of the hazard quotient [9]:

Hazard quotient (HQ) = Measured concentration (MC)/Environment quality standards EQS_{DW}

In case of HQ >1.0, arsenic is considered as a potential hazard for water medium and, respectively, for population health.

The following EQS boundary values have been used:

drinking water: 0.01 mg/l (maximum permissible concentrations according to the Decree no. 58 on Approval of Technical Regulations for Drinking Water protection from Pollution in Georgia) [10].

Analyses have been conducted using the up-to-date methods and equipment, which meet the requirements and comply with European standards, in particular:

1. Spectrophotometric method - SPECORD 205; ISO 7150-1: 2010;
2. Ion-chromatographic method IC-1000; ISO 10304-1:2007
3. Plasma-emission spectrometer - ICP-OES; Epa method 200.8;
4. Field portable apparatus - Hanna Combo pH/EC/TDS/PPM Tester HI98129;
5. IDEXX-Apparatus - ISO 9308-3
6. pH-meter - Milwaukee-Mi 150.

Results and discussion

Results of hydrochemical and microbiological analyses of artesian and spring drinking waters are given in Table 1.

Table 1. Results of hydrochemical and microbiological analyses of artesian and drinking waters
June, October 2022.

#	Ingredients	Spring water in the territory of Uravi 2 (150-200 m away)	Spring water from the mountain in the direction of Tsana	Acidic water (spring) above Lentekhi	MPC *
		X-359777 Y-4722474	X-316809 Y-4741183	X-313288 Y-4741009	
		June			
1	pH	8.0	7.1	6.5	6-9
2	Electrical conductivity, μsms/cm	89	345	1125	
3	BOD_5, mg/l	1.25	2,10	0,95	
4	Hardness, mg.seq./l	0.97	5,53	18,57	7-10
5	Ammonium, mgN/l	0.221	0,098	0,469	0,39
6	Nitrites, mgN/l	0.022	0.075	132.05	1.0
7	Nitrates, mgN/l	0.113	0.029	0.070	10
8	Phosphates, mg/l	0.072	0.196	0.156	3.5

9	Sulfates, mg/l	1.29	53.67	12.51	250
10	Chlorides, mg/l	0.46	0.06	81.99	250
11	Bromine, mg/l	0.170	0.101	0.667	
12	Fluoride, mg/l	0.072	0.041	0.040	0.7
13	Hydrocarbons, mg/l	74.42	189,10	502,64	
14	Potassium, mg/l	0.88	0,95	80,5	
15	Sodium, mg/l				
16	Calcium, mg/l	10.44	84,27	220,15	
17	Magnesium, mg/l	5.52	16,19	10,98	
18	Mineralization, mg/l	93.14	341,28	921,76	1000-1500
19	Arsenic-As, mg/l	0.0097	0.0123	0.0013	0.01
20	E-Coli, in 250 ml	8	10	N.D	not allowed
21	Total coliforms in 250 ml	25	32	N.D	
22	Fecal streptococci, in 300 ml	5	3	N.D	
		October			
1	Arsenic-As, mg/l	0.0016	0.0111	0.0024	0.01

MPC* - maximum permissible concentrations according to Technical Regulations for Drinking Water (Decree №58 of the Georgian government as of 15th January of 2014, Tbilisi) [10]

As is seen from Table 1, pH of artesian and spring drinking waters varies within the limits of 6.5-8.0. pH (medium reaction) equal to 6.5 is peculiar for spring acid water. It should be especially noted an increase of hardness of spring acid water (18.57 mg.eq/l) compared to MPC. Content of hydrocarbonates is 502.64, Ca^{++} – 220.15, $Na^{+} + K^{+}$ – 80.5 and Mg^{++} – 10.98 mg/l.

Biogenic elements (nitrogen, phosphorus), which reflect surface water pollution degree and are indicators of anthropogenic load, are important components. It is especially important to control the content of their separate forms (NH_4^+, NO_2^-, NO_3^-, PO_4^{3-}) in water, which point at the intensification of such processes as fecal contamination induced by discharge of household and agricultural waste waters. Among nitrogen mineral forms there are identified high contents of ammonia (0.469/1.2 MPC) and nitrite forms (132.05/132.1 MPC) that is presumably stipulated by the impact of fecal waste waters, causing pollution of the mentioned spring water. Nitrate and phosphate values don't exceed the respective MPCs. Mineralization of this spring comprises 921.76 mg/l so it is ranked among the waters with moderate mineralization (500-1000 mg/l) [11], while a spring water flowing from mountains towards Tsana, belongs to the category of medium-salt (average mineralization) waters (341.28 mg/l).

In samples taken from the spring waters in June (Table 1), arsenic content at the territory of Uravi 2 (at 150-200 m distance) almost equals to one MPC, while in the spring water flowing from mountains towards Tsana, arsenic concentration is 0.0123 mg/l and its ratio to MPC is 1.2, i.e. arsenic concentration 1.2-times exceeds MPC. It should be mentioned the fact that this water is heavily used for drinking by population. Arsenic content in the spring's acid water above Lentekhi is low and its concentration comprises 0.0013 mg/l. Arsenic concentration higher than MPC in the spring water flowing from mountains towards Tsana was recorded again in October (0.0111 mg/l), and in other cases arsenic concentration is within the norm.

Based on this fact, a hazard quotient (HQ_{dw}) in both months varies in artesian drinking waters from 0.0013 to 0.0123 mg/l and create a hazard, since all measured concentrations were not lower than MPC.
Pollution is resulted not only in change of physical properties of water (color, odour, muddiness), but also chemical composition (organic, biogenic substances, heavy metals etc.) and microflora. River water bacteriological purity is evaluated by means of intestinal bacteria (E-coli) quantity per 1 liter of water (Coli index). High value of Coli index is an indicator of fecal contamination of water (MPC - not allowed), (Table 1), [11].

In Tables 2 and 3 there are given the results of hydrochemical analyses of artesian and spring drinking waters in 2023-2024.

As is seen from Table 2, a srping's acid water above Lentekhi stands out here too, according to its hydrochemical parameters. Water hardness comprises 18.44 that exceeds MPC. Chloride content is high, as well, and surpasses MPC, spring water mineralization is 2612.22 mg/l and this water belongs to the category of highly mineralized waters.

Among mineral forms it should be noted high content of ammonia (0.44 mg/l) and nitrite nitrogen (11.70 mg/l), which equals 1.1 and 58.5 MPC, respectively.

Arsenic content is high in the spring water flowing from mountains towards Tsana, where arsenic content 1.3- and 1.9-times surpasses MPC.

As can be seen from the conducted results, similarly to Table 1, in the month of October (Table 2, Fig. 1), a spring water at the Uravi 2 territory and towards Tsana contains E-coli, total coliforms and fecal streptococci, which are not permitted according to Georgian legislation, while for acid waters pollution in terms of microbiological parameters was not registered.

Table 2. Results of hydrochemical analyses of artesian and spring waters, May, 2023.

#	Ingredients	Spring water above Uravi 1	Spring water in the territory of Uravi 2 (150-200 m away)	Spring water from the mountain in the direction of Tsana	Spring water from the mountain (in the middle)	Spring water from the mountain (in last)	Acidic water (spring) above Lentekhi	MPC *
			X-359777 Y-4722474	X-316809 Y-4741183	X-316833 Y-4741198	X-316930 Y-4741232	X-313288 Y-4741009	
		May						
1	pH	7.9	7.8	8.2	7.9	8.1	7.0	6-9
2	Electrical conductivity, µsms/cm	105	85	350	170	190	2558	
3	BOD_5, mg/l	0.98	1.45	2.25	0.75	1.35	0.78	
4	Hardness, mg.seq./l	1.30	1.03	4.49	1.93	2.07	18.44	7-10
5	Ammonium, mgN/l	0.44	0.053	0.058	0.059	0.054	0.212	0.39
6	Nitrites, mgN/l	0.021	0.095	0.216	0.052	0.126	11.70	0.2
7	Nitrates, mgN/l	1.072	0.320	0.237	1.304	1.202	0.084	50
8	Phosphates, mg/l	0.085	0.142	0.153	0.112	0.241	0.094	3.5
9	Sulfates, mg/l	2.94	2.86	78.89	4.22	12.28	24.40	250
10	Chlorides, mg/l	3.77	2.29	2.27	3.38	3.30	376,84	250
11	Bromine, mg/l	0.120	0.142	0.381	0.210	0.059	0.910	
12	Fluoride, mg/l	0.111	0.016	0.200	0.023	0.060	0.042	0.7
13	Hydrocarbons, mg/l	75.64	59.78	180.56	124.44	136.64	1526.22	
14	Potassium, mg/l	3.08	2.05	4.5	6.0	4.0	333.88	
15	Sodium, mg/l							
16	Calcium, mg/l	13.17	10.61	71.81	26.63	26.51	291.71	
17	Magnesium, mg/l	7.85	6.04	10.99	7.33	9.07	47.26	
18	Mineralization, mg/l	107.62	84.03	349.56	172.18	192.01	2612.22	1000-1500
19	Arsenic-As, mg/l	0.0072	0.0086	0.0133	0.0092	0.0190	0.0022	0.01
		October						
1	Arsenic-As, mg/l		0.0004	0.0025	0.0144	0.0093	0.0149	0.01
2	E-Coli, in 250 ml		5	3	4	11	N.D	not allowed
3	Total coliforms in 250 ml		11	8	10	21	N.D	
4	Fecal streptococci, in 300 ml		N.D	N.D	2	7	N.D	

MPC* - maximum permissible concentrations according to Technical Regulations for Drinking Water. (Decree №58 of the Georgian government as of 15th January of 2014, Tbilisi) [10]

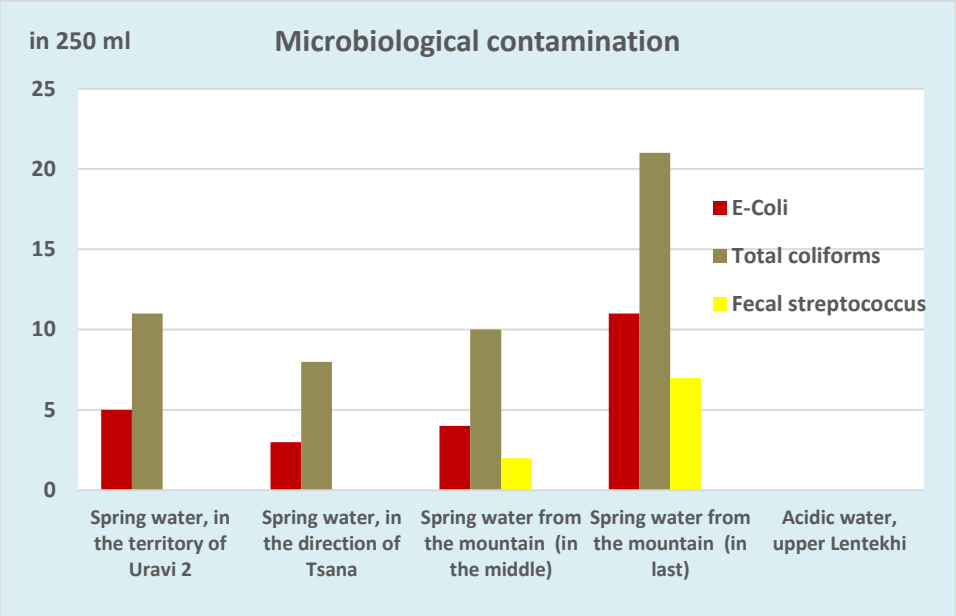

Fig. 1. Microbiological pollution in spring water, October, 2023
(MPC – is not permitted).

Table 3. Results of hydrochemical analysis of artesian and drinking waters, April, 2024.

#	Ingredients	Spring water above Uravi 1	Spring water in the territory of Uravi 2 (150-200 m away)	Spring water from the mountain in the direction of Tsana	Spring water from the mountain (in the middle)	Spring water from the mou-ntain (in last)	Acidic water (spring) above Lentekhi	MPC*
1	pH	7.6	7.8	8.0	8,1	8.3	6.9	6-9
2	Electrical conductivity, µsms/cm	135	98	365	220	310	390	
3	BOD_5, mg/l	1.32	1.52	1.95	1.25	0.95	5.27	
4	Hardness, mg.seq./l	1.53	1.09	2.93	3.15	2.45	3.58	7-10
5	Ammonium, mgN/l	0.226	0.217	0.252	0.236	0.302	0.318	0.39
6	Nitrites, mgN/l	0.170	0.051	0.044	0.111	0.124	0.050	0.2
7	Nitrates, mgN/l	0.624	0.756	2.114	1.326	3.321	0.203	50
8	Phosphates, mg/l	0.171	0.084	0.147	0.139	0.088	0.018	3.5
9	Sulfates, mg/l	4.63	6.46	58.65	8.24	52.34	28.55	250
10	Chlorides, mg/l	2.66	2.97	3.23	2.78	3.09	12.22	250
11	Bromine, mg/l	0.046	0.016	0.036	0.048	0.015	0.092	
12	Fluoride, mg/l	0.237	0.488	0.108	0.131	0.178	0.321	0.7
13	Hydrocarbons, mg/l	96.16	65.88	0.178	0.205	0.269	239.12	
14	Potassium, mg/l	4.5	5.0	5.5	4.0	4.5	36.25	
15	Sodium, mg/l							
16	Calcium, mg/l	17.82	11.24	65.42	52.25	32.86	51.42	
17	Magnesium, mg/l	7.82	6.49	9.133	10.02	8.53	11.89	
18	Mineralization, mg/l	133.23	99.14	345.55	238.60	345.88	380.12	1000-1500
19	Arsenic-As, mg/l	0.0093	0.0023	0.0123	0.0140	0.0152	0.0072	0.01

MPC* - maximum permissible concentrations according to Technical Regulations for Drinking Water (Decree №58 of the Georgian government as of 15th January of 2014, Tbilisi) [10]

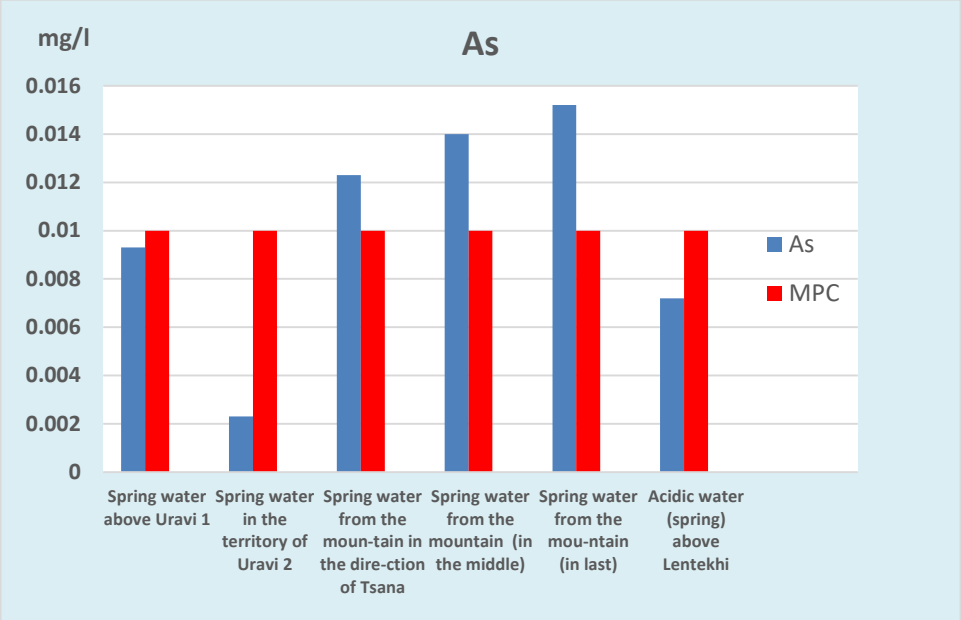

Fig. 2. Arsenic concentration content in artesian and drinking waters, April 2024.

According to hydrochemical parameters, a spring acid water, which is located above Uravi 1, with observed water hardness increase (3.58 mg.eq/l), stands out again (Table 3). Hydrocarbonate content comprises 239.12; Ca^{++} – 51.42, $Na^{+} + K^{+}$ – 36.25 and Mg^{++} – 11.89 mg/l, though none of these parameters surpasses MPC.

Among mineral forms of nitrogen, high contents of ammonia and nitrite forms are not registered, and nitrate and phosphate values don't exceed respective MPCs.

In the spring water flowing from the mountains towards Tsana, arsenic concentration comprises 0.0123-0.0140 and 0.0152 mg/l and its ratio to MPC is equal to 1.2, 1.4 and 1.5, i.e. arsenic concentration 1.2-1.5-times surpasses MPC (Fig. 2). It should be mentioned the fact that waters of all three springs are used for drinking by population. Proceeding from this fact, hazard quotient (HQ_{dw}) of spring water flowing from mountains towards Tsana exceeds permissible standards in April and poses a danger, since all measured concentration were not lower than MPC. In other cases, arsenic concentration is within the norm.

Conclusions

- in some cases, among ingredients polluting artesian and spring waters there has been registered increase of some components (mineral forms of nitrogen, water hardness, sulfates, mineralization, microbiological indicators) compared to respective MPCs, these waters belong to the category of medium-salt (average mineralization) waters, while an acid water of the spring located below Lentekhi belongs to the category of highly mineralized waters;
- in spring water flowing towards Tsana, arsenic concent in 2022-2024 has exceeded MPC and arsenic hazard quotient HQ_{Dw} >1, so these waters are at risk;
- arsenic concentration in other spring waters is within the norm.

Acknowledgments

This work is done with the assistance of the Shota Rustaveli National Science Foundation Grant project №FR-21-427

References

[1] Alexidze G., Lolishvili R. Basic Aspects of Georgia's Environmental Pollution. Materials of International Scientific Conference "Modern Technologies of Eco-friendly Products for Sustainable Development of Agriculture", Tbilisi, 2016, pp. 33-45.

[2] Bagrationi N. Study of the conditions of arsenic industrial waste disposal and ecological assessment of their distribution area, avtoreferat, Tbilisi, 2016.

[3] Avkopashvili G.,Avkopashvili M., Gongadze A., Gakhokidze R. Eco-Monitoring of Georgia's Contaminated Soil and Water with Heavy Metals. Carpathian Journal of Earth and Environmental Sciences - vol. 12, No. 2, 20017, pp. 595-604.

[4] Shavliashvili L., Bakradze E., Arabidze M., Kuchava G. Arsenic pollution study of the rivers and soils in some of the regions of Georgia". International Journal of Current Research Vol.9, Issue, 02, 2017, pp. 47002-47008.

[5] Shavliashvili L., Arabidze M., Bakradze E., Kuchava G., Tabatadze M. Chemical study of arsenic in soils of the municipality of Ambrolauri. Scientific reviewed proceedings of the institute of Hydrometeorology of the Georgian Technical University, Vol. 129, 2020, pp. 84-90.

[6] Arsenic and Arsenic Compounds IARC Monographs – 100C, (IARC, 1980, 1987, 2004).

[7] Фомин Г.С., Фомин А.Г. Вода. Контроль качества и экологической безопасности по международным стандартам. Справочник, Москва, 2001.

[8] Руководство по методам гидробиологического анализа поверхностных вод и донных отложений. Гидрометеоиздат, Ленинград, 1982, 240 с.

[9] Risk Analysis Methodology of the Arsenic Impact on the Water Resources and its Application in Pilot Basin Water Researcher Institute of Slovak Republic, 2019.

[10] Decree of the Government of Georgia N 58 on the approval of technical regulations for protection against drinking water pollution in Georgia, January 15, 2014.

[11] Supatashvili G. Environmental Chemistry (Ecochemistry) - Tbilisi, University Publishing House, 187, 2009.

რაჭა-ლეჩხუმის და ქვემო სვანეთის რეგიონის 2022-2024 წწ. არტეზიული და წყაროს წყლების ჰიდროქიმიური კვლევა

ლ. შავლიაშვილი, გ. კუჭავა, ე. შუბლაძე, მ. ტაბატაძე

რეზიუმე

ნაშრომში განხილულია 2022-2024 წწ რაჭა-ლეჩხუმი და ქვემო სვანეთის რეგიონის დარიშხანის გადამამუშავებელი საწარმოების მიმდებარე ტერიტორიებზე არსებული არტეზიული და წყაროს (სასმელი) წყლების ჰიდროქიმიური დახასიათება.

გამოვლენილია სხვადასხვა ინგრედიენტებით დაბინძურებული არტეზიული და წყაროს წყლები.

ჩატარებული კვლევების საუძველზე მიღებულია შემდეგი დასკვნები:

- არტეზიულ და წყაროს წყლებში დამაბინძურებელი ინგრედიენტებიდან ზოგიერთ შემთხვევაში აღინიშნება კომპონენტების (აზოტის მინერალური ფორმები, წყლის სიხისტე, სულფატები, მინერალიზაცია, მიკრობიოლოგიური მაჩვენებლები) მატება შესაბამის ზდკ-სთან. ისინი მიეკუთვნებიან საშუალო მინერალიზირებული წყლების კატეგორიას, ხოლო მჟავე წყაროს წყალი ლენტეხის ქვევით, მიეკუთვნება მაღალ მინერალიზირებულ წყლების კატეგორიას;

- წყაროს წყლებში ცანას მიმართულებით 2022-2024 წწ დარიშხანის საერთო შემცველობა აღემატება ზდკ-ს და დარიშხანის საშიშროების ინდექსი (HQ_{Dw} >1), ამრიგად, ეს წყლები არის რისკის ქვეშ;
- დანარჩენ წყაროს წყლებში დარიშხანის კონცენტრაცია ნორმის ფარგლებშია.

საკვანძო სიტყვები: არტეზიული წყლები, წყაროს წყლები, ჰიდროქიმია, დარიშხანი, დაბინძურება.

Гидрохимическое исследование артезианских и родниковых вод региона Рача-Лечхуми и Квемо Сванети за 2022-2024 гг.

Л. Шавлиашвили, Г. Кучава, Е. Шубладзе, М. Табатадзе

Резюме

В работе рассмотрена гидрохимическая характеристика артезианских и родниковых (питьевых) вод, имеющихся на территории, прилегающей к предприятиям по переработке мышьяка региона Рача-Лечхуми и Квемо Сванети за 2022-2024 гг. Выявлены артезианские и родниковые воды, загрязненные различными ингредиентами.

На основании проведенных исследований сделаны следующие выводы:

- среди ингредиентов, загрязняющих артезианские и родниковые воды, в некоторых случаях отмечено превышение компонентов (минеральные формы азота, жесткость воды, сульфаты, микробиологические показатели) по сравнению с соответствующими ПДК; данные воды относятся к категории вод средней минерализации, а кислая родниковая вода ниже Лентехи относится к категории высокоминерализованных вод;
- в родниковой воде, текущей в направлении Цана, общее содержание мышьяка в 2022-2024 гг. превышает ПДК, а индекс опасности мышьяка HQ_{Dw} >1, т.е. данные воды находятся под угрозой;
- в остальных родниковых водах концентрация мышьяка находится в пределах нормы.

Ключевые слова: артезианские воды, родниковые воды, гидрохимия, мышьяк, загрязнение.

Journal of the Georgian Geophysical Society, e-ISSN: 2667-9973, p-ISSN: 1512-1127
Physics of Solid Earth, Atmosphere, Ocean and Space Plasma, v. 27(1), 2024, pp. 33 - 35

Some Results of Radioecology Monitoring of Black Earth Soils of Georgia

[1]Sophiko B. Matiashvili, [2]Zaur J. Chanqseliani

[1]M. Nodia Institute of Geophysics of the I. Javakhishvili Tbilisi State University, Tbilisi, Georgia
[2]Soil Fertility Research Service of LEPL Agricultural Scientific Research Center, Tbilisi, Georgia
[1]e-mail:sophiko.matiashvili@tsu.ge

ABSTRACT

Based on radioecological monitoring data, the average content of ^{137}Cs and ^{90}Sr in 2019-2023 in the black earth soils of Georgia was studied. The obtained results are marked with the corresponding coordinates and given on the map. The average content of ^{137}Cs in black earth soils was determined to be 13.9 Bq/kg. The standard deviation is 14.0 Bq/kg. The content of ^{137}Cs in almost 95% of black earth soils does not exceed 32 Bq/kg. The average content of ^{90}Sr in soils is 4.1 Bq/kg. The highest ^{137}Cs contamination is recorded in the Samtskhe–Javakheti region of Georgia (Akhalkalaki, Akhaltsikhe, Vale, Ninotsminda, Adigeni, Aspindza, Akhaldaba). Radionuclides in the mentioned soils, namely ^{226}Ra content is 23 Bq/kg, ^{232}Th is 31 Bq/kg. As for ^{40}K-500 Bq/kg. The role of long-term decay products ^{210}Pb in the contamination of agricultural products is discussed.

Key words: *radioecology, soils, radionuclides.*

Introduction

Black soils are quite widespread in Georgia, both in eastern and western Georgia. Black soils are characterized by a large thickness of humus horizons and a high content of humus. These soils are characterized by high fertility and are intensively used for growing perennial crops and various agricultural crops (Akhalkalaki, Akhaltsikhe, Vale, Ninotsminda, Adigeni, Aspindza, Akhaldaba - Fig.1)

Materials and methods

After the accident at the Chernobyl power plant, soil radiation monitoring and environmental assessment of agricultural fields became important. Based on local monitoring data, we estimated the dose rate of gamma radiation exposure and the contamination levels of ^{137}Cs and ^{90}Sr in agricultural black earth soil types.

Agro-ecological soil monitoring and long-term observation system, determining the condition in space and time, beyond the processes and changes taking place in them, is the most important component of ensuring environmental safety [1]. The dynamics of radionuclide content was monitored at local monitoring reference sites. Constituent analyzes of the research are presented from 10 units. The dynamics of ^{137}Cs, ^{90}Sr, ^{226}Ra, ^{232}Th and ^{40}K in black soil were studied.

Results

Statistical processing of the data was carried out, the obtained results are presented in Table 1. The contamination with ^{137}Cs in black soils in the territory of Georgia does not exceed 31 Bq/kg. The average concentration of ^{90}Sr in the mentioned soils is 4.1 Bq/kg. The level of pollution is 1.2-5.1 Bq/kg. In the range. Studies indicate that the results are concentrated in the set near the mean value. Extreme values are quite rare. The average values of changes over time in the content of ^{137}Cs and 90Sr in black earth soils in

2019-2023 are presented in Fig. 1. The content of ^{137}Cs in the study soils in 2019 was 13.4 Bq/kg, slightly decreased in 2022 - 11.2 Bq/kg. And the content of ^{90}Sr in the same years was - 4.3 Bq/kg, later it decreased - 2.2 Bq/kg [2].

The half-life of the named radionuclide is equal to 30.0 years. The decrease of ^{137}Cs occurs in the spring, during the flood period, this season is characterized by the cleaning of contaminated areas from ^{137}Cs.

Fig.1. Black earth soils of Georgia.

By 2023, the radiation situation in the region will be improved, the radiation pollution levels of specific agricultural fields will decrease.

Transfer of ^{137}Cs from black earth soil to plants is the smallest compared to other types of soil. ^{137}Cs is involved in isotope exchange reactions in soil that occur as a mixture of potassium in soil-forming minerals and fertilizers. The content of ^{90}Sr in black soil in the area contaminated with ^{137}Cs is 2-26 Bq/kg. An important way of action is to reduce the contribution of radionuclides by humans to soils from the point of view of agriculture [3].

This study presents data from the statistical evaluation of all land soils. Analyzes were conducted at the Agricultural Research Center, the results are presented in Tables 1.

The decay products of long-lived elements - ^{226}Ra, ^{228}Ra, ^{210}Pb - have radiological importance and considerably more radiation.

Table 1. Levels of radionuclide contamination in the mentioned regions.

Sampling location	Radionuclide Content Bq/kg			Sampling location	Radionuclide Content Bq/kg		
	^{226}Ra	$^{232}Th(^{228}Ra)$	^{40}K		^{226}Ra	$^{232}Th(^{228}Ra)$	^{40}K
Akhalqalaqi	26.5	29.2	490	Adigeni	14.9	31.7	480
Vale	19.9	22.8	390	Aspindza	24.8	28.0	480
Adigeni	24.2	36.4	510	Akhaltsikhe	16.5	32.6	440

It should be noted here that the introduction of increased doses of mineral fertilizers into the soil creates desorption in the soil, which leads to an increase in radionuclides. In terms of radiation - ^{210}Pb is a very toxic radionuclide [4].

Conclusion

From the point of view of radiation safety, the conditions of provision should preferably be controlled - the content of ^{226}Ra in agricultural black soil.

Thus, the transfer of natural radionuclide isotopes from agricultural soils to plants was determined as ^{226}Ra and ^{228}Ra. High concentrations of these radionuclides in soil can lead to increased levels of contamination in food products.

References

[1] Chankseliani Z., Zardalishvili O. Ecological principles of agrochemistry. (book). Tbilisi, 1992, 107 p.
[2] Standards of content of heavy metals and metalloids in soil. Soil science, No. 3, 2012, pp. 368-375
[3] Matiashvili S., Chankseliani Z., Meparidze E. Comparison of the Distribution of Radionuclides and Heavy Metals in Georgian Soils. Journal of the Georgian Geophysical Society, e-ISSN: 2667-9973, p-ISSN: 1512-1127, Physics of Solid Earth, Atmosphere, Ocean and Space Plasma, v. 25(1), 2022, pp. 29-32.
[4] Vakulovskii, S.M. (ed.). Dannye po radioaktivnomu zagryazneniyu territorii naselennykh punktov Rossiiskoi Federatsii ^{137}Cs, ^{90}Sr, $^{239+240}$Pu [Data on radioactive contamination of the territory of settlements of the Russian Federation ^{137}Cs, ^{90}Sr, $^{239+240}$Pu]. Obninsk, FBU "Typhoon" NPO, 2015, 225 p.

საქართველოს შავმიწა ნიადაგების რადიოეკოლოგიური მონიტორინგის ზოგიერთი შედეგი

ს. მათიაშვილი, ზ. ჩანქსელიანი

რეზიუმე

რადიოეკოლოგიური მონიტორინგის მონაცემებზე დაყრდნობით, შესწავლილია ^{137}Cs და ^{90}Sr-ის საშუალო შემცველობა 2019-2023 წლებში, საქართველოს შავმიწა ნიადაგებში. მიღებული შედეგები დატანილია შესაბამისი კოორდინატებით და მოცემულია რუკაზე. შავმიწა ნიადაგებში ^{137}Cs საშუალო შემცველობა დადგინდა 13.9 ბკ/კგ. სტანდარტული გადახრა არის 14.0 ბკ/კგ. თითქმის 95% შავმიწა ნიადაგებში ^{137}Cs-ის შემცველობა არ აღემატება 32 ბკ/კგ. ^{90}Sr -ის საშუალო შემცველობა ნიადაგებში არის 4.1 ბკ/კგ. ^{137}Cs-ის ყველაზე მაღალი დაბინძურება ფიქსირდება სამცხე-ჯავახეთის რეგიონში (ახალქალაქი, ახალციხე, ვალე, ნინოწმინდა, ადიგენი, ასპინძა, ახალდაბა). აღნიშნულ ნიადაგებში რადიონუკლიდები, კერძოდ ^{226}Ra - შემცველობა არის 23 ბკ/კგ. ^{232}Th - კი 31 ბკ/კგ. რაც შეეხება ^{40}K-500 ბკ/კგ. გრძელვადიანი დაშლის პროდუქტების ^{210}Pb როლი, განხილულია სოფლის მეურნეობის პროდუქტების დაბინძურებაში.

საკვანძო სიტყვები: რადიოეკოლოგია, რადიონუკლიდები, ნიადაგები

Некоторые результаты радиоэкологического мониторинга черноземных почв Грузии

С. Матиашвили З. Чанкселиани

Резюме

По данным радиоэкологического мониторинга в черноземных почвах Грузии в 2019-2023 гг. изучено среднее содержание ^{137}Cs и ^{90}Sr. Полученные результаты отмечены соответствующими координатами и указаны на карте. Установлено, что среднее содержание ^{137}Cs в черноземных почвах равно 13.9 Бк/кг. Стандартное отклонение составляет 14.0 Бк/кг. Содержание ^{137}Cs почти в 95% черноземных почв не превышает 32 Бк/кг. Среднее содержание ^{90}Sr в почвах составляет 4.1 Бк/кг. Наибольшее загрязнение ^{137}Cs зафиксировано регионе Самцхе-Джавахети Грузии (Ахалкалаки, Ахалцихе, Вале, Ниноцминда, Адигени, Аспиндза, Ахалдаба). Содержание радионуклидов в указанных почвах, а именно ^{226}Ra, составляет 23 Бк/кг. ^{232}Th составляет 31 Бк/кг. Что касается ^{40}K -500 Бк/кг. Обсуждается роль продуктов длительного распада ^{210}Pb в загрязнении сельскохозяйственной продукции.

Ключевые слова: радиоэкология, почвы, радионуклиды.

Journal of the Georgian Geophysical Society, e-ISSN: 2667-9973, p-ISSN:1512-1127
Physics of Solid Earth, Atmosphere, Ocean and Space Plasma, v. 27(1), 2024, pp. 36 - 41

On the Potential of Geospatial Artificial Intelligence - GeoAl in Solving Problems of Development of Metal-Bearing Technogenic Deposits

[1]Gigo V. Jandieri, [2]Inga S. Janelidze, [3]Onise B. Zivzivadze, [4]Giorgi G. Loria

[1] Independent Researcher, Leipzig, Germany
[2]Georgian Technical University Tbilisi, Georgia
[3]Akaki Tsereteli State University, Kutaisi, Georgia
[4]Georgian Aviation University, Tbilisi, Georgia
[1]e-mail: gigo.jandieri@gmail.com; [2]e-mail: ingajanelidze9@gmail.com;
[3]e-mail: onise.zivzivadze@gmail.com; [4]e-mail: giorgiloria1979@gmail.com

ABSTRACT

Solid mineral wastes generated as a result of mining and processing of minerals represent a significant environmental problem of the geosphere. Their accumulations in terms of scale and content are deservedly referred to technogenic deposits, the development of which is of great interest both for modern and upcoming digital-industrial revolution called "Industry-4.0". It is noted that the effectiveness of this activity will depend on the efficiency and adequacy of the assessment of the environmental and economic feasibility of extracting the target components, on the quantitative assessment of the volume of accumulation of the extracted element, the possibility of extending its life cycle, on the expected composition of by-products and their consumer value, on the minimum acceptable level of profitability of the selected development technology, as well as - on the rate of re-accumulation and environmental inertness of the waste generated during recycling. In connection with the above, this study emphasizes the importance and necessity of the application of modern hybrid geospatial artificial intelligence (GeoAI), which includes the synergy of general artificial intelligence (AI) based on adaptive neuro-fuzzy inference system (ANFIS) with geographical information systems (GIS). Consequently, in order to increase the efficiency of GeoAI application and to obtain accurate and effective results in solving the set tasks, it is recommended and justified the expediency of combining the knowledge of neural networks and fuzzy logic with GIS data, where the latter will serve as a source-storage of reference (initial/boundary) data on the current and desired for achieving the set goal changes in the developed technogenic deposits.

Key words*: ecology of the geosphere, technosphere, secondary resources, GeoAI, Industry-4.0.*

Introduction

It is known that geospatial artificial intelligence (GeoAI) is a hybrid of artificial intelligence (AI) and geographic information system (GIS) with inherent spatial data and geospatial analysis technologies, the purpose of which is to adequately identify spatial problems accumulating in the technosphere and search for optimal options for their successful solution [1]. GeoAI functionality also includes the use of spatially oriented artificial intelligence methods [2], based on the adaptive neuro-fuzzy inference system (ANFIS) [3], which is designed to solve spatial problems through the analysis of spatial data and includes methods for detecting patterns, making forecasts, spatio-temporal forecasting of upcoming/expected changes, etc.

GeoAI can play a critical role in solving spatial problems across a wide range of application areas. An important aspect of GeoAI is the application of traditional artificial intelligence methods in obtaining spatial data by extracting, classifying and discovering information from/in structured and unstructured data. This data includes tabular data, remote sensing data (including rasters, images, lidar point clouds, video, and others), and even text data. When obtaining spatial data, it is necessary to solve problems such as searching and organizing objects in images, creating 3D data using lidar, or extracting location information from unstructured text for subsequent geocoding [4].

Another key aspect of GeoAI is the application of machine learning and deep learning techniques, including spatial statistical methods and machine learning techniques, to analyze spatial data for applications such as spatial pattern detection and forecasting, including spatiotemporal forecasting. Using new machine learning and deep learning tools with spatial data gives practitioners new opportunities to explore complex problem spaces. Using machine learning techniques on spatial data, as well as incorporating spatially-aware models that incorporate some geographic aspects (location, shape, proximity, etc.) directly into the forecasting algorithm, can not only make the models more efficient, but also more accurate. reflecting the reality that they are trying to model. These methods can be used to allocate, conserve, or exploit mineral natural or secondary resources based on meaningful spatial patterns, to identify trends and anomalies in space and time, and to incorporate spatial relationships into forward-looking planning processes.

Based on the above, it is indisputable that GeoAI can play a vital role in solving optimization problems related to the formation, conservation or development of deposits of technogenic origin that are harmful to the geosphere. Therefore, assessing the state of development, deep learning and effectively exploiting the potential of GeoAI seems to be a very urgent task.

Features of the formation of technogenic deposits and the role of GeoAI in their management

Solid mineral waste, as a rule, is formed due to a discrepancy between the composition of the subsoil and the needs of society. They can be divided into mining waste (overburden) and mineral processing waste (tailings). The amount of mineral waste generated mainly depends on the characteristics of a particular deposit: the conditions of occurrence of the mineral, the method and technology of development, the content of the useful component, enrichment technologies, etc. Waste generated as a result of mining or processing of minerals is stored using special storage facilities. Since these can be quite large formations containing under-extracted mineral components, the term “technogenic deposits” was introduced in many countries of the world, including Georgia [5]. This means that under certain conditions (for example, after a change in the degree of conditionality), it becomes advisable to selectively extract minerals from these accumulations of mineral mass on an industrial scale [6].

As a rule, technogenic deposits are represented by two types of objects: dumps and tailings dumps. The former is formed due to the accompanying extracted rock mass, the latter are waste from pyro - or hydrometallurgical processing of primary mineral raw materials. Accordingly, they differ from each other in mineralogical and granulometric composition. According to the possibilities of use, solid mineral waste can be divided into three groups: waste for which there are no technologies for their processing or the volume of their formation exceeds the needs of the economy for this type of resource; waste for which processing technologies are available, but production capacity is insufficient; waste that is secondary raw materials and included in material balances, but not yet used by enterprises.

The most significant ways to reduce the scale of accumulation of mineral waste include: reclamation of dumps and tailings, use of waste to fill mined-out space, recycling of depleted technogenic raw materials, as well as additional extraction of useful components present in waste [7, 8].

The primary role of GeoAI in the management of marked technogenic mineral accumulations is to identify them, map them, inventory them, assess the degree of their growth/decrease and the actual impact on the environment, in order to prevent possible environmental disasters. This is especially true for tailings ponds of ore processing plants, where large quantities of sludge with a high-water content accumulate, the safe retention of which requires the construction of especially expensive reinforced dams. For Georgia, such objects that are in dire need of servicing GeoAI systems are the Gurgumel tailings dump of the Chiatura manganese mining and processing plant [9] and the tailings of the Kazretsky complex RMG-Cooper, which mines gold and copper [10].

Features of the environmental and economic impact of technogenic deposits and the possibility of their mitigation using GeoAI

The negative impact of these storage facilities on the environment occurs mainly in the following areas: pollution of the atmosphere surrounding the facility, surface and underground water bodies, and soil. Substances released by these objects may have toxic or radioactive properties. In addition, in some places the height of mineral mass storages can reach 100 meters or more, which contributes to changes in the wind regime and, accordingly, the climatic conditions of the area. A significant mass of stored substance puts pressure on the surface of the earth and can lead to changes in the hydrogeological regime. Accumulated dumps and tailings ponds occupy large areas, thereby removing potentially useful lands from circulation. For enterprises, these environmental problems result in increased tax payments for negative impacts on the environment [11].

The peculiarities of the influence of the process of accumulation and exploitation of technogenic deposits on mining and metallurgical production is that enterprises are forced to bear certain costs, while receiving additional products and economic results. In particular, the costs of utilization or recycling of technogenic deposits are formed by costs associated directly with the extraction, transportation, processing of mineral mass and the sale of the resulting finished product. At the same time, positive economic results should include income from the sale of additional products, a reduction in environmental damage, a reduction in the costs of disposal and maintenance of mineral waste and reclamation costs, a reduction in payments for the disposal of solid waste into the environment and for the withdrawal of land suitable for agricultural land [12]. Along with the positive environmental effect, there is also a negative one associated with technological processing processes. It occurs during mining, enrichment processing, transportation of rocks, enrichment tailings or metallurgical slag. During the development of the noted technogenic deposits, the area of withdrawn land may temporarily increase, and the number of emissions into the atmosphere and aquatic environment may increase [13]. It is here, to control and prevent random (unforeseen) environmental violations, that the first need arises for the use of GeoAI, which includes the synergy of general artificial intelligence (AI), adaptive neuro-fuzzy inference system (ANFIS) and geographic information systems (GIS) with human intelligence [14], authorized to make decisions.

Based on the above analysis, it follows that the development processes of the mentioned fields require dynamic optimization in real operating time, both from the point of view of increasing technical and economic and environmental efficiency. Solving optimization problems with dynamically changing input parameters is not possible without the use of the modern hybrid intelligent system GeoAI. Here GeoAI can certainly play a key role, both in monitoring and managing the processes of accumulation and targeted consumption (recycling) of technogenic raw materials. In this case, data obtained from GeoAI can serve as a generator of confirmed reference information for solving problems of mitigating the overall environmental load, including minimizing land taken out of production and reducing the impact on adjacent above-ground and underground water bodies. Based on the noted data, decisions made on the general feasibility of developing a specific technogenic deposit, on the quantity and degree of extraction of the components contained in it and their beneficial use, should be based on a summary environmental and economic assessment that takes into account all of the above factors.

In this case, the criterion for environmental and economic assessment of the degree of development of technogenic deposits used in GeoAI must satisfy the following basic conditions: take into account all the main costs associated with the utilization of technogenic raw materials and the technical results obtained; do not contradict various environmental indicators of production; not violate the maximum permissible standards for the emission (discharge) of associated mineral or chemical formations and fully reflect the benefit of these decisions for the interested party, i.e. the owner of the technogenic deposit. The last condition is justified by the fact that the process of using technogenic deposits is most often internal to a typical mining and metallurgical enterprise and is carried out at its own expense. Therefore, the assessment does not require comparison of its efficiency with competitive production processes at other enterprises and should be made according to internal indicators. This methodology is carefully described and algorithmized in the study [8], where, using the example of manganese-containing industrial waste, a solution to the problem of their highly efficient, economically break-even internal recycling is proposed.

The criterial framework developed in this way will make it possible to create on its basis new

mathematical models suitable for training GeoAI. The created economic and mathematical models must include a target function, by value, which selects the optimal technical and economic solution and a number of boundary (ecological) conditions necessary for the objectivity of decision-making and reducing the duration of the estimated time.

Such boundary conditions include: the total amount of technogenic mass in dumps and tailing dumps planned for targeted use; annual amount of utilised technogenic mass; the amount of contained components extracted during the disposal of solid mineral waste (degree of conditionality), the degree of extraction of each component, the potential for replacing mined ore (Ore Substitution Index), the long-term scale of extending the life cycle of existing mines and quarries, etc. As a current indicator of the degree of useful use, it is recommended to take the coefficient of use of mineral mass, which is the ratio of the amount of mineral mass extracted from a technogenic deposit to the volume of products obtained as a result of metallurgical restoration of this mass. It should also be noted that when determining the number of extracted components, one should be guided not only by their value, but also by the scale (volume) of their recycling, which is very important for mitigating the anthropogenic load on the environment.

Conclusion

Carried out using geospatial artificial intelligence -GeoAI, the collection of geospatial information and dynamic observation data of technogenic deposits and adjacent lands, combined with environmental, socio-economic and other statistical data, will provide authorized decision-making bodies with a unique digital contribution to preparation and monitoring and assessing the effectiveness of the chosen policy for the re-development and use of accumulated secondary metal-containing resources. The scale of the formed digital portfolio, along with digital developments and industry innovations of the fourth industrial revolution "Industry 4.0" will play a decisive role in the global management of technogenic accumulations, allowing humanity to take timely, more accurate and environmentally softened, biosphere-friendly steps in the development of the technosphere.

References

[1] Choi Y. GeoAI: Integration of Artificial Intelligence, Machine Learning, and Deep Learning with GIS. Applied Sciences, 13(6), 2023, 3895. https://doi.org/10.3390/app13063895

[2] Nishant R., Kennedy M., Corbett J. Artificial intelligence for sustainability: Challenges, opportunities, and a research agenda. International Journal of Information Management, 53, 2020, 102104. https://doi.org/10.1016/j.ijinfomgt.2020.102104

[3] Cabalar A.F., Cevik A., Gokceoglu C. Some applications of Adaptive Neuro-Fuzzy Inference System (ANFIS) in geotechnical engineering. Computers and Geotechnics, Volume 40, 2012, pp. 14-33, https://doi.org/10.1016/j.compgeo.2011.09.008

[4] GeoAI - Geospatial workflows driven by artificial intelligence. Electronic resource, accessed at: https://www.esri.com/ru-ru/capabilities/geoai/overview (in Russian)

[5] Law of Georgia on Subsoil. Parliamentary Gazette, 16, 17/05/1996. Consolidated publications 22/04/2024. Accessed - https://matsne.gov.ge/en/document/view/33040?publication=17

[6] Jandieri G. Increasing the efficiency of secondary resources in the mining and metallurgical industry. Journal of the Southern African Institute of Mining and Metallurgy, 123(1), 2023, 1-8. http://dx.doi.org/10.17159/2411-9717/1092/2023

[7] Potravny I., Novoselov A., Novoselova I., Gassiy V., Nyamdorj D. The Development of Technogenic Deposits as a Factor of Overcoming Resource Limitations and Ensuring Sustainability (Case of Erdenet Mining Corporation SOE in Mongolia). Sustainability, 15(22), 2023, 15807. https://doi.org/10.3390/su152215807

[8] Jandieri G. A generalized model for assessing and intensifying the recycling of metal-bearing industrial

waste: A new approach to the resource policy of manganese industry in Georgia. Resources Policy, 75, 2022. https://doi.org/10.1016/j.resourpol.2021.102462
[9] Georgian Manganese – Company profile. 2017. Electronic resource, accessed at: https://greenalt.org/app/uploads/2021/04/GM_Company_Profile_2017.pdf
[10] Avkopashvili M., Avkopashvili G., Avkopashvili I., Asanidze L., Matchavariani L., Gongadze A., Gakhokidze R. Mining-Related Metal Pollution and Ecological Risk Factors in South-Eastern Georgia. Sustainability, 14(9), 2022, 5621. https://doi.org/10.3390/su14095621
[11] Georgian Manganese – Company Profile March, 2021. Electronic resource, accessed at: https://greenalt.org/app/uploads/2021/05/GM_Eng_2021.pdf
[12] Umnov V.A. Ecological and economic assessment of technogenic deposits management. Bulletin of the Russian State University for the Humanities. Series Economics. Management. Law, (2), 2017, 21-29, (In Russian).
[13] Jandieri G., Janelidze I. On Climate Change Mitigation Measures in Ferrous and Non-Ferrous Metallurgy (General Analysis). International Scientific Conference „Natural Disasters in the 21st Century: Monitoring, Prevention, Mitigation“. Proceedings, ISBN 978-9941-491-52-8, Tbilisi, Georgia, December 20-22, 2021. Publish House of Iv. Javakhishvili Tbilisi State University, Tbilisi, 2021, 42-45, URL: http://openlibrary.ge/bitstream/123456789/9574/1/12_Conf_ND_2021.pdf
[14] Jandieri G., Janelidze I., Sakhvadze D. Theoretical prerequisites fot the formation of a paradigm of synergy between human and artificial intelligence in solving the problems of circular transformation of metallurgical enterprises. Sciences of Europe, 114, 2023, 96–101. https://doi.org/10.5281/zenodo.7811570

გეოსივრცული ხელოვნური ინტელექტის (GeoAI) პოტენციალის შესახებ ლითონშემცველი ტექნოლოგიური საბადოების დამუშავების პრობლემების გადაჭრისათვის

გ. ჯანდიერი, ი. ჯანელიძე, ო. ზივზივაძე, გ. ლორია

რეზიუმე

სასარგებლო წიაღის მოპოვებისა და გადამუშავების შედეგად წარმოქმნილი მყარი მინერალური ნარჩენები მნიშვნელოვან ეკოლოგიურ საფრთხეს უქმნიან გეოსფეროს. აღნიშნული ანთროპოგენული წარმონაქმნები, თავისი მასშტაბებისა და შემცველობის მიხედვით, დამსახურებულად კლასიფიცირდება როგორც ტექნოგენური საბადოები, რომელთა სასარგებლო გადამუშავებაც, როგორც თანამედროვეობის, ასევე - ინტენსიური ფორმირების სტადიაში მყოფი «Industry 4.0» სახელით ცნობილი მეოთხე ინდუსტრიული რევოლუციისშემდგომი პერიოდისათვისაც ერთ-ერთი პრიორიტეტული ამოცანა იქნება. სტატიაში გამოკვეთილია აღნიშნული ანთროპოგენული აქტივობის ეფექტურობის ამაღლების შესაძლებლობა ფასეული კომპონენტების მეორადი მოპოვების ეკოლოგიური და ეკონომიკური მიზანშეწონილობის კომპლექსური შეფასების გზით. მათ შორის ხაზგასმულია ისეთი კრიტერიუმების გათვალისწინების აუცილებლობა, როგორებიცაა მიზნობრივი ელემენტების აკუმულირებისა და მათი სასიცოცხლო პერიოდის შესაძლო გაფართოების მასშტაბები, გადამუშავებისას წარმოქმნილი თანმდევი (არამიზნობრივი) პროდუქტების ქიმიურ-მინერალური შემადგენლობა და მათი სამომხმარებლო ფასეულობა, გადამუშავებისათვის შერჩეული ტექნოლოგიის რენტაბელობის მინიმალური დასაშვები ზღვარი, და ბოლოს, - გადამუშავებისას ემისირებული ნარჩენების ეკოლოგიური უვნებლობის ხარისხი. შესრულებული ანალიზის საფუძველზე, დასახული მიზნის მისაღწევად შემოთავაზებულია

ისეთი ჰიბრიდული გეოსივრცითი ხელოვნური ინტელექტის (GeoAI) შექმნა და გამოყენება, რომელიც დაფუძნებული იქნება ადაპტირებულ ნეირო-არამკაფიო სისტემის (ANFIS) ფუნქციონირების პრინციპით შექმნილი ხელოვნური ინტელექტის (AI) და გეოგრაფიულ ინფორმაციულ სისტემების (GIS) სინერგიაზე, სადაც ეს უკანასკნელი შეასრულებს მიზნობრივ ტექნოგენურ საბადოში, მისი დამუშავებისას მიმდინარე ფაქტობრივი და დაგეგმილი ცვლილებების შესახებ ანალიტიკურ მონაცემებთა ბაზის ფორმირებისა და ხელოვნური ინტელექტის ნეიროქსელებში მოთხოვნისამებრ მიწოდების ფუნქციას.

საკვანძო სიტყვები: გეოსფეროს ეკოლოგია, ტექნოსფერო, მეორადი რესურსები, GeoAI, ინდუსტრია-4.0.

О потенциале геопространственного искусственного интеллекта - GeoAl для решения задач разработки металлсодержащих техногенных месторождений

Г. Джандиери, И. Джанелидзе, О. Зивзивадзе , Г. Лория

Резюме

Твердые минеральные отходы, образующиеся в результате добычи и переработки полезных ископаемых, представляют собой существенную экологическую проблему геосферы. Их скопления по масштабам и содержанию заслуженно относят к техногенным месторождениям, разработка которых представляет собою большой интерес, как для современной, так и — предстоящей цифрово-промышленной революции, называемой «Индустрией-4,0». Отмечено, что эффективность данной деятельности будет зависеть от оперативности и адекватности оценки эколого-экономической целесообразности извлечения целевых компонентов, от количественной оценки объема накопления извлекаемого элемента, возможности расширения его жизненного цикла, от ожидаемого состава получаемых побочных продуктов и их потребительской ценности, от минимально допустимого уровня рентабельности выбранной технологии разработки, а также — от темпов повторного накапливания и экологической инертности образующийся при повторной переработке отвальных отходов. В связи с отмеченным, в данной исследовании, подчеркнута важность и необходимость применения современного гибридного геопространственного искусственного интеллекта (GeoAI), включающее в себя синергию общего искусственного интеллекта (ИИ), основанной на адаптивной системе нейронечеткого вывода (ANFIS) с географическими информационными системами (GIS). Следовательно, для повышения эффективности применения GeoAI и получения точных и эффективных результатов в решении поставленных задач, рекомендовано и обосновано целесообразность объединения знаний нейронных сетей и нечеткой логики с данными GIS, где последний будет служить в качестве источника-хранилища опорных (исходных/граничных) данных о текущих и желаемых для достижения поставленной цели изменениях в разрабатываемом техногенном месторождений.

Ключевые слова: экология геосферы, техносфера, вторичные ресурсы, GeoAI, Индустрия-4,0.

Journal of the Georgian Geophysical Society, e-ISSN: 2667-9973, p-ISSN: 1512-1127
Physics of Solid Earth, Atmosphere, Ocean and Space Plasma, v. 27(1), 2024, pp. 42 - 51

Impact of Current Climate Change on Frost Characteristic Parameters in Western Georgia using 2007-2022 Year Meteorological Data

Naili I. Kapanadze, Marika R. Tatishvili, Irina P. Mkurnalidze, Ana M. Palavandishvili

Institute of Hydrometeorology of Technical University of Georgia, Tbilisi, Georgia
knaili1990@gmail.com; n.kapanadze@gtu.ge

ABSTRACT

According to the weather stations 2007-2022 data in Western Georgia, the distribution of the intensity of frosts of different intensity has been studied. The early, average and late dates of the last spring and the first autumn frost in the research period have been determined. In 2007-2022 period in comparison with the 1951-1965 one, a shift in the average values of freezing has been revealed for the last spring frosts for about 1-14 days earlier, and for the first autumn frosts 7-10 days later, which increased the duration of frost-free periods and, accordingly, the duration of the vegetation period by 11- 21 days, which corresponds to 10-17%. An exception is Akhaltsikhe, where the reduction of frost-free periods by 15 (9%) days has been detected against the background of climate change. The dependence of frost-free periods on the Arctic Oscillation has been found.

Key words: *freezing, frost-free period, freezing intensity, arctic oscillation.*

Introduction

The modern world is facing many challenges. Among them, the most important and large-scale climate change poses a great threat to the country's sustainable development. The consequences of climate change are already visible, which is evidenced by the increase in temperature, change in precipitation regime, limitation of water availability, rise in the level of the Black Sea, increase in the frequency and intensity of floods, landslides and mudslides.

Almost half of the population of our country is involved in the agricultural sector, which makes the country highly sensitive to changes in weather and climatic conditions. The negative impact of climate change on agriculture is reflected in the direct connection with the increase in the level of poverty and socio-economic development, which implies an increase in the income of the population to the level that should actually ensure the population's access to sufficient, safe and quality food. Freezing is one of the problems of getting abundant and quality food from unfavorable hydro-meteorological events.

It is true that, considering the types of threats, the conditions of occurrence, the type of events and the main consequences, such a dangerous event as frost for agriculture was not included in the international classified standard list of dangers, but considering the damage caused by it to Georgia and other countries of the world, it is worth thinking about its negative consequences and taking certain actions [1,2].

In Georgia, the researches about glaciations have a long history and have been studied in great detail by our great scientists: T. Davitaia, Sh. Tsertsvadze, M. Zakashvili, E. Elizbarashvili, J. Vachnadze, R. Samukashvili, G. Meladze, M. Meladze and others. However, in the results of the research based on the materials of the 70s of the last century, the influence of the current climate change on the characteristic parameters of freezing was clearly not reflected. Therefore, we considered it appropriate, similar to the studies conducted for the territory of Eastern Georgia [3], to find out whether the characteristic parameters of freezing have changed in the territory of Western Georgia and, if so, what are the quantitative indicators of this change.

The North Atlantic Oscillation (NAO)

The North Atlantic Oscillation (NAO) is a prominent "seesaw" of atmospheric surface pressure fluctuation between the Azores and Iceland that has been meteorologically well defined since at least the late 19th century (e.g., Hurrell, Kushnir, Ottersen, & Visbeck, 2003). It is defined using the NAO index, which is typically a normalized mean sea-level pressure (SLP) index between a southern station located in the Azores or continental Iberia and a northern station in western Iceland (Cropper, Hanna, Valente & Jónsson, 2015; Hurrell, 1995; Jones, Jónsson, & Wheeler, 1997; van Loon & Rogers, 1978). The NAO has historically been recognized since at least the time of the Vikings; pioneering work based on early instrumental meteorological records was undertaken by Hildebrandsson (1897), who using surface air pressure data discovered the inverse relation between Iceland and Azores pressure, and by Sir Gilbert Walker who in works published in 1924 and 1932 (the latter with Bliss) undertook correlation analysis and constructed a robust multivariate NAO index based on surface air pressure and surface air temperature data from several European stations (Stephenson, Wanner, Brönnimann, & Luterbacher, 2003) [4].

The strength of the pressure difference between the high- and low-SLP centers of action exerts a strong control over the strength and direction of the mid-latitude westerly storm tracks. As such, the NAO has been linked to a variety of climatological, biological, hydrological, and ecological variables across several locations (Ottersen et al., 2001; Westgarth-Smith, Roy, Scholze, Tucker, & Sumpter, 2012) but is most frequently recognized as directly affecting the west of Europe (from Iberia to Scandinavia) and North America. A greater than normal pressure difference between the Azores and Iceland is a positive NAO, and a weaker than normal pressure difference is a negative NAO. During the winter months, a positive NAO is associated with warmer and wetter conditions across northwest Europe and cooler and drier conditions across southern Europe as the stronger pressure gradient between the Azores and Iceland drives the storm tracks poleward (Fig. 1). The opposite is generally true for negative NAO conditions as the weaker pressure gradient generally results in southward-shifted storm tracks, and a SLP reversal will typically result in more easterly conditions. As such, the NAO index is strongly related to favored positions of the North Atlantic atmospheric polar jet stream (Hall, Erdélyi, Hanna, Jones & Scaife, 2015; Overland et al., 2015; Woollings et al., 2015) [4].

The NAO and AO are preferred modes of variability of atmospheric circulation in the Northern Hemisphere. The alternative designation Northern Annular Mode (NAM, which is the same as the AO) is not as widely used as its southern counterpart the Southern Annular Mode (Abram et al., 2014). The NAO can be regarded as an Atlantic sector regional expression of the hemisphere-wide AO (or NAM). The NAO reflects changes in the position and strength of the North Atlantic polar front jet stream and has associated effects on the weather and climate of mid-to-high latitudes within and around the Atlantic (Fig. 1). A more positive (negative) NAO/AO index represents stronger (weaker) airflow around the Northern Hemisphere and a jet stream that is shifted further north (south) over the North Atlantic.

The NAO/NAM pattern is a result of the eddy-driven extratropical atmospheric circulation: specifically, the transport of heat and momentum by stationary eddies (longwaves or planetary waves in the northern polar jet stream) and transient eddies (cyclones and anticyclones forming within or along the jet stream) (e.g., Kaspi & Schneider, 2013). The polar jet stream is directly related to NAO changes and has a mean latitude somewhere between 50°N and 60°N over the eastern North Atlantic. The strongest westerly winds (of up to about 200 km/hr in the core of the jet near the tropopause) are typically experienced at these latitudes, and there is a clear clustering of extratropical storm tracks along the polar jet stream. The prevailing direction is westerly due to the Coriolis Effect of earth's rotation, which deflects air masses to the right of their direction of motion in the Northern Hemisphere. Longwaves develop in the jet stream because of orographic obstacles (e.g., the Rocky Mountains over North America) or east–west heating contrasts between land and sea, or variations in latent heating due to condensation and rainfall. Low- and high-pressure systems form due to strong horizontal contrasts in temperature, typically where cold polar air meets relatively warm tropical air masses. These transient eddies are very important in providing energy for maintaining the polar jet stream flow and mid-latitude westerlies, otherwise friction with the surface would slow and eventually halt the winds. However, a significant contribution to maintaining the westerlies—greater than in the Southern Hemisphere—comes from the stationary eddies: this is due to the much stronger land–ocean contrast effects in northern mid-latitudes [4].

Being linked with the jet stream, there is a deep and pronounced vertical structure to the AO and NAO, which extends up into the stratosphere; this is most notable for the AO, which lies further north and is more directly linked with the polar vortex. What happens in the stratosphere in polar winter can also have a big

bearing on conditions in the troposphere: for example, stratospheric sudden warmings are associated with a weakening and sometimes reversal of the polar vortex and development of negative NAO/ AO that sometimes occurs in mid- to late winter (e.g., Cohen et al., 2014; Marshall & Scaife, 2010). Stratosphere–troposphere interaction and coupling is not very well understood, yet is important for NAO dynamics (Kidston et al., 2015). It appears from theory and observations that planetary-scale Rossby waves can propagate upwards from the troposphere into the stratosphere under conditions of moderate westerly flow during boreal winter; the stratosphere is effectively decoupled from the troposphere in other seasons. If the wintertime polar vortex is weak (strong), the upward-propagating waves can (cannot readily) interact with and slow the upper-level westerly flow. There is also a kind of reverse effect where airflow anomalies in the stratosphere can propagate down to affect the near-surface circulation (Baldwin & Dunkerton, 2001). The time of operation of these changes is typically 2–3 weeks, although dynamical couplings range over timescales from daily to multidecadal (Kidston et al., 2015) [4].

The NAO/AO exist in atmosphere-only computer models of the global climate system, so the NAO does not depend on the ocean for its existence. However, it is thought that low-frequency variations of oceanic circulation in the Atlantic—which comprise the Atlantic Multidecadal Oscillation (AMO)—are driven at least partly by the NAO (Clement et al., 2015). The AMO may in turn drive the NAO in a distinctly seasonal response, with a warm AMO phase promoting a negative NAO in winter (Gastineau & Frankignoul, 2015) [4].

The AO and NAO tend to be strongest in winter because this is when one of the key factors driving the jet stream—the equator-pole temperature gradient—is greatest, due to less seasonal cooling in the tropics than the polar regions. The jet stream and NAO correspondingly tend to weaken in summer. The summertime NAO is shifted northwards, having its southern node over northwest Europe and a smaller accompanying pressure pattern. A detailed discussion of NAO patterns and changes during this season is provided by Folland et al. (2009), who develop a summer NAO index that they compare with changes in European summertime climate. These authors also note a small but significant link of interannual variation in SNAO with La Niña sea-surface temperatures in the eastern tropical Pacific, as well as a persistent link with the AMO.

Due to the seasonal migration of the jet stream, which generally lies further south (north) in winter (summer), the association between NAO and, for example, British weather conditions varies markedly depending on the season. Thus, in winter, a positive (negative) NAO is generally associated with mild, wet (cold, dry) weather over the United Kingdom but a positive (negative) NAO in summer is often linked with dry and sunny (wet and cool) conditions. Key examples are the exceptionally cold 2009/2010 U.K. winter, with a record low (Hurrell PC) NAO value of -2.93 and the exceptionally wet 2007 and 2012 U.K. summers with low NAO values of -1.15 and -1.59. However, the NAO-U.K. weather relation in summer is less clear than in winter: for example, summer 2015 had a similarly low NAO value of -1.61 but had only slightly above average rainfall, e.g., 113% of the 1981–2010 summer average for U.K. precipitation (http://www.metoffice.gov.uk/climate/ uk/summaries/2015/summer). While the NAO is the single most important factor determining changes in weather and climate over the North Atlantic region, it does not explain everything, and most notably the East Atlantic and Scandinavian atmospheric circulation patterns—with respective main centers to the west of Ireland and around Bergen, Norway—also need to be considered (Moore, Renfrew, & Pickart, 2013) [4].

The North Atlantic Oscillation is usually described as a movement of atmospheric mass between the Arctic and the subtropical Atlantic (Wanner et al. 2001). There is no unique way to define the NAO. However, there are two pressure areas often used when describing the phenomenon, the Icelandic low- and the Azores high-pressure systems. The variations in sea level pressure between these two areas generate a pressure gradient. Because of this pressure gradient, westerly winds over the North Atlantic are generated (Wanner et al. 2001). The westerly winds, also known as “jets”, reach their maximum speed of 40 m/s at about 12 km up in the troposphere (Hurrell et al. 2003). When measuring the NAO different statistical methods can be used, either station-based or pattern based (Wanner et al. 2001). A station-based index is measured as the normalized sea level pressure differences between two monitoring stations in the vicinity of the Icelandic low and Azores high. Alternatively, a spatial-based index, or a principal component-based index, can be calculated from performing principle component analysis on the mean sea level pressure anomalies over the North Atlantic sector (usually beween 20-80ºN and 90ºW-40ºE) (Wanner et al. 2001) The NAO is described as being in an either positive or negative phase (see Figure 1). These phases are describing the strength of the circulation pattern. In a positive (NAO+) state the Icelandic low and the Azores high are well developed, resulting in a greater pressure gradient between these two areas. A greater pressure gradient causes stronger and more northern westerly winds. In a negative (NAO-) phase the pressure anomalies at the nodes of the NAO are less developed than normal and as a result the westerly winds get weaker and are positioned further south.

However, it is important to point out, is that there is not only a confined positive and negative phase of the NAO, but also everything in between (Wanner 2001). The NAO affects the climate mainly during wintertime when the NAO accounts for more than one-third of the total sea level pressure variance over the North Atlantic Ocean (Hurrell et al. 2003). During summertime the spatial extent of the NAO and the sea level pressure variance are smaller than during winter. Atmospheric variations are lager during wintertime which makes the effect of the NAO on surface climate bigger than during summertime. Because of this, most research on the NAO is restricted to wintertime, however the NAO is still noticeable all year around (Hurrell et al. 2003). There have been periods when the NAO persisted in an either positive or negative phase. During the beginning of the last century until approximately 1930 the NAO winters were characterized by a positive phase. During the 1960s the NAO winters instead showed persistent negative NAO anomalies (Hurrell et al. 2003). Although decadal NAO trends is shown, it is observed that variations in the NAO can occur on very different timescales, making it hard to assess any preferred timescale of the NAO variability.

The different wind patterns as a result of the various phases of the NAO are accompanied by different patterns of temperature and precipitation over the North Atlantic area. It has been shown that there are statistically significant correlations between sea level pressure anomalies and air temperature anomalies over a wide region in the northern hemisphere (Van Loon & Rogers 1978). Normally during strong positive NAO phases, warm maritime air is moved over the North Atlantic Ocean because of the enhanced westerly winds (Hurrell et al. 2003). This makes winter temperatures higher than normal in eastern United States and over northern Europe. Simultaneously in Greenland and the Mediterranean area temperatures are normally below average. During strong negative NAO phases the temperature pattern is opposite (Wanner et al. 2001). This reversing temperature pattern is often referred to as the Greenland seesaw (Van Loon & Rogers 1978). The positive and negative NAO phases are also connected to different patterns of precipitation as a result of variations in the strength and paths of storms generated over the Atlantic. During a positive NAO the North Atlantic storm track is usually directed more north-eastward over northern Europe than during negative NAO winters (Hurrell et al. 2003). This makes positive NAO phases associated to precipitation anomalies above normal in northern Europe and Scandinavia, while the precipitation levels over southern and central Europe are below average. The opposite precipitation pattern is notable during negative NAO phases (Wanner et al. 2001). It is seen that the ocean and the atmosphere interact, which makes variations in the ocean affect the NAO (Visbeck et al. 2013). The NAO is also known to force responses in different layers of the ocean (Visbeck et al. 2013). It is shown that NAO variations cause responses in the ocean on multiple time scales. Fluctuations in the NAO seems to be synchronized with interdecadal changes in convection triggering the renewal of intermediate and deep water in the Labrador Sea. On a decadal time, scale this has been shown to affect the thermohaline circulation and thereby also of sea surface temperatures.

The NAO has been linked with a variety of meteorological and non-meteorological effects across a wide spatial and multiple temporal scales, and only a selection of these impacts can be mentioned here. For example, Nesje, Lie, and Dahl (2000) showed a strong relationship between the mass balance of Scandinavian glaciers and the NAO due to the controlling influence of the storm tracks by the NAO, which influenced precipitation amounts, and glacier mass balance as a result. Coincidentally, the NAO has been shown to explain a large amount of the variance in Norwegian streamflow (55%) and hydropower output (30%), influencing electricity consumption and prices (Cherry et al., 2005). Baltic sea-ice extent is also strongly related to NAO changes (Karpechko, Peterson, Scaife, Vainiko, & Gregow, 2015). Cropper, Hanna, and Bigg (2014) found an influence of the NAO as far south as 20°N in coastal upwelling-inducing winds along the northwest African coastline. The great-circle distance between northwest Africa and Scandinavia is ~5,700 km, indicating the great spatial extent of the NAO influence. Recent NAO–climate linkages literature includes a strong signal of the (non-summer) NAO on precipitation in Iraq (Khidher & Pilesjö, 2015), an influence on sea-ice breakup date in south-central Ontario (Fu & Yao, 2015) and even a Southern Hemisphere influence, via a decadal-scale mechanism, on subtropical eastern Australian rainfall.

The NAO has also been shown to directly influence energy-generating capabilities. Colantuono, Wang, Hanna, and Erdélyi (2014) identify a negative relationship between the NAO and solar radiation availability across the United Kingdom, also showing a clear and intriguing zonal contrast between west and east regions, which they attribute to a topographic rain-shadow effect (more clouds and rain in the west of the United Kingdom under a positive NAO can sometimes be linked with cloud breakup and clear, sunnier weather in eastern England). Jerez et al. (2013) identify that for southern Europe, negative NAO conditions enhance hydropower resources and wind power by up to 30% while diminishing solar potential by 10–20% (the contrasting influence on solar availability in these studies is a function of the spatial locations analyzed, e.g., Fig. 1 shows they are regions which correlate differently with the NAO). Curtis, Lynch, and Zubiate (2016)

show that the NAO-induced variability in the Irish electrical grid could cause detectable signals in the total carbon dioxide emissions from the system. Ely, Brayshaw, Methven, Cox, and Pearce (2013) call for improved understanding of the potential effects of the NAO on European power generation, as they surmise that under negative NAO conditions, lower temperatures, and less wind power generation across the United Kingdom/Scandinavia lead to an increased demand and lowered supply. On this note, while negative NAO conditions may be less favorable for the U.K.-Scandinavian renewable energy system, for regions like Iberia, the European Alps, or the Middle East, negative NAO conditions may be more favorable (Beniston, 2012; Sowers, Vengosh, & Weinthal, 2011; Trigo et al., 2004). The energy industry is already very weather-dependent due not only to demand fluctuations with temperature and hence the NAO but also because Germany and other countries rely so heavily on wind power. Therefore, NAO predictability will be an even more valuable asset in the medium- to long-term future, when renewable energy sources are expected to contribute much more significantly toward total power generation.

It is still unclear what will happen to the NAO with ongoing anthropogenic climate change, even discounting other external forcing factors and natural (internal) variability. The tropopause is highest at the equator (about 15 km above the surface) and slopes down toward the poles (about 10 km altitude). With increasing greenhouse gas levels, temperatures warm at the surface and in the lower troposphere while the stratosphere cools. This effect has been well observed in recent decades and is due to a denser blanket of greenhouse gases trapping infrared radiation in the lower atmosphere. At the same time, the surface has been warming most rapidly at high latitudes: called polar (or here Arctic) amplification of global warming (Overland et al., 2014). This latter change has the effect of reducing the meridional (north–south) temperature gradient, which might be expected to reduce the amount of energy available for driving the polar jet stream, all other factors being equal (Francis & Vavrus 2015; Overland et al., 2015). But this is just a (near-)surface expression of global warming. Meanwhile, in the upper troposphere at low latitudes, there is a higher specific humidity under global warming, and this raises the tropopause and increases upper troposphere temperatures near the equator (about 15 km up) while the same altitude near the poles (i.e., well within the stratosphere at these high latitudes) significantly cools with global warming. Therefore, there is a significantly enhanced meridional temperature gradient at this higher altitude just at the same time that the north–south temperature gradient reduces near the surface (Harvey, Shaffrey, & Woollings, 2015) [4]. Thus, there are two competing influences that can result in changes in mid-latitude (i.e., polar) jet-stream dynamics under conditions of global warming. One recent model-based study (Harvey et al., 2015) suggests that the near-surface meridional temperature gradient change is most important for determining changes in the wintertime North Atlantic storm track, but overall this is far from certain and more work is undoubtedly needed.

Data and method

In order to solve the task, we obtained data from the National Environment Agency for meteorological stations in Western Georgia (Mta- Sabueti, Sachkhere, Zestafoni, Kutaisi, Zugdidi, Poti, Kobuleti, Khulo, Keda, Ambrolauri, Shovi) for 2007-2022. Based on the data, we studied the intensity of late spring and early autumn frosts, estimated the impact of climate change on the dates of the last spring and first autumn frosts and the average, minimum and maximum values of frost-free periods as a temperature characteristic of climate change in 2007-2022. and 1951-1965 By comparing the corresponding data of the periods [3,5,6]. We also wanted to assess the extent to which the global climate determines the climate of our study region, using the so-called Arctic Oscillation (AO) index graph. Comparison of the positive and negative deviations of the template [5] with the course of the graph depicting the frost-free periods of Western Georgia.

Discussion

The Table 1 shows the change in frost intensity of the meteorological stations in the territory of Western Georgia in 2007-2022. According to the data. As can be seen from the table, 345 frosty days were recorded during the study period, of which 59% (205 days) were frosts of weak intensity, 36% (125 days) were moderate. Frosts of moderate and severe intensity will be observed only in 3% (10 days) and 1% (4 days) cases respectively.

Table 1. Distribution of the intensity of the first autumn frosts and the last spring frosts in Western Georgia in the period 2007-2022.

Station	Intensity							
	Weak 0.1-(-1.0)		Moderate -1.1-(-3.0) °C		Average -3.1- (-4.0) °C		Strong -4.1- (-8.0) °C	
	I frost Day %	Last frost day	I frost Day %	Last frost day	I frost Day %	Last frost day	I frost Day %	Last frost day
Mta-Sabueti	9	6	5	9			1 (33)	1
Sachkhere	9	9	7	6		1		
Zestaphoni	9	13	5	3	2			
Kutaisi	13	11	1	3				
Zugdidi	7	9	9	6		1		
Poti	11	12	5	3				
Qobuleti	6	9	9	5		1		
Khulo	9	14	4	11	1	1	1	
Qeda	7	6	5	7	1			
Ambrolauri	10	8	5	7		1	1	
Shovi	11	8	5	5		1		
Total	101 (29)	105 (30)	60 (17)	65(19)	4 (1)	6 (2)	3 (1)	1(0)

Table 1 shows that at the meteorological stations of Western Georgia, as well as at most stations of Eastern Georgia, the majority of freezing days - 206 days - are of weak intensity, of which 101 cases belong to the first frosts of autumn, and 105 to the last frosts of spring. The first autumn and last spring frosts of moderate intensity vary almost equally according to the meteorological stations and amount to 60 (17%) and 65 (19%) days, respectively. The number of frosts of medium intensity is relatively small and is equal to 4 (1%) days for the first frosts of autumn, and 6 (2%) days for the last frosts of spring. As for frosts of strong intensity, only 4 cases were noted during the observation period at the research meteorological stations of the entire Western Georgia. One case of severe frost was recorded in autumn and spring in Mta-Sabueti, Khulo and Ambrolauri. Very strong frosts (<-8°C) did not occur at all at the meteorological station in Western Georgia during the period 2007-2022.

Table 2 shows the early, average and late values of the dates of the last spring and the first autumn frosts in the territory of Western Georgia.

Table 2. Dates of the last spring and first autumn frosts in the territory of Western Georgia in the period 2007-2022.

Station	H elevation, m	Dates of the last spring frosts					Dates of the first autumn frosts				
		Early	Year	Ave.	Late	Year	Early	Year	Ave.	Late	Year
Mta-Sabueti	1242	6/X	2013	2/XI	24/XI	2012	3/IV	2012	21/IV	11/V	2021
Sachkhere	415	22/X	2014	16/XI	21/XII	2010	19/II	2009	29/III	26/IV	2017
Zestaphoni	160	15/XI	2011	21/XII	26/I	2009	29/I	2016	10/III	17/IV	2007
Kutaisi	114	26/XI	2016	8/I	26/I	2022	11/I	2015	25/II	28/III	2012
Zugdidi	117	15/XI	2011	14/XII	21/I	2020	1/II	2017	9/III	13/IV	2009
Poti	3	26/XI	2016	1/I	26/I	2022	10/I	2015	19/II	18/III	2022
Qobuleti	7	15/XI	2011	16/XII	22/I	2020	19/II	2020	14/III	28/III	2012
Khulo	92	I/IX	2020	5/XI	11/XII	2008	18/III	2008	17/IV	11/V	2021
Qeda	256	20/X	2011	1/XII	1/I	2022	4/XII	2013	5/III	23/IV	2019
Ambrolauri	544	20/X	2014	13/XI	22/XII	2022	11/III	2015	31/III	26/IV	2017
Shovi	1507	26/IX	2016	21/X	17/XI	2012	1/IV	2013	25/IV	15/V	2021

The comparison of the average values of frosts with the corresponding values of multi-year data (1891-1960) showed us that in the period 2007-2022, similar to the studies conducted in East Georgia [6], the average

frosts of spring moved earlier, and the average of the last autumn frosts - later (nine 3). This shift for spring frosts was particularly high for Kutaisi, Kobuleti and Keda (16-16 days), Zestafoni (25 days) is distinguished by the maximum shift for the last autumn freezes, followed by Poti (17 days), Shovi (16 days), Sachkhere and Zugdidi (15 -15 days) etc. Khulo is the only station where, compared to previous years, the onset of frost was 3 days later in spring, and it stopped 1 day earlier in autumn.

Table 3. Comparison results of the average dates of frost occurrence for the periods 1891-1960 (I) and 2007-2022 (II).

Station	Period					
	I	II	II-I	I	II	II-I
Mta-Sabueti	25/IV	21/IV	-4	25/X	2/XI	8
Sachkhere	8/IV	29/III	-10	I/XI	16/XI	15
Zestaphoni	20/III	10/III	-10	26/XI	21/XII	25
Kutaisi	12/III	25/II	-16	26/XII	8/I	13
Zugdidi	23/III	9/III	-14	29/XI	14/XII	15
Poti	3/III	19/II	-12	14/XII	1/I	17
Qobuleti	30/III	14/III	-16	2/XII	16/XII	14
Khulo	14/IV	17/IV	3	6/XI	5/XI	-1
Qeda	21/III	5/III	-16	4/XII	1/XII	-3
Ambrolauri	7/IV	31/III	-6	12/XI	13/XI	1
Shovi	6/V	25/IV	-10	5/X	21/X	16

The shift of the average values of freezing increased the duration of frost-free periods at all weather stations of Western Georgia, exception is Khulo, where the reduction of the frost-free period by 3 days was noted (Table 4).

Table 4. Comparison of average, minimum and maximum values of frost-free periods between the first (1951-1965) and second (2007-2022) periods.

Station	Duration of frost-free days by periods (%)			Least values of frost-free periods %			Highest values of frost-free periods %		
	I	II	II-I	I	II	II-I	I	II	II-I
Mta-Sabueti	182	195	13	149	163	14	152	234	82
Sachkhere	206	232	26	187	190	3	233	282	49
Zestaphoni	250	286	36	192	221	29	322	342	20
Kutaisi	268	317	49	222	271	49	330	343	13
Zugdidi	250	277	27	196	223	27	317	337	20
Poti	280	317	37	224	272	48	347	370	23
Qobuleti	246	275	29	202	244	42	290	337	47
Khulo	205	202	-3	160	131	-29	238	267	29
Qeda	257	268	11	167	179	12	322	364	42
Ambrolauri	218	226	8	180	190	10	247	267	20
Shovi	151	177	26	112	137	25	180	224	44

A comparison of the average, minimum and maximum values of the frost-free periods of 1951-1965 and 2007-2022 showed us that in the last period, compared to the previous one, the average duration of the frost-free period increased by 49 days in Kutaisi, by 37 days in Poti, and by 36 days in Zestafon. A significant increase was also noted in Zugdidi (27 days), Shov and Sachkhere (26-26 days). A similar result was observed for extreme values of the duration of the frost-free period. The minimum values of frost-free periods range from 3-49 days, and the maximum values - from 13 to 82 days. An exception is Khulo, where there is a decrease in the average and minimum values of frost-free periods, and an increase in the maximum value.

The change of the average values of frost-free periods for visibility between the mentioned periods of time is presented in Figure 1, from which it is clear that in the second period, compared to the previous one, the duration of the frost-free periods has significantly increased.

It is known from the literature that frost occurs mainly in cloudless calm weather and is especially noticeable during the invasion of arctic air masses from dry latitudes [8]. Along with this, the Arctic Oscillation (AO) is an important indicator of the Arctic climate, which with its positive and negative phases determines the state of the atmospheric circulation in the Arctic. In order to determine the influence of AO on the climate of Georgia, we compared the graph showing the frost-free periods calculated for the meteorological stations of Western Georgia with the graph of the arctic oscillation indices as a template (Fig. 1 and Fig. 2).

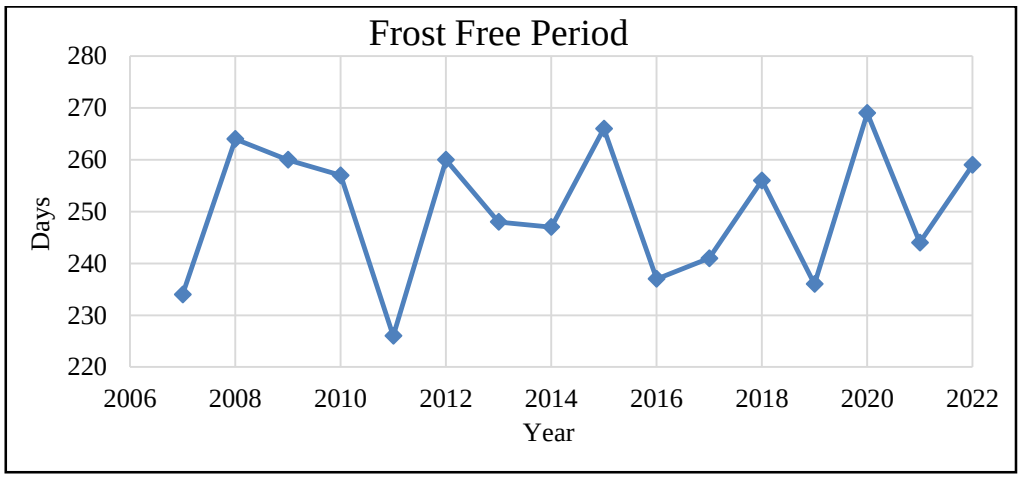

Fig. 1. Change of the average values of durations of frost-free periods in the territory of Western Georgia (2007-2022).

Comparison of Fig. 1 and 2 shows that the duration of frost-free periods in Western Georgia follows the positive and negative phases of the Arctic Oscillation almost proportionally. In particular, a relatively long frost-free period corresponds to each positive phase of the AO indices, and when moving to a negative phase, a decrease in the frost-free period is also recorded in the second diagram. If there was a small shift of positive and negative phases in eastern Georgia until 2012, the exception is 2010 in Samtskhe-Javakheti, where in the case of a negative phase of the AO, a relatively long frost-free period was observed in Samtskhe-Javakheti [8], in western Georgia there are arctic oscillations and frost-free periods. representing the harmonious flow of graphs. After all that, we can confirm that the global climate really determines the climate of Georgia.

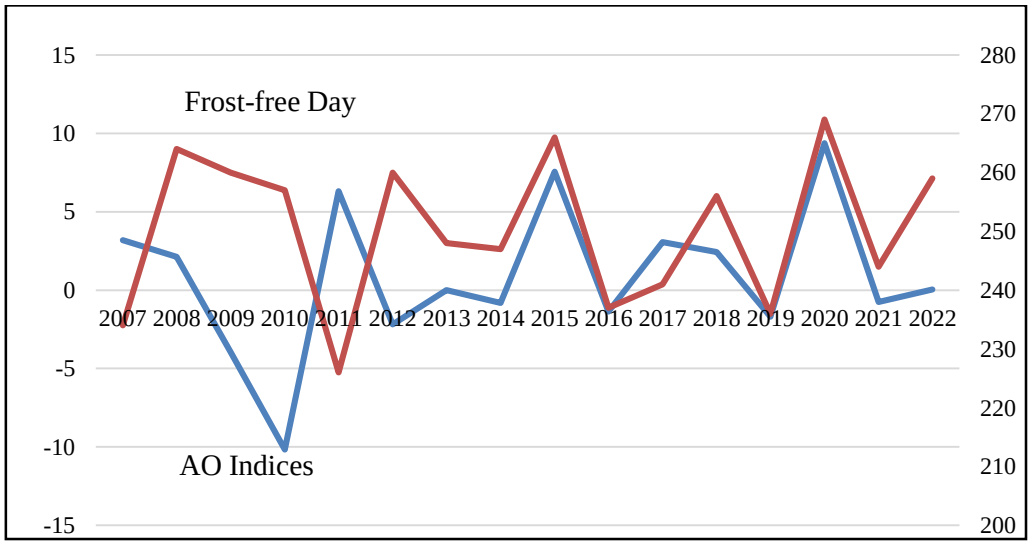

Fig. 2. Distribution of average values of arctic oscillation indices and durations of frost-free periods in the territory of Western Georgia in the period 2007-2022.

Conclusion

The NAO is the primary variation in barometric pressure variation over the North Atlantic that affects the weather and climate of much of Europe. It is subject to internal variability or chaos in the climate system but is also influenced by slowly varying climatic forcing factors including anthropogenic greenhouse warming and solar and volcanic variability, which makes the NAO inherently predictable—at least in part—on a timescale of up to at least several months. Between the 1960s and 1990s the NAO was becoming more positive, but since then this trend has tended to reverse. Recently updated observational records and reanalyses show increasing variability of winter NAO and AO, which is a feature not just of the 2000s and early 2010s but has been ongoing during the 20th century. We have also noted during the last 20–30 years a statistically significant decline in the NAO in summer—and to a lesser extent winter (with a recent record negative December value, although the winter negative trend appears strongest during the period 1989–2011 but has returned to more positive/neutral values in the last 5–6 years)— whereas no significant change has occurred in spring and autumn. This asymmetric seasonal response of the NAO, and its increased winter variability, was not foreseen in previous general circulation climate model predictions analyzed here but may have resulted from several climatic forcing factors and feedbacks conspiring together: these include enhanced blocking arising from cryosphere–atmosphere couplings, solar variability, and/or changes in North Atlantic sea temperatures. The increasingly more variable winter NAO that we have detected based on the last century or so of observations appears to be a seasonally uneven change and does not show up as a forced response—i.e., responding to an external climatic driving factor—in state-of-the-art (CMIP5) climate models. Although the winter increase in NAO variance was sustained over the 20th century and there may be errors in climate models, we still cannot discount the possibility that this feature is due to internal variability (random noise and chaos generation in the climate system), particularly as there was no prior reason to expect this change to occur in winter as opposed to some other season. It is currently uncertain how the NAO will change during the rest of the current century, as both the climate models and our understanding of the physical processes causing NAO variations need to be improved. Whatever the reason(s) behind the observed seasonal NAO changes, there are also clearly important consequences for the heavily populated circum–North Atlantic land masses if these changes continue.

Based on the analysis of the results of our research, it can be concluded that the current climate change has a certain influence on the characteristic parameters of freezing. This influence is manifested by the shift of the average values of the dates of occurrence of frosts and the increase of frost-free periods, or what is the same, the length of the vegetation period by 8-49 days, which is based on the high and quality harvest of agricultural crops in the subtropical zone of Western Georgia, the success of agriculture and socio-economic conditions. It guarantees development

References

[1] Kapanadze N., Tatishvili M., Mkurnalidze I., Palavandishvili A. Classification of hazardous events according to international standards. International Scientific Conference "Geophysical Processes in the Earth and its Envelopes". Tbilisi, Georgia, November 16-17, 2023.pp. 175-180. ISBN 978-9941-36-147-0

[2] Mkurnalidze I., Kapanadze N. Methods for protecting vineyards and orchards from early frosts. Scientific Reviewed Proceedings of the Institute of Hydrometeorology of the GTU, V.133, 2023, pp 124-128, ISSN 1512 – 0902, doi.org/10.36073/ 1512 – 0902.

[3] Handbook on the climate of the USSR, vol. 14, part I. Air temperature. Gidrometeoizdat, Leningrad, 1971.

[4] Hanna E., Cropper T.E. North Atlantic Oscillation. Oxford Research Encyclopedia of Climate Science. 2017. DOI: 10.1093/acrefore/9780190228620.013.22

[5] Handbook on the climate of the USSR, vol. 14, part II. Air and soil temperature Gidrometeoizdat, Leningrad, 1967.

[6] https://www.cpc.ncep.noaa.gov/products/precip/CWlink/daily_ao_index/ao.shtml

[7] Kapanadze N., Tatishvili M., Mkurnalidze I., Palavandishvili A. Anomalies of frost characteristic parameters in the territory of Eastern Georgia in the background of current climate change**.** International Scientific Conference "Geophysical Processes in the Earth and its Envelopes ", Tbilisi, Georgia, November 16-17, 2023, pp.175-180

[8] Chogovadze I.V. Study of the statistical structure of frosts and frosts on the territory of the Georgian SSR. Report on NIP, NTBZakNIGMI, Tbilisi, 1975.

კლიმატის მიმდინარე ცვლილების გავლენა წყინვის მახასიათებელ პარამეტრებზე დასავლეთ საქართველოში მეტეოროლოგიური სადგურების მიხედვით

ნ. კაპანაძე, მ. ტატიშვილი, ი. მკურნალიძე, ა. ფალავანდიშვილი

რეზიუმე

დასავლეთ საქართველოში არსებული მეტეოსადგურების 2007-2022 წწ. მონაცემების მიხედვით შესწავლილია სხვავასხვა სიმძლავრის წყინვების ინტენსივობის განაწილება. დადგენილია საკვლევ პერიოდში გაზაფხულის ბოლო და შემოდგომის პირველი წყინვის დადგომის თარიღების ნაადრევი, საშუალო და ნაგვიანები მნიშვნელობები. გამოვლენილია 2007-2022 წწ პერიოდში 1951-1965 წწ პერიოდთან შედარებით წყინვის საშუალო მნიშვნელობების წანაცვლება გაზაფხულის ბოლო წყინვებისთვის 1-14 დღით უფრო წინ, ხოლო შემოდგომის პირველი წყინვებისთვის 7-10 დღით უფრო გვიან, რამაც გაზარდა უყინვო პერიოდებისა და, შესაბამისად, სავეგეტაციო პერიოდის ხანგრძლივობები 11-21 დღით, რაც 10-17 %-ს შეესაბამება. გამონაკლისს წარმოადგენს ახალციხე, სადაც გამოვლენილია კლიმატის ცვლილების ფონზე უყინვო პერიოდების შემცირება 15 (9%) დღით. აღმოჩენილია უყინვო პერიოდების არქტიკულ ოსცილაციაზე დამოკიდებულება.

საკვანძო სიტყვები: წყინვა, უყინვო პერიოდი, წყინვის ინტენსივობა, არქტიკული ოსცილაცია.

Влияние современных изменений климата на характеристики заморозков в Западной Грузии по метеорологическим данным за 2007-2022 гг.

Н. Капанадзе, М. Татишвили, И. Мкурналидзе, А. Палавандишвили

Резюме

По данным метеостанций 2007-2022 гг. в Западной Грузии изучено распределение интенсивности заморозков разной интенсивности. Определены ранние, средние и поздние сроки последних весенних и первых осенних заморозков за период исследований. В период 2007-2022 гг. по сравнению с 1951-1965 гг. выявлено смещение средних значений замерзания последних весенних заморозков примерно на 1-14 дней раньше, а первых осенних заморозков на 7-10 дней позже, что увеличило продолжительность безморозного периода и, соответственно, продолжительность вегетационного периода на 11-21 день, что соответствует 10-17%. Исключением является Ахалцихе, где на фоне изменения климата зафиксировано сокращение безморозных периодов на 15 (9%) дней. Обнаружена зависимость безморозных периодов от арктического колебания.

Ключевые слова: заморозки, безморозный период, интенсивность замерзания, арктическое колебание.

Journal of the Georgian Geophysical Society, e-ISSN: 2667-9973, p-ISSN: 1512-1127
Physics of Solid Earth, Atmosphere, Ocean and Space Plasma, v. 27(1), 2024, pp. 52 - 57

About the Representativeness of Data from Meteorological Stations in Georgia for Monthly Sum of Atmospheric Precipitation Around of These Stations

[1]Avtandil G. Amiranashvili, [1]Tamaz L. Chelidze,
[1]David T. Svanadze, [2]Tamar N. Tsamalashvili, [1]Nodar D. Varamashvili

[1]M. Nodia Institute of Geophysics of I. Javakhishvili Tbilisi State University, Tbilisi, Georgia
avtandilamiranashvili@gmail.com
[2]A. Janelidze Geological Institute of I. Javakhishvili Tbilisi State University, Tbilisi, Georgia

ABSTRACT

Results of study of the representativeness of data from 39 meteorological stations in Georgia for monthly sum of atmospheric precipitation around of these stations are presented. Period of observation – from 1936 to 2015. In particular, it was found that the representativeness of these stations in terms of monthly precipitation varies from 14 km (Akhalkalaki, January) to 90 km (Akhaltsikhe, October).

Key words: *atmospheric precipitations, correlation and regression analysis, natural catastrophe, landslides.*

Introduction

As is known, precipitation is one of the most important components of climate [1-3], bioclimate [3,4], and the state of ecosystems [5]. Atmospheric precipitation often has an extremely negative impact on the human environment. Their deficiency leads to droughts, while their excess can provoke floods, flooding, mudflows, landslides and other dangerous natural phenomena [5-10]. In particular, the time scale of the impact of atmospheric precipitation on provoking various natural disasters (including landslides) has a wide range - from several tens of minutes to several days, months and years (climatic time scale) [8-18]. Since the number of weather stations is usually limited, to study the impact of precipitation on the environment it is necessary to have data on the representativeness of these stations depending on their distance from them.

In [19] results of study of the representativeness of data from 39 meteorological stations in Georgia for annual and semi-annual sum of atmospheric precipitation around of these stations are presented. It was found that in general for the year data of meteorological stations on precipitations are representative around these stations on distance from 19 km (Mta-Sabueti, Kobuleti) to 46 km (Gori); in cold period of year - from 13 km (Mta-Sabueti) to 49 km (Zugdidi); in warm period of year - from 20 km (Chokhatauri) to 43 km (Pasanauri).

This work is a continuation of the study [19]. Results of study of the representativeness of data from 39 meteorological stations in Georgia for monthly sum of atmospheric precipitation around of these stations are presented below.

Study area, material and methods

Study area – territory of Georgia.

The data of Georgian National Environmental Agency about monthly sum of atmospheric precipitations for 39 meteorological stations are used. Period of observation: 1936-2015 (80 years). The locations of meteorological stations and their names are shown below (in Fig. 1, 2-4 and Table 1).

In the proposed work the analysis of data is carried out with the use of the standard statistical analysis methods.

The following designations will be used below: R^2 – coefficient of determination; R – coefficient of linear correlation; α - the level of significance; a – coefficient of regression equation; L – distance around meteorological station, km.

The degree of correlation was determined in accordance with [20]: very high correlation ($0.9 \leq R \leq 1.0$); high correlation ($0.7 \leq R < 0.9$); moderate correlation ($0.5 \leq R < 0.7$); low correlation ($0.3 \leq R < 0.5$); negligible correlation ($0 \leq R < 0.3$).

As in [19] determination of the representativeness of data meteorological stations for sum of atmospheric precipitation around of these stations was carried out in two stages.

1. The linear correlation coefficient R of each meteorological station with all other stations on the monthly sum of atmospheric precipitation was calculated.
2. The dependence of this correlation coefficient on distance L between meteorological station from all other stations was determined. This dependence for each station has the form: $L = (1-R)/a \cdot R$, $\alpha(R^2)<0.01$. A representative value of L was considered when R values were not less than 0.7 (high correlation).

Results and discussion

Results in Fig. 1-4 and Table 1 are presented.

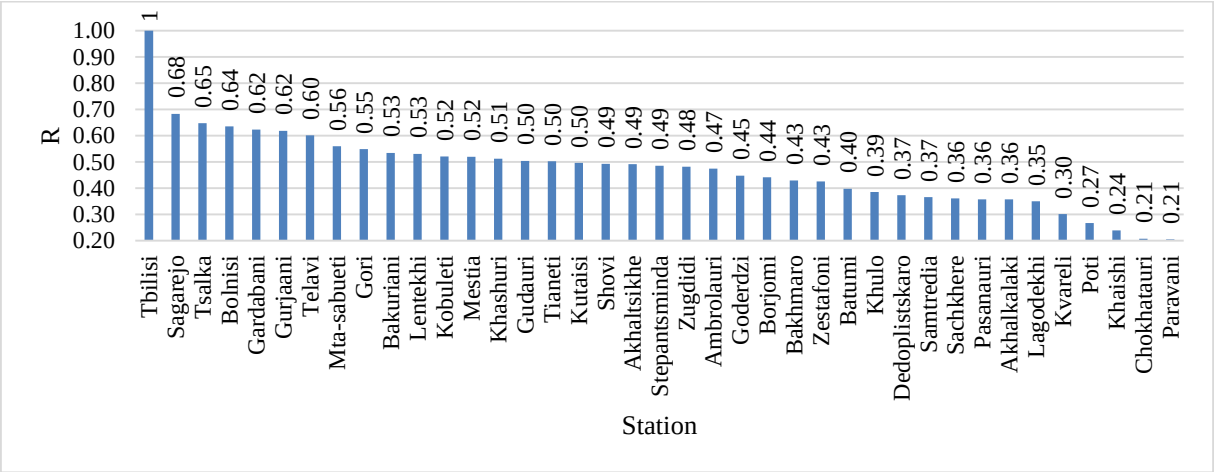

Fig.1. Example of linear correlation between monthly sum of atmospheric precipitations in Tbilisi with monthly sum of atmospheric precipitations on each meteorological stations in Georgia in July.

In Fig.1 the example of linear correlation between monthly sum of atmospheric precipitations in Tbilisi with monthly sum of atmospheric precipitations on each meteorological stations in Georgia in July is presented. As follows from this Fig. 1 coefficient of correlation for this case changes from 0.21 (Parvani, negligible correlation) to 0.68 (Sagarejo, moderate correlation).

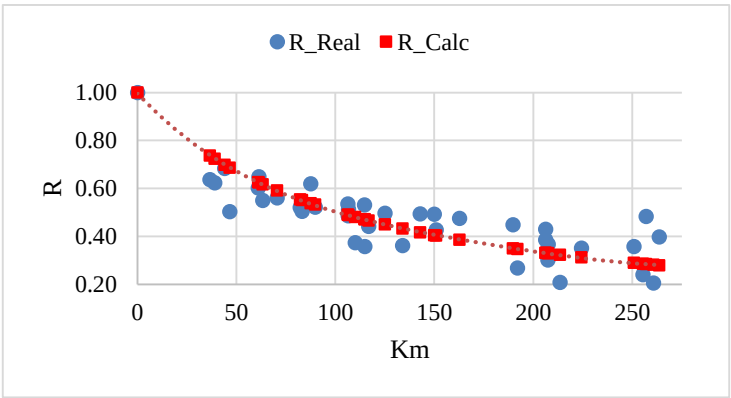

Fig. 2. Dependency example of coefficient of linear correlation between monthly sum of atmospheric precipitations in Tbilisi and monthly sum of atmospheric precipitations on each of meteorological stations with distance for these stations in July.

In Fig. 2 the dependency example of coefficient of linear correlation between monthly sum of atmospheric precipitations in Tbilisi and monthly sum of atmospheric precipitations on each of meteorological stations with distance for these stations in July is presented. The distance L can be determined from the regression curve and in this case it is equal to 44 km.

Table 1. The radius of the circle L, within which the data of meteorological stations on the monthly precipitation amounts are applicable with a high level of representativeness. $L = (1-R)/a \cdot R$, $\alpha(R^2)<0.01$.

Stations	Jan	Feb	Mar	Apr	May	Jun	Jul	Aug	Sep	Oct	Nov	Dec
Akhalkalaki	14	35	28	48	27	17	19	26	39	79	69	27
Akhaltsikhe	40	49	37	50	31	17	33	31	44	90	59	55
Ambrolauri	42	34	36	64	33	29	35	43	36	70	73	52
Bakhmaro	33	32	29	41	33	27	38	21	35	53	55	34
Bakuriani	44	47	37	57	37	22	32	26	43	82	67	44
Batumi	61	58	47	52	46	25	51	23	52	68	89	41
Bolnisi	19	26	22	51	36	27	30	38	54	64	43	26
Borjomi	38	44	36	51	27	21	33	31	53	77	60	41
Chokhatauri	34	53	32	49	32	17	21	28	33	71	63	37
Dedoplistskaro	17	41	30	38	43	19	26	46	42	80	63	58
Gardabani	19	22	21	38	31	21	36	38	43	79	50	35
Goderdzi	38	36	23	43	31	19	36	23	39	55	68	40
Gori	49	51	52	44	34	27	32	31	42	69	61	60
Gudauri	39	44	29	39	28	26	34	42	50	87	57	53
Gurjaani	34	46	28	36	23	28	30	42	58	70	54	49
Khaishi	47	34	43	35	26	27	31	46	44	68	73	60
Khashuri	31	34	41	54	29	26	31	40	40	66	49	41
Khulo	44	35	29	55	38	21	31	26	38	53	64	43
Kobuleti	40	58	60	65	42	18	40	18	53	82	72	30
Kutaisi	49	42	41	52	31	20	24	29	32	67	46	57
Kvareli	31	52	38	57	26	28	28	33	53	84	56	60
Lagodekhi	30	55	33	42	37	23	36	33	39	81	53	44
Lentekhi	40	36	41	40	33	26	28	38	26	72	47	43
Mestia	41	35	53	37	23	19	28	61	34	83	73	44
Mta-sabueti	19	27	20	50	40	24	34	37	42	54	44	27
Paravani	42	52	31	47	28	25	31	34	43	74	60	34
Pasanauri	42	58	41	51	36	31	33	51	58	87	60	52
Poti	41	71	50	72	33	20	23	40	57	48	74	39
Sachkhere	44	40	47	62	30	25	25	39	40	77	71	54
Sagarejo	30	28	20	40	34	29	33	47	39	80	38	30
Samtredia	46	59	42	58	33	22	34	27	28	85	62	57
Shovi	44	42	38	42	29	26	41	47	38	79	54	47
Stepantsminda	30	50	25	34	25	23	38	44	22	59	50	33
Tbilisi	23	28	21	59	27	20	44	28	45	67	47	29
Telavi	33	39	32	57	38	27	33	42	56	72	67	52
Tianeti	49	50	41	47	21	26	21	44	39	76	55	58
Tsalka	23	28	16	33	29	24	37	38	34	62	47	26
Zestafoni	33	36	38	51	33	20	24	25	34	52	42	41
Zugdidi	58	48	53	70	33	22	49	42	28	57	79	79
Max	61	71	60	72	46	31	51	61	58	90	89	79
Min	14	22	16	33	21	17	19	18	22	48	38	26
Range	47	49	44	39	25	14	32	43	36	42	51	53
Mean	36.7	42.4	35.4	49.0	31.9	23.4	32.4	35.8	41.7	71.3	59.3	44.4
St Dev	10.9	11.2	10.6	10.0	5.6	3.8	7.0	9.4	9.2	11.3	11.5	12.2
C_v, %	29.8	26.4	30.0	20.5	17.6	16.2	21.7	26.1	22.1	15.8	19.3	27.4

Table 1 presents information for all 39 meteorological stations on the values of L for all months of year. In particular, the representativeness of these stations in terms of monthly precipitation varies from 14 km (Akhalkalaki, January) to 90 km (Akhaltsikhe, October).

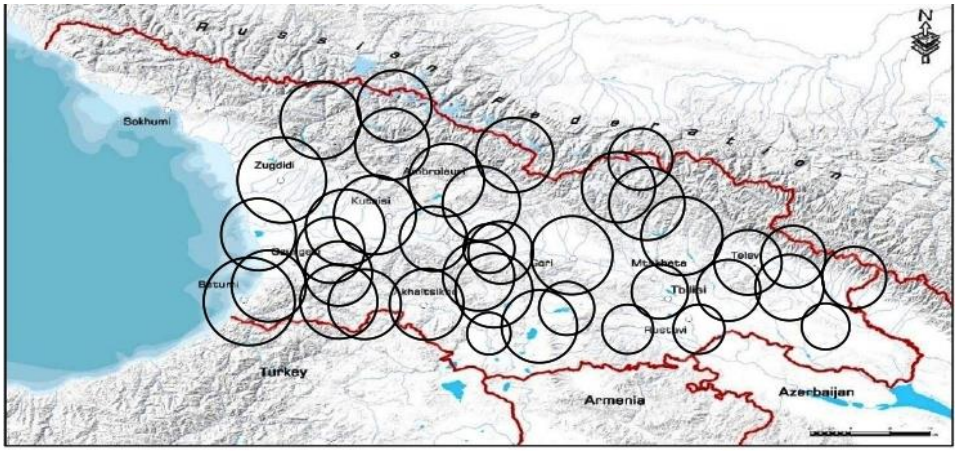

Fig. 3. Example of the areas of circles around meteorological stations within which the data of these stations on the sum of atmospheric precipitation in January with a high level of representativeness can be used.

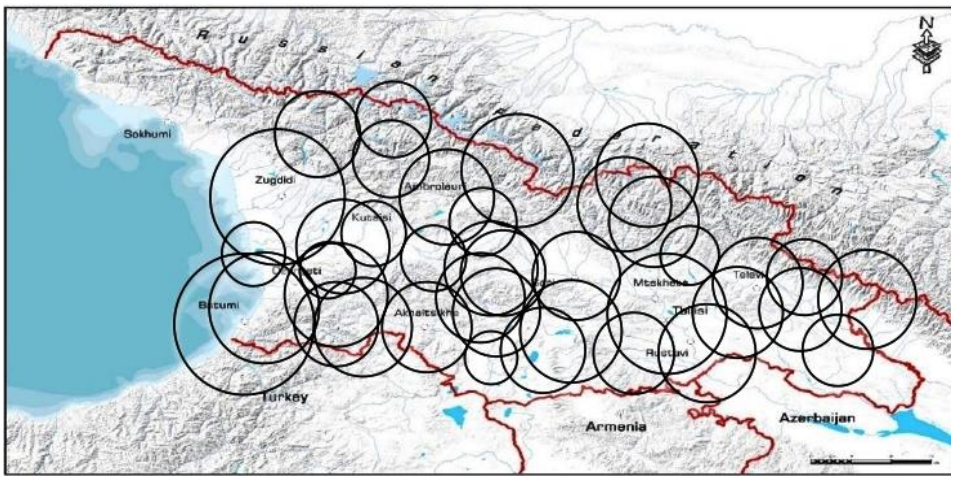

Fig. 4. Example of the areas of circles around meteorological stations within which the data of these stations on the sum of atmospheric precipitation in July with a high level of representativeness can be used.

Finally, for clarity in Fig. 3 and 4 examples of the areas of circles around meteorological stations within which the data of these stations on the monthly sum of atmospheric precipitation in January and July with a high level of representativeness can be used are presented.

Conclusion

In the future, these studies will be continued for daily data of atmospheric precipitation.

Acknowledgments

This work was supported by Shota Rustaveli National Science Foundation of Georgia (SRNSFG), Grant number FR-23-5466, “Machine Learning Approach to the Landslide Activation Prediction in Georgia”.

References

[1] Tavartkiladze K., Begalishvili N., Kharchilava J., Mumladze D., Amiranashvili A., Vachnadze J., Shengelia I., Amiranashvili V. Contemporary Climate Change in Georgia. Regime of Some Climate Parameters and their Variability. Monograph, ISBN 99928-885-4-7, Tbilisi, 2006, 177 p., (in Georgian).

[2] Amiranashvili A. Changeability of Air Temperature and Atmospheric Precipitations in Tbilisi for 175 Years. International Scientific Conference "Natural Disasters in Georgia: Monitoring, Prevention, Mitigation". Proceedings, ISBN 978-9941-13-899-7, Publish House of Iv. Javakhishvili Tbilisi State University, December 12-14, Tbilisi, 2019, pp. 86-90.

[3] Kartvelishvili L., Tatishvili M., Amiranashvili A., Megrelidze L., Kutaladze N. Weather, Climate and their Change Regularities for the Conditions of Georgia. Monograph, Publishing House "UNIVERSAL", ISBN: 978-9941-33-465-8, Tbilisi 2023, 406 p., https://doi.org/10.52340/mng.9789941334658

[4] Amiranashvili A.G., Revishvili A.A., Khazaradze K.R., Japaridze N.D. Connection of Holiday Climate Index with Public Health (on Example of Tbilisi and Kakheti Region, Georgia). Journal of the Georgian Geophysical Society, e-ISSN*:* 2667-9973, p-ISSN: 1512-1127, Physics of Solid Earth, Atmosphere, Ocean and Space Plasma, v. 24(1), 2021, pp. 63-76.

[5] Varazanashvili O., Tsereteli N., Amiranashvili A., Tsereteli E., Elizbarashvili E., Dolidze J., Qaldani L., Saluqvadze M., Adamia Sh., Arevadze N., Gventcadze A. Vulnerability, Hazards and Multiple Risk Assessment for Georgia. Natural Hazards, Vol. 64, Number 3, 2012, pp. 2021-2056. DOI: 10.1007/s11069-012-0374-3, http://www.springerlink.com/content/9311p18582143662/fulltext.pdf.

[6] Opasnyye gidrometeorologicheskiye yavleniya na Kavkaze. Pod red. Svanidze G.G. i Tsutskiridze Ya.A., L., Gidrometeoizdat, 1980, 288 s., (in Russian).

[7] Elizbarashvili E.Sh., Elizbarashvili M.E. Stikhiynyye meteorologicheskiye yavleniya na territorii Gruzii. Tbilisi, Zeon, 2012, 104 s., (in Russian).

[8] Erener A., Düzgün H.B.S. A regional scale quantitative risk assessment for landslides: case of Kumluca watershed in Bartin, Turkey. // Landslides, 10.1, 2013, pp. 55-73, DOI 10.1007/s10346-012-0317-9

[9] Segoni S., Piciullo L., Gariano S.L. A review of the recent literature on rainfall thresholds for landslide occurrence. Landslides, 15, 2018, pp. 1483–1501, DOI 10.1007/s10346-018-0966-4.

[10] Kirschbaum D., Stanley T. Satellite-Based Assessment of Rainfall-Triggered Landslide Hazard for Situational Awareness. Earth's Future, 6, 2018, pp.505-523, https:// doi.org/10.1002/, 2017EF000715

[11] Amiranashvili A., Chelidze T., Dalakishvili L., Svanadze D., Tsamalashvili T., Tvauri G. Preliminary Results of a Study of the Relationship Between the Monthly Mean Sum of Atmospheric Precipitation and Landslide Cases in Georgia. Journal of the Georgian Geophysical Society, ISSN: 1512-1127, Physics of Solid Earth, Atmosphere, Ocean and Space Plasma, v. 23(2), 2020, pp. 37 – 41.

[12] Amiranashvili A., Chelidze T., Dalakishvili L., Svanadze D., Tsamalashvili T., Tvauri G. Preliminary Results of a Study of the Relationship Between the Variability of the Mean Annual Sum of Atmospheric Precipitation and Landslide Processes in Georgia. Int. Sc. Conf. „Modern Problems of Ecology", Proc., ISSN 1512-1976, v. 7, Tbilisi-Telavi, Georgia, 26-28 September, 2020, pp. 202-206.

[13] Chelidze, T., Tsamalashvili, T., Fandoeva, M. Mass-movement stationary hazard maps of Georgia including precipitation triggering effect: fuzzy logic approach. Bull. Georg. Nat. Acad. Sci., vol. 16, no. 2, 56-63, 2022, http://science.org.ge/bnas/t16-n2/07_Chelidze_Geophysics.pdf

[14] Amiranashvili A., Chelidze T., Svanadze D., Tsamalashvili T., Tvauri G. Comparison of Data from Ground-Based and Satellite Measurements of the Monthly Sum of Atmospheric Precipitation on the Example of Tbilisi City in 2001-2020. Int. Conf. of Young Scientists "Modern Problems of Earth Sciences". Proceedings, ISBN 978-9941-36-044-2, Publish House of Iv. Javakhishvili Tbilisi State University, Tbilisi, November 21-22, 2022, pp. 154-158. http://openlibrary.ge/bitstream/123456789/10251/1/37_YSC_2022.pdf

[15] Amiranashvili A., Chelidze T., Svanadze D., Tsamalashvili T., Tvauri G. Some Results of a Study of the Relationship Between the Mean Annual Sum of Atmospheric Precipitation and Re-Activated and New Landslide Cases in Georgia Taking into Account of Climate Change. Journal of the Georgian Geophysical Society, e-ISSN: 2667-9973, p-ISSN: 1512-1127, Physics of Solid Earth, Atmosphere, Ocean and Space Plasma, v. 25(2), 2022, pp. 38–48. https://openjournals.ge/index.php/GGS/article/view/5959, DOI: https://doi.org/10.48614/ggs2520225959

[16] Chelidze T., Amiranashvili A., Svanadze D., Tsamalashvili T., Tvauri G. Terrestrial and Satellite-Based Assessment of Rainfall Triggered Landslides Activity in Georgia, Caucasus. Bull. Georg. Nat. Acad. Sci., vol. 17, no. 2, 71-77, 2023, http://science.org.ge/bnas/vol-17-2.html

[17] Amiranashvili A., Chelidze T., Svanadze D., Tsamalashvili T., Tvauri G. Abnormal Precipitation Before the Landslide in Akhaldaba (A Suburb of Tbilisi, Georgia) on June 13, 2015 According to Radar Measurements. Journal of the Georgian Geophysical Society, e-ISSN: 2667-9973, p-ISSN: 1512-1127, Physics of Solid Earth, Atmosphere, Ocean and Space Plasma, v. 26(1), 2023, pp. 30–41.
[18] Amiranashvili A., Chelidze T., Svanadze D., Tsamalashvili T., Tvauri G. Study of the Relationship Between the Mean Annual Sum of Atmospheric Precipitation and Re-Activated and New Mudflow Cases in Georgia. Journal of the Georgian Geophysical Society, e-ISSN: 2667-9973, p-ISSN: 1512-1127, Physics of Solid Earth, Atmosphere, Ocean and Space Plasma, v. 26(1), 2023, pp. 19–29. https://ggs.openjournals.ge/index.php/GGS/article/view/6958;
DOI: https://doi.org/10.48614/ggs2620236958
[19] Amiranashvili A., Chelidze T., Svanadze D., Tsamalashvili T., Tvauri G. On the Representativeness of Data from Meteorological Stations in Georgia for Annual and Semi-Annual Sum of Atmospheric Precipitation Around of These Stations. International Scientific Conference „Natural Disasters in the 21st Century: Monitoring, Prevention, Mitigation“. Proceedings, ISBN 978-9941-491-52-8, Tbilisi, Georgia, December 20-22, 2021. Publish House of Iv. Javakhishvili Tbilisi State University, Tbilisi, 2021, pp. 79 - 83. http://openlibrary.ge/bitstream/123456789/9566/1/20_Conf_ND_2021.pdf
[20] Hinkle D. E., Wiersma W., Jurs S. G. Applied Statistics for the Behavioral Sciences. // Boston, MA, Houghton Mifflin Company, 2003.

საქართველოს მეტეოროლოგიური სადგურების მონაცემების რეპრეზენტულობა ნალექების თვიური რაოდენობის მიხედვით ამ სადგურების ირგვლივ

ა.ამირანაშვილი, თ.ჭელიძე, დ.სვანაძე, თ.წამალაშვილი, ნ.ვარამაშვილი

რეზიუმე

წარმოდგენილია საქართველოს 39 მეტეოროლოგიური სადგურების მონაცემების რეპრეზენტულობა ამ სადგურების ირგვლივ ნალექების თვიური რაოდენობის მიხედვით კვლევის შედეგების გათვალისწინებით. დაკვირვების პერიოდი 1936 - 2015 წწ. კერძოდ, დადგინდა რომ ამ სადგურების რეპრეზენტულობა თვიური ნალექების მიხედვით მერყეობს 14 კმ-დან (ახალქალაქი, იანვარი) 90 კმ-მდე (ახალციხე, ოქტომბერი).

საკვანძო სიტყვები: ნალექი, კორელაციური და რეგრესიული ანალიზი, სტიქიური უბედურებები, მეწყერები.

О репрезентативности данных метеостанций Грузии по месячной сумме атмосферных осадков вокруг этих станций

А. Амиранашвили, Т. Челидзе, Д. Сванадзе, Т. Цамалашвили, Н. Варамашвили

Резюме

Представлены результаты исследования репрезентативности данных 39 метеорологических станций Грузии по месячной сумме атмосферных осадков вокруг этих станций. Период наблюдений – с 1936 по 2015 годы. В частности, установлено, что репрезентативность этих станций по месячному количеству осадков варьирует от 14 км (Ахалкалаки, январь) до 90 км (Ахалцихе, октябрь).

Ключевые слова: атмосферные осадки, корреляционно-регрессионный анализ, природные катастрофы, оползни.

Journal of the Georgian Geophysical Society, e-ISSN: 2667-9973, p-ISSN: 1512-1127
Physics of Solid Earth, Atmosphere, Ocean and Space Plasma, v. 27(1), 2024, pp. 58 - 66

Variability in the Number of Days with Hail in the Warm Half of the Year in Bolnisi and Tsalka in 1941-2021 and their Expected Change until 2045

[1,2]Mikheil G. Pipia, [1]Avtandil G. Amiranashvili, [2,3]Nazibrola G. Beglarashvili, [2]Elizbar Sh. Elizbarashvili, [1]Otar Sh. Varazanashvili

[1]M. Nodia Institute of Geophysics of the I. Javakhishvili Tbilisi State University, Georgia
[2]Institute of Hydrometeorology of the Georgian Technical University, Georgia
[3]Samtskhe-Javakheti State University

e-mail: mikheil.pipia@tsu.ge

ABSTRACT

The paper presents the results of a study of the features of variations in the number of days with hail in the warm half of the year (HD) in Bolnisi and Tsalka in 1941-2021 and their expected change until 2045. The stability of time series of the number of days with hail at the indicated points was studied by determining the HD correlations with time (linear correlation, Kendall's and Spearmen's rank correlation). The level of autocorrelation in HD time series in Bolnisi and Tsalka was determined. The periodicity of these time series has been studied. Interval forecasting of the number of days with hail in Bolnisi and Tsalka until 2045 was carried out, taking into account the periodicity in the HD time series.

Key words: *Natural disasters, number of days with hail, statistical analysis, long-term interval forecast.*

Introduction

Almost all types of geophysical disasters occur in Georgia, including hydrometeorological ones [1-4]. Regarding hail processes, Georgia is one of the hail-prone regions of the world [1-3]. As in other countries, in Georgia hail regularly causes serious material damage to agriculture, buildings, structures, infrastructure, transport, etc. Therefore, given the importance of the problem, special attention has always been paid to the study of hail processes here, especially taking into account climate change [5-7].

Most studies of hail processes are usually associated with the analysis of weather station data on the number of days with hail, as well as assessment of damage from hail in various regions of Georgia [8-18], and especially in Kakheti, the main wine-growing region of Georgia [8,15,16,18] .

However, in recent years, it has become possible, based on radar data [19,20], to study various characteristics of hail processes in Eastern Georgia and its neighboring countries (Azerbaijan, Armenia), including determining the maximum size of hail in the clouds and simulating the size of fallen hail [21-26].

For example, works [21,22] present the results of modeling the distribution of hailstones by average maximum diameter (D) on the territory of Kakheti (Georgia) using data on the freezing level in the atmosphere and radar measurements of the maximum size of hail in the clouds. Maps of hail distribution according to the average maximum diameter on the territory of Kakheti for individual months were constructed - from April to September. The vertical distribution of D in the specified territory was studied in the altitude range from 0.11 to 3.84 km, etc.

The works [23-25] present a preliminary analysis of data from radar studies of hail processes in Georgia, Armenia and Azerbaijan. In [26] the results of the analysis of radar studies of hail processes over the territories of Georgia and Azerbaijan on May 28 and July 13, 2019 are presented. Based on the values of the maximum size of hailstones in clouds, using the Zimenkov-Ivanov model, the expected sizes of hailstones falling on the earth's surface are calculated. The degree of damage to vineyards, wheat and corn, depending on the size of the hail, was determined by summarizing the known data on damage to these crops at different kinetic energy of hail and data on the average kinetic energy of hail of different magnitudes. Based on this compilation, regression equations were obtained for the relationship between the degree of damage to these crops and the size of hailstones, which have the form of a sixth degree of a polynomial.

According to this equation, calculations were made of the degree of maximum damage to vineyards, wheat and corn along the trajectories of hail clouds over the territories of Georgia and Azerbaijan.

In 2022-2023, work was carried out to prepare [27,28] and create [29] a systematized catalog for five types of natural disasters in Georgia (landslides, mudflows, hurricane winds, floods and hail), as well as ways to interpret the data from this catalog [30 ,31].

In particular, using the data from this catalog, work was carried out on a statistical analysis of the number of days with hail in Georgia in 2006-2021 [32], as well as an analysis of damage from hail to agricultural crops in Kvemo Kartli (Georgia) [33]. The work [34] studied the long-term variability of the number of days with hail in Tbilisi (1891-2021).

In continuation of work [34] in [35] predictive estimates of the number of hail days (HD) and their moving averages (for 3, 5, 7, 9 and 11 years – HD_3…HD_11) per warm period of year to 2050 and 2085 an example of Tbilisi was performed. Forecasting was carried out using the AAA version of the exponential smoothing (ETS) algorithm taking into account the periodicity in the pre-forecast time series. In particular, the following results were obtained.

For the time series of the measured number of days with hail and HD_11 years, no pronounced peak in periodicity is observed. For time series HD_3, the periodicity is 14 years, HD_5 – 32 years, HD_7 and HD_9 – 31 years.

In the period from 2022 to 2050, the range of variability of the average values of the central points of the forecast for the number of days with hail and the values of their 95% upper level is as follows: HD - from 0.9 to 3.8, HD_3 - from 1.0 to 3.0, HD_11 – from 1.0 to 1.6. In the period from 2022 to 2085, the range of variability of the average values of the central points of the forecast for the number of days with hail and the values of their 95% upper level is as follows: HD_5 - from 0.4 to 3.0, HD_7 - from 0.7 to 1.8, HD_9 - from 0.5 to 3.

Our last paper [36] presents some results of a statistical analysis of data from 30 meteorological stations of Georgia on the number of days with hail in the warm half of the year in 1941-2021.

This work is a continuation of previous studies [32-36]. Results of a study of the features of variations in the number of days with hail in the warm half of the year in Bolnisi and Tsalka in 1941-2021 and their expected change until 2045 are presented below.

Study area, material and methods

Study area – Bolnisi (41.45° N, 44.54° E, 550 m a.s.l.) and Tsalka (41.60° N, 44.09° E, 1450 m a.s.l.) – Kvemo Kartli region of Georgia.

The work used catalog data on the number of days with hail in the warm season of the year (April-October) in Bolnisi and Tsalka from 1941 to 2021 [29].

In the proposed work the analysis of data is carried out with the use of the standard statistical analysis methods of random events and methods of mathematical statistics for the non-accidental time-series of observations [37-40].

Forecasting the number of hail days was performed using the AAA version of the exponential smoothing (ETS) algorithm taking into account the periodicity in the pre-forecast time series [40].

The following designations will be used below: Mean – average values; Min – minimal values; Max - maximal values; St Dev - standard deviation; R – coefficient of linear correlation; R_k - Kendall's rank correlation coefficient; R_s - Spearmen's rank correlation coefficient; R_a – autocorrelation coefficient; Lag = 1, 2…27 years; HD - the number of days with hail in the warm season; Forecast - forecast center point; 67%_Upp...99.99%_Upp - 67%...99.99% upper forecast level of HD; Lower forecast level of HD is 0.

The degree of correlation was determined in accordance with [37]: very high correlation ($0.9 \leq R \leq 1.0$); high correlation ($0.7 \leq R < 0.9$); moderate correlation ($0.5 \leq R < 0.7$); low correlation ($0.3 \leq R < 0.5$); negligible correlation ($0 \leq R < 0.3$).

The statistical programs Mesosaur and Excel 19 were used for calculations.

Results

Results in Table 1,2 and Fig. 1-8 are presented.

In Table 1 data about correlation level of the number of days with hail in the warm season in Bolnisi and Tsalka in 1941-2021 with years are presented.

Table 1. Correlation of the number of days with hail in the warm season in Bolnisi and Tsalka in 1941-2021 with years.

Location	Bolnisi					
Parameter	R	α (R)	R_k	α(R_k)	R_s	α(R_s)
Value	-0.16	0.2	-0.14	0.074	-0.13	0.233
Location	Tsalka					
Parameter	R	α (R)	R_k	α(R_k)	R_s	α(R_s)
Value	-0.62	<0.005	-0.44	<0.005	-0.59	<0.005

As follows from Table 1, in general, the correlation of HD with years in both Bolnisi and Tsalka is negative. However, the level of all types of HD correlations with the years in Bolnisi is lower than in Tsalka ("Negligible correlation" for Bolnisi, and "Low correlation" and "Moderate correlation" for Tsalka).

That is, the dependence HD on time in Bolnisi is lower than in Tsalka. The data in Table 1 confirms the results of work [36], which in particular shows that in 1981-2021 compared to 1941-1980 the average number of days with hail in Bolnisi decreased by 0.6 (43% of the average number of days with hail in 1941-2021), while in Tsalka by 2.5 (81% of the average number of days for the entire observation period).

The level of autocorrelation in the HD time series in Bolnisi is also lower than in Tsalka (Fig. 1,2).

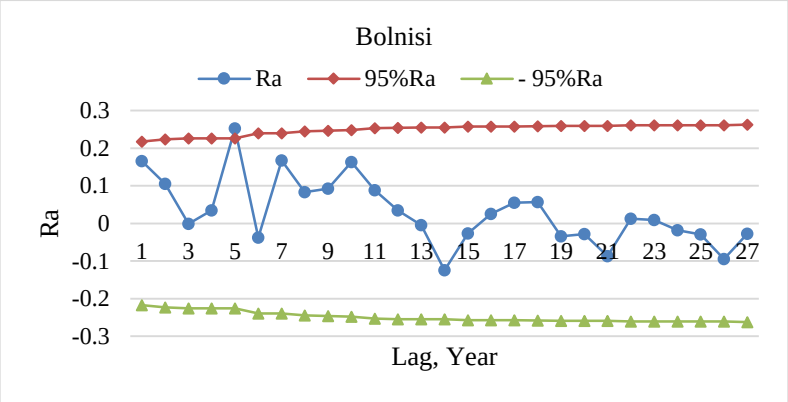

Fig. 1. Autocorrelation in time-series of observations on the number of days with hail in the warm season in Bolnisi from 1941 to 2021.

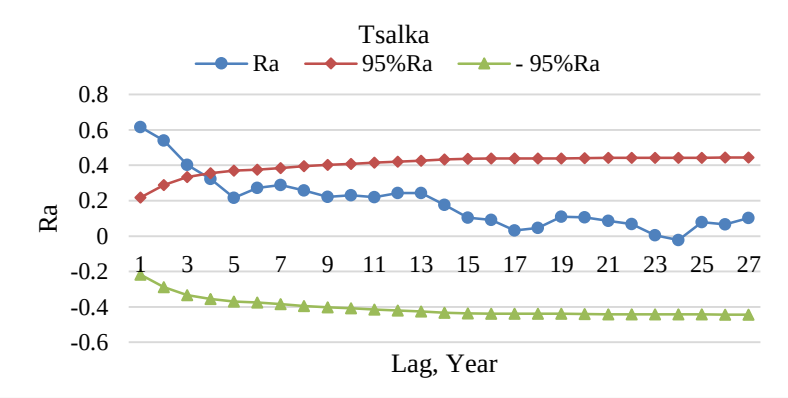

Fig. 2. Autocorrelation in time-series of observations on the number of days with hail in the warm season in Tsalka from 1941 to 2021.

Thus, in Bolnisi, autocorrelation appears only in the fifth lag (R_a = 0.26), while in Tsalka in the first three lags (R_a = 0.62, 0.54 and 0.40, respectively).

In Bolnisi, the HD time series shows two periodicity peaks – the main one ≈ 6 years and the auxiliary one ≈ 10 years (Fig. 3).

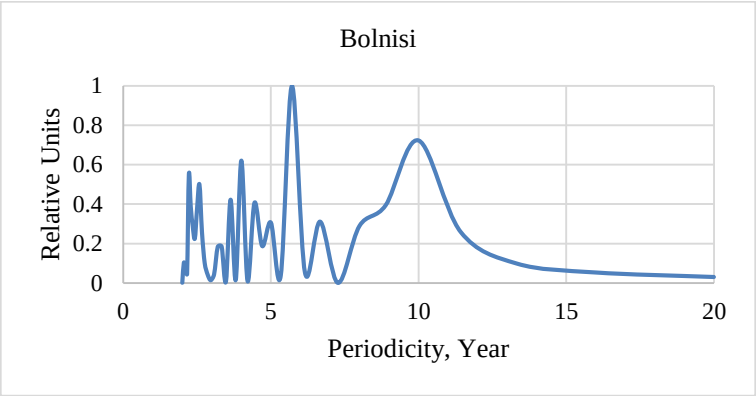

Fig. 3. Periodicity of the number of days with hail in the warm season in Bolnisi from 1941 to 2021.

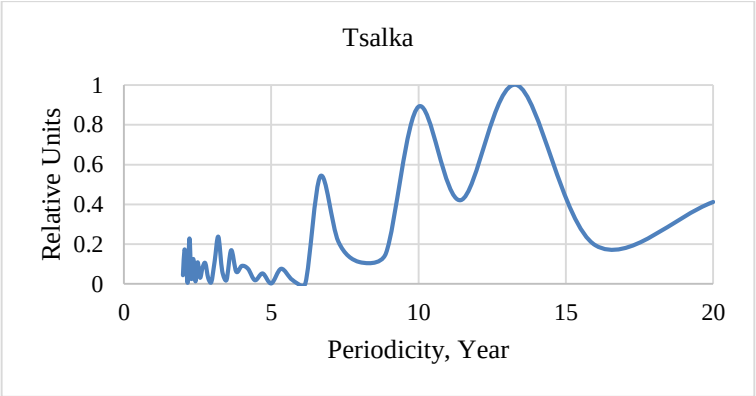

Fig. 4. Periodicity of the number of days with hail in the warm season in Tsalka from 1941 to 2021.

In Tsalka, the HD time series shows three periodicity peaks – the main one ≈ 13 years and two auxiliary ones ≈ 10 years and ≈ 7 years (Fig. 4).

Data on the main peak periodicity values in the HD time series are taken into account when conducting interval forecasting of the number of days with hail in Bolnisi and Tsalka until 2045 (Fig. 5-8).

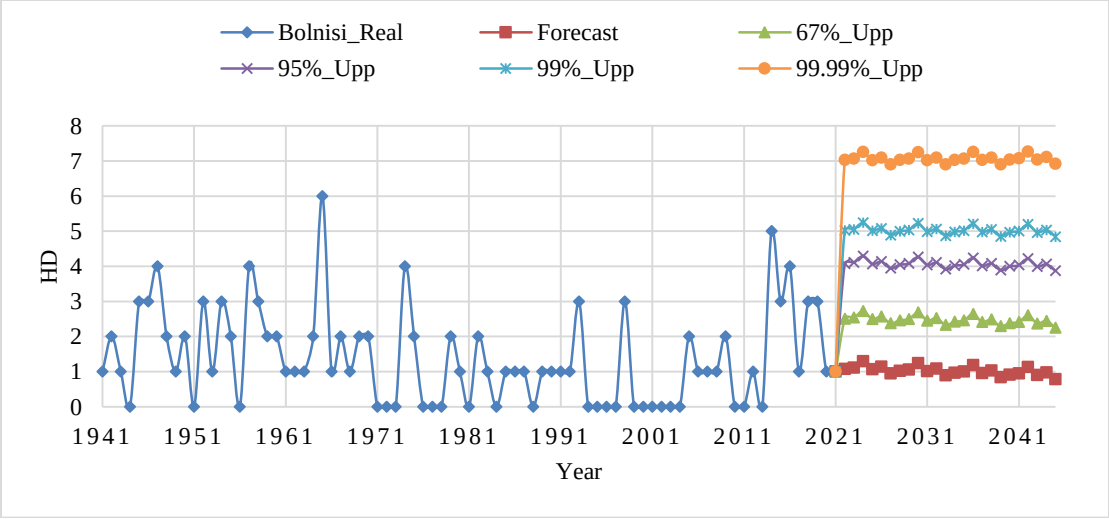

Fig. 5. Time-series of real (1941-2021) and forecasting (2022-2045) values of the number of days with hail in the warm season in Bolnisi.

In particular, the five-year average values of the central points of the HD forecast in 2026-2045 in Bolnisi they vary from 0.9 to 1.1 (Fig. 6), and in Tsalka – from 0.5 to 1.1 (Fig. 8).

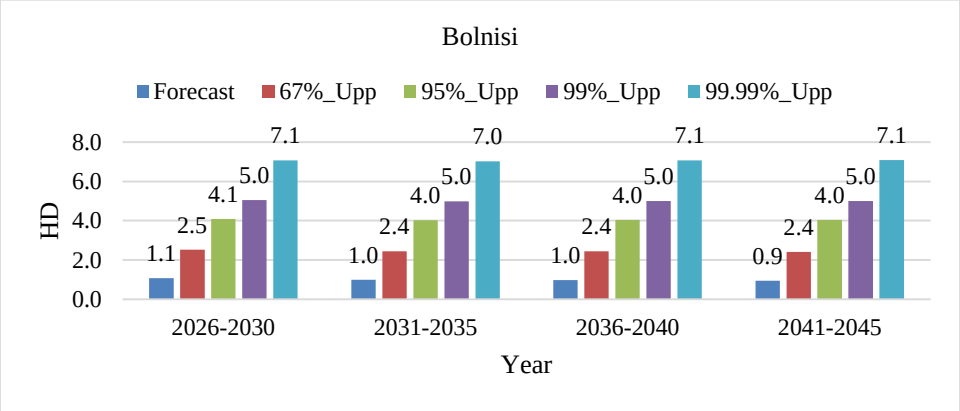

Fig. 6. Five-year averages forecasting values of the number of days with hail in the warm season in Bolnisi from 2026 to 2045.

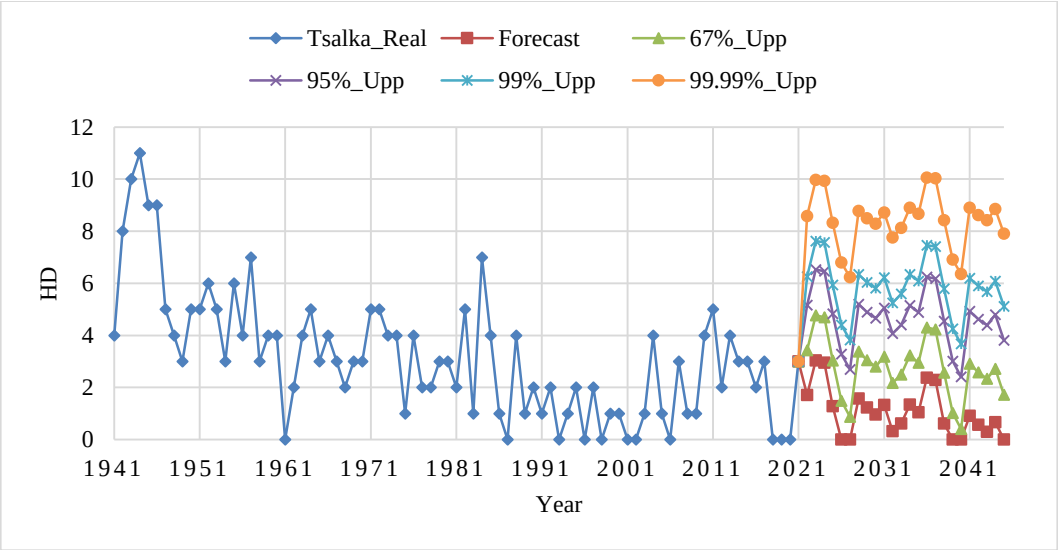

Fig. 7. Time-series of real (1941-2021) and forecasting (2022-2045) values of the number of days with hail in the warm season in Tsalka.

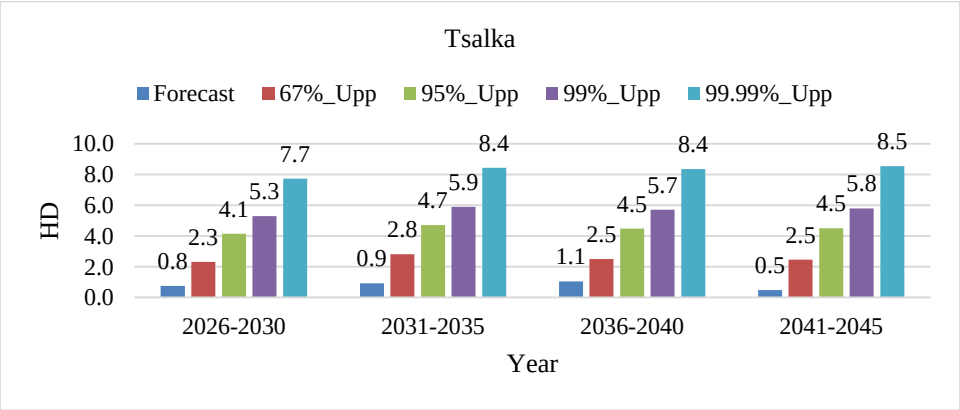

Fig. 8. Five-year averages forecasting values of the number of days with hail in the warm season in Tsalka from 2026 to 2045.

The five-year average values of the 99.99% upper level of HD forecast points in Bolnisi vary from 7.0 to 7.1 (Fig. 6), and in Tsalka – from 7.7 to 8.5 (Fig. 8).

Table 2 compares the actual average HD values in Bolnisi and Tsalka in 1941-2021 and 2002-2021 with their prognostic values in 2026-2045.

Table 2. Statistical characteristics of real (1941-2021, 2002-2021) and forecasting (2026-2045) values of the number of days with hail in the warm season in Bolnisi and Tsalka.

Years	1941-2021	2002-2021	2026-2045				
Variable	Real	Real	Forecast	67%_Upp	95%_Upp	99%_Upp	99.99%_Upp
Location	Bolnisi						
Max	6.0	5.0	1.2	2.7	4.3	5.2	7.3
Min	0.0	0.0	0.8	2.3	3.9	4.8	6.9
Mean	1.4	1.5	1.0	2.5	4.1	5.0	7.1
StDev	1.3	1.5	0.1	0.1	0.1	0.1	0.1
Location	Tsalka						
Max	11	5.0	2.4	4.3	6.2	7.5	10.1
Min	0	0.0	0.0	0.4	2.4	3.7	6.2
Mean	3.1	2.0	0.8	2.5	4.5	5.7	8.3
StDev	2.4	1.6	0.7	1.0	1.0	1.0	1.0

In particular, as follows from Table 2, in Bolnisi the average real HD values during the indicated time periods fall into their forecast range “Forecast - 67%_Upp”, and in Tsalka – into the range “Forecast - 95%_Upp”.

Conclusion

In the future, similar forecast estimates of the number of days with hail (HD) will be carried out for other individual settlements in Georgia, both for annual data and moving averages of these data.

It is also planned to study of the variability of the number of days with hail in the warm half of the year (April-October) for 22 weather stations of Georgia from 1941 to 2021, on average for five climatic zones, which includes four climatic groups according to the Köppen classification, and conducting HD interval forecasting for indicated climate zones.

Acknowledgments

This work was supported by Shota Rustaveli National Science Foundation of Georgia (SRNSFG), Grant Number YS-22-1062.

References

[1] Opasnyye gidrometeorologicheskiye yavleniya na Kavkaze. Pod red. Svanidze G.G. i Tsutskiridze Ya.A., L., Gidrometeoizdat, 1980, 288 s., (in Russian).

[2] Elizbarashvili E.Sh., Elizbarashvili M.E. Stikhiynyye meteorologicheskiye yavleniya na territorii Gruzii. Tbilisi, Zeon, 2012, 104 s., (in Russian).

[3] Varazanashvili O., Tsereteli N., Amiranashvili A., Tsereteli E., Elizbarashvili E., Dolidze J., Qaldani L., Saluqvadze M., Adamia Sh., Arevadze N., Gventcadze A. Vulnerability, hazards and multiple risk assessment for Georgia. Natural Hazards, Vol. 64, Number 3, 2012, 2021-2056, DOI: 10.1007/s11069-012-0374-3, http://www.springerlink.com/content /9311p18582143662/fulltext.pdf

[4] Amiranashvili A.G. Increasing Public Awareness of Different Types of Geophysical Catastrophes, Possibilities of Their Initiation as a Result of Terrorist Activity, Methods of Protection and Fight with their Negative Consequences. Engaging the Public to Fight Consequences of Terrorism and Disasters. NATO Science for Peace and Security Series E: Human and Societal Dynamics, vol. 120. IOS Press, Amsterdam•Berlin•Tokyo•Washington, DC, ISSN 1874-6276, 2015, pp.155-164. http://www.nato.int/science; http://www.springer.com; http://www.iospress.nl

[5] Berdzenishvili N., Kirkitadze D. Review of some Studies of Hail and Thunderstorm Processes in Georgia. Transactions of Mikheil Nodia Institute of Geophysics, ISSN 1512-1135, vol. LXXV, 2022, pp. 57-75, (in Russian).

[6] Tatishvili M.R., Kartvelishvili L.G., Mkurnalidze I.P. Thunderstorm and Hail Processes over Georgian Territory. Against Global Climate Change Background. Journal of the Georgian Geophysical Society, ISSN: 1512-1127, Iss. B, Physics of Atmosphere, Ocean and Space Plasma, vol. 19B, Tb., 2016, pp. 111-119.
[7] Kartvelishvili L., Tatishvili M., Amiranashvili A., Megrelidze L., Kutaladze N. Weather, Climate and their Change Regularities for the Conditions of Georgia. Monograph, Publishing House "UNIVERSAL", ISBN: 978-9941-33-465-8, Tbilisi 2023, 406 p., https://doi.org/10.52340/mng.9789941334658
[8] Kurdiani I.G. O grozakh i gradobitiyakh v Kakhetii. Tbilisi, Gruz. geogr. obshch., 1935, (in Russian).
[9] Gigineyshvili V.M. Gradobitiya v Vostochnoy Gruzii. Leningrad, Gidrometeoizdat, 1960, 123 s., (in Russian).
[10] Sulakvelidze G.K. Livnevyye osadki i grad. L., Gidrometeoizdat, 1967, 412 s.
[11] Amiranashvili A.G., Nodia A.G., Toronjadze A.F., Khurodze T.V. Some Statistical Characteristics of the Number of Days with Hail into the Warm Half-Year in Georgia in 1941-1990. Trans. of Institute of Geophysics of Acad. of Sc. of Georgia, ISSN 1512-1135, v. 58, 2004, pp. 133-141, (in Russian).
[12] Amiranashvili A.G., Amiranashvili V.A., Nodia A.G., Khurodze T.V., Toronjadze A.F., Bibilashvili T.N. Spatialtemporary characteristics of number of days with a hails in the warm period of year in Georgia. Proc. 14th Int. Conf. on Clouds and Precipitation, Bologna, Italy, 18-July 2004, pp. 2_2_215.1-2_2_215.2.
[13] Amiranashvili A., Varazanashvili O., Nodia A., Tsereteli N., Khurodze T. Statistical Characteristics of the Number of Days with Hail Per Annum in Georgia. Trans. of the Institute of Hydrometeorology, ISSN 1512-0902, vol. 115, Tb., 2008, pp. 427 – 433, (in Russian).
[14] Elizbarashvili E., Amiranashvili A., Varazanashvili O., Tsereteli N., Elizbarashvili M., Elizbarashvili Sh., Pipia M. Hailstorms in the Territory of Georgia. European Geographical Studies, Vol. 2, No. 2, 2014. Tbilisi, pp. 55-69, (in Russian).
[15] Amiranashvili A., Dzodzuashvili U., Lomtadze J., Sauri I., Chikhladze V. Some Characteristics of Hail Processes in Kakheti. Trans. of Mikheil Nodia Institute of Geophysics, ISSN 1512-1135, vol. 65, Tb., 2015, pp. 77 – 100, (in Russian).
[16] Amiranashvili A.G., Bliadze T.G., Jamrishvili N.K., Khurodze T.V., Pipia M.G., Tavidashvili Kh. Z. Comparative Analysis of the Distribution of Number of Days with Hail Per Annum on the Territory of Kakheti According to the Data of the Meteorological Stations and State Insurance Service of Georgia. Journal of the Georgian Geophysical Society, Issue A. Physics of Solid Earth, v.20A, 2017, Tbilisi, pp.44 -56.
[17] Janelidze I., Pipia M. Hail Storms in Georgia in 2016-2018. Int. Sc. Conf. "Natural Disasters in Georgia: Monitoring, Prevention, Mitigation". Proc., ISBN 978-9941-13-899-7, Publish House of Iv. Javakhishvili Tbilisi State University, December 12-14, Tbilisi, 2019, pp. 144 -146.
[18] Beglarashvili N., Janelidze I., Pipia M., Varamashvili N. Hail Storms in Kakheti (Georgia) in 2014-2018. Int. Sc. Conf. „Modern Problems of Ecology". Proc. v. 7. Tbilisi-Telavi, Georgia, 26-28 September, 2020, pp. 176-179.
[19] Amiranashvili A., Chikhladze V., Dzodzuashvili U., Ghlonti N., Sauri I., Telia Sh., Tsintsadze T. Weather Modification in Georgia: Past, Present, Prospects for Development. Int. Sc. Conf. "Natural Disasters in Georgia: Monitoring, Prevention, Mitigation". Proceedings, ISBN 978-9941-13-899-7, Publish House of Iv. Javakhishvili Tbilisi State University, December 12-14, Tbilisi, 2019, pp. 216-222.
[20] Amiranashvili A., Chikhladze V., Kveselava N., Kvilitaia N., Sauri I., Shavlakadze Sh. Some Characteristics of Hail Processes in Kakheti (Georgia) According to Radar Observations into 2016-2019. Journal of the Georgian Geophysical Society, ISSN: 1512-1127, Physics of Solid Earth, Atmosphere, Ocean and Space Plasma, v. 23(2), 2020, pp. 50 – 56. DOI: https://doi.org/10.48614/ggs2320202729
[21] Amiranashvili A., Bolashvili N., Gulashvili Z., Jamrishvili N., Suknidze N., Tavidashvili Kh. Distribution of Hail by Mean Max Size on the Territories of Municipalities of the Kakheti Region of Georgia. International Scientific Conference „Natural Disasters in the 21st Century: Monitoring, Prevention, Mitigation". Proceedings, ISBN 978-9941-491-52-8, Tbilisi, Georgia, December 20-22, 2021. Publish House of Iv. Javakhishvili Tbilisi State University, Tbilisi, 2021, pp. 84 - 87.
[22] Amiranashvili A.G., Bolashvili N.R., Gulashvili Z.M., Jamrishvili N.K., Suknidze N.E., Tavidashvili Kh.Z. Modeling the Distribution of Hailstones by Mean Max Sizes on the Territory of Kakheti (Georgia) using Data of the Freezing Level in the Atmosphere and Radar Measurements. Journal of the Georgian Geophysical Society, e-ISSN*:* 2667-9973, p-ISSN*:* 1512-1127, Physics of Solid Earth, Atmosphere, Ocean and Space Plasma, v. 24(1), 2021, pp. 25-36. DOI: https://doi.org/10.48614/ggs2420212881
[23] Gvasalia G., Kekenadze E., Mekoshkishvili N., Mitin M. Radar Monitoring of Hail Processes in Eastern

Georgia and its Neighboring Countries (Azerbaijan, Armenia). Int. Sc. Conf. „Natural Disasters in Georgia: Monitoring, Prevention, Mitigation“. Proc., Tbilisi, Georgia, December 12-14, 2019, pp. 170-174.

[24] Amiranashvili A., Bliadze T., Jamrishvili N., Kekenadze E., Tavidashvili Kh., Mitin M. Some Characteristics of Hail Process in Georgia and Azerbaijan on May 28, 2019. Journal of the Georgian Geophysical Society, Physics of Solid Earth, Atmosphere, Ocean and Space Plasma. v. 22(2), 2019, pp. 40–54.

[25] Kekenadze E., Samkharadze I. Preliminary Analysis of the Hail Process Above the Territory of Georgia, Armenia and Azerbaijan on July 13, 2019. Int. Sc. Conf. „Modern Problems of Ecology“. Proc. v. 7. Tbilisi-Telavi, Georgia, 26-28 September, 2020, pp. 167-171.

[26] Pipia M., Amiranashvili A., Beglarashvili N., Elizbarashvili E., Varazanashvili O. Analysis and Damage Assessment of Hail Processes in Georgia and Azerbaijan Using Radar Data (On the Example of May 28 and July 13, 2019). Reliability: Theory & Applications, ISSN: 1932-2321, vol. 18, iss. SI 5 (75), 2023, pp. 267-274, DOI: 10.24412/1932-2321-2023-575-267-274, https://cyberleninka.ru/article/n/analysis-and-damage-assessment-of-hail-processes-in-georgia-and-azerbaijan-using-radar-data-on-the-example-of-may-28-and-july-13

[27] Varazanashvili O.Sh., Gaprindashvili G.M., Elizbarashvili E.Sh., Basilashvili Ts.Z., Amiranashvili A.G. Principles of Natural Hazards Catalogs Compiling and Magnitude Classification. Journal of the Georgian Geophysical Society, e-ISSN*:* 2667-9973, p-ISSN*:* 1512-1127, Physics of Solid Earth, Atmosphere, Ocean and Space Plasma, v. 25(1), 2022, pp. 5-11. DOI: https://doi.org/10.48614/ggs2520224794

[28] Gaprindashvili G., Varazanashvili O., Elizbarashvili E., Basilashvili Ts., Amiranashvili A., Fuchs S. GeNHs: the First Natural Hazard Event Database for the Republic of Georgia. EGU General Assembly 2023, EGU23-1614, https://doi.org/10.5194/egusphere-egu23-1614; https://meetingorganizer.copernicus.org/EGU23/EGU23-1614.html

[29] Varazanashvili O., Gaprindashvili G., Elizbarashvili E., Basilashvili,Ts., Amiranashvili A., Fuchs S. The First Natural Hazard Event Database for the Republic of Georgia (GeNHs). Catalog, 2023, 270 p. http://dspace.gela.org.ge/handle/123456789/10369; DOI: 10.13140/RG.2.2.12474.57286

[30] Varazanashvili O., Gaprindashvili G., Elizbarashvili E., Amiranashvili A., Basilashvili Ts., Fuchs S. New Parametric Catalogs of Natural Hazard Events for Georgia. Transactions of Mikheil Nodia Institute of Geophysics, ISSN 1512-1135, vol. LXXVI, 2023, pp. 168-177, (in Georgian), http://dspace.gela.org.ge/bitstream/123456789/10483/1/12_Tr_IG%2876%29_2023.pdf

[31] Varazanashvili O., Gaprindashvili G., Elizbarashvili E., Amiranashvili A., Basilashvili Ts., Fuchs S. New Natural Hazard Event Database for the Republic of Georgia (GeNHs): Catalogs Compiling Principles and Results. Int. Sc. Conf. "Geophysical Processes in the Earth and its Envelopes". Proceedings, ISBN 978-9941-36-147-0, Publish House of Iv. Javakhishvili Tbilisi State University, November 16-17, 2023, pp. 185-187, (in Georgian). http://109.205.44.60/bitstream/123456789/10431/1/44_IG_90.pdf

[32] Amiranashvili A., Basilashvili Ts., Elizbarashvili E., Gaprindashvili G., Varazanashvili O. Statistical Analysis of the Number of Days with Hail in Georgia According to Meteorological Stations Data in 2006-2021. Int. Conf. of Young Scientists “Modern Problems of Earth Sciences”. Proceedings, ISBN 978-9941-36-044-2, Publish House of Iv. Javakhishvili Tbilisi State University, Tbilisi, November 21-22, 2022, pp. 164-168. http://openlibrary.ge/handle/123456789/10249

[33] Amiranashvili A., Bolashvili N., Elizbarashvili E., Liparteliani G., Suknidze N., Tsirgvava G., Varazanashvili O. Statistical Analysis of the Number of Days with Hail and Damage to Agricultural Crops from it in Kvemo Kartli (Georgia). Int. Sc. Conf. "Geophysical Processes in the Earth and its Envelopes". Proceedings, ISBN 978-9941-36-147-0, Publish House of Iv. Javakhishvili Tbilisi State University, November 16-17, 2023, pp. 133-137. http://www.openlibrary.ge/bitstream/123456789/10419/1/33_IG_90.pdf

[34] Amiranashvili A., Elizbarashvili E., Varazanashvili O., Pipia M. Statistical Analysis of the Number of Days with Hail During the warm Season in Tbilisi in 1891-2021. Transactions IHM, GTU, ISSN: 1512-0902ISSN: 1512-0902, vol.133, 2023, pp.74-77, (in Georgian), doi.org/10.36073/1512-0902-2023-133-74-77; http://openlibrary.ge/bitstream/123456789/10340/1/133-14.pdf

[35] Amiranashvili A., Elizbarashvili E., Pipia M., Varazanashvili O. Expected Changes of the Number of Days with Hail in Tbilisi to 2085. Int. Sc. Conf. "Geophysical Processes in the Earth and its Envelopes". Proceedings, ISBN 978-9941-36-147-0, Publish House of Iv. Javakhishvili Tbilisi State University, November 16-17, 2023, pp. 138-142. http://www.openlibrary.ge/handle/123456789/10420

[36] Amiranashvili A., Beglarashvili N., Elizbarashvili E., Varazanashvili O., Pipia M. Statistical analysis of data from 30 meteorological stations of Georgia on the number of days with hail in the warm half of the year in 1941-2021. Transactions of IHM, GTU, vol. 135, 2024, pp. 32-38 (in Georgian).
[37] Hinkle D. E., Wiersma W., Jurs S. G. Applied Statistics for the Behavioral Sciences. Boston, MA, Houghton Mifflin Company, ISBN: 0618124055; 9780618124053, 2003, 756 p.
[38] Förster E., Rönz B. Methoden der korrelations - und regressionsanalyse. – Ein Leitfaden für Ökonomen. Verlag Die Wirtshaft Berlin, 1979, 324 p.
[39] Kendall M.G. Time-series. Moscow, 1981, 200 s., (in Russian).
[40] Box G.E.P, Jenkins G.M., Reinsel G.C. Time Series Analysis: Forecasting & Control (3rd Edition). ISBN10: 0130607746, ISBN13: 9780130607744. Prentice Hall, 1994, 592 p.

სეტყვათა დღეთა რაოდენობის ცვალებადობა ბოლნისსა და წალკაში წლის თბილ ნახევარში 1941-2021 წლებში და მოსალოდნელი ცვლილება 2045 წლამდე

მ. ფიფია, ა. ამირანაშვილი, ნ. ბეგლარაშვილი, ე. ელიზბარაშვილი, ო. ვარაზანაშვილი

რეზიუმე

ნაშრომში წარმოდგენილია ბოლნისსა და წალკაში სეტყვათა დღეთა რაოდენობის წლის თბილ ნახევარში (HD) 1941-2021 წლებში ცვალებადობის მახასიათებლების შესწავლის შედეგები და მათი მოსალოდნელი ცვლილება 2045 წლამდე. აღნიშნულ პუნქტებში შესწავლილი იქნა სეტყვათა დღეთა რაოდენობის დროის სერიების სტაბილურობა HD-ს დროთან კორელაციების განსაზღვრით (წრფივი კორელაცია, კენდალის და სპირმანის რანგის კორელაცია). განისაზღვრა ავტოკორელაციის დონე HD-ს დროის რიგებში ბოლნისსა და წალკაში. შესწავლილია ამ დროის რიგების პერიოდულობა. განხორციელდა ბოლნისსა და წალკაში სეტყვათა დღეთა რაოდენობის ინტერვალური პროგნოზირება 2045 წლამდე HD-ს დროის რიგებში პერიოდულობის გათვალისწინებით.

საკვანძო სიტყვები: სტიქიური მოვლენები, სეტყვათა დღეთა რაოდენობა, სტატისტიკური ანალიზი, მრავალწლიანი ინტერვალური პროგნოზი.

Вариации числа дней с градом в теплое полугодие в Болниси и Цалке в 1941-2021 гг. и их ожидаемое изменение до 2045 г.

М. Пипиа, А. Амиранашвили, Н. Бегларашвили, Э. Элизбарашвили, О. Варазанашвили

Резюме

В работе представлены результаты исследования особенностей вариаций числа дней с градом в теплое полугодие (HD) в Болниси и Цалке в 1941-2021 гг. и их ожидаемое изменение до 2045 г. Изучена устойчивость временных рядов числа дней с градом числа в указанных пунктах путем определения корреляционных связей HD со временем (линейная корреляция, ранговая корреляция Кендалла и Спирмена). Определен уровень автокорреляции во временных рядах HD в Болниси и Цалке. Изучена периодичность указанных временных рядов. Проведено интервальное прогнозирование числа дней с градом в Болниси и Цалке до 2045 г. с учетом периодичности во временных рядах HD.

Ключевые слова: Стихийные бедствия, количество дней с градом, статистический анализ, многолетний интервальный прогноз.

Journal of the Georgian Geophysical Society, e-ISSN: 2667-9973, p-ISSN: 1512-1127
Physics of Solid Earth, Atmosphere, Ocean and Space Plasma, v. 27(1), 2024, pp. 67 - 76

Some Results of an Expeditionary Study of the Tornado Distribution Area in Kakheti on June 25, 2024

[1]Avtandil G. Amiranashvili, [1]Victor A. Chikhladze, [1,2]Mikheil G. Pipia, [1]Nodar D. Varamashvili

[1]M. Nodia Institute of Geophysics of I. Javakhishvili Tbilisi State University, Tbilisi, Georgia
avtandilamiranashvili@gmail.com
[2]Institute of Hydrometeorology of the Georgian Technical University, Tbilisi, Georgia

ABSTRACT

Some results of an expeditionary study of the tornado distribution area in Kakheti on June 25, 2024 are presented. The team of researchers visiting the Alaverdi Cathedral, had a meeting with His Eminence, Bishop of Alaverdi, Metropolitan David. The damage to the Alaverdi Cathedral and its surroundings was discussed in detail. Important information has been received regarding this issue. Further research was continued in the area surrounding the Alaverdi Cathedral and in the direction of the villages of Kvemo and Zemo Alvani. The probable place of origin of the tornado and the trajectory and area of its spread were determined. The damage caused by the tornado on the propagation trajectory was studied. More detailed studies of this natural phenomenon are planned in the near future.

Key words: *natural disasters, hurricane winds, tornadoes, distribution area, damage to facilities.*

Introduction

Wind is one of the main climate-forming factors. Georgia is characterized by complex physical-geographical and climatic conditions, as a result of which significant and abrupt changes in a number of meteorological parameters may be observed in certain regions. Therefore, in Georgia, as in other countries, special attention is paid to the study of wind regimes [1-6].

Wind frequency is influenced by local winds, so-called breezes, which cause seasonal and diurnal variations in the wind and cause changes in its regime [1, 3-5]. Research on the wind regime is important for the development of wind energy, the agricultural sector of the economy [3] and other areas. Strong winds often cause damage and destruction of residential and industrial facilities, shutdown of airports, snowstorms, and enhance the negative consequences of other dangerous hydrometeorological phenomena (intense precipitation, hail, etc.), casualties, etc. [7-10]. Wind speed determines the level of air pollution [11,12]. Wind is also one of the most important bioclimatic factors. Therefore, information about the wind regime is important for the development of the economy, resort and tourism sector [13] and for assessing various simple and complex bioclimatic characteristics for specific territories [14, 15].

The assessment of extreme wind values is especially important from the point of view that such phenomena, as a result of their destructive effects, can cause significant damage to the agro-economic and other infrastructure of the country [7,8,16-22]. In particular, article [23] presents information about the tornado in Kobuleti, and also discusses the issue of a more detailed study of these events in Georgia.

In the study [24], as a special case, considered a tornado that took place on September 25, 2021 in the terminal space of the city of Poti, which caused significant damage to one of the cargo terminals.

To assess the specified damage, photographic materials were used, filmed in automatic mode by video cameras of the surveillance system located on the territory of the terminal. With the help of these data, it was possible to estimate the speed of the vortex flows of the above spontaneous process (tornado). To determine the speed of movement of objects inside the tornado, the deceleration program "Mivavi Video Editor Plus" was used.

As a result of subsequent processing of the received video image, it was found that at one of the points in time, the speed of objects inside the tornado was 190 - 265 km/h. According to the so-called Fujita scale, the strength of a tornado is determined by the wind speed inside the tornado and related phenomena

(degree of destruction). As a result, it was found that the strength of the tornado in the considered territory of the terminal corresponds to the F2 value of the Fujita scale, which was due to the specifics of the location of the territory and the synoptic processes recorded in the considered period of time.

In this work some results of an expeditionary study of the tornado distribution area in Kakheti on June 25, 2024 are presented.

Study area, material and methods

Study area - Akhmeta municipality of Kakheti region of Georgia (Alaverdi Cathedral and surrounding areas, the villages of Kvemo Alvani and Zemo Alvani). On June 29, 2024, the authors of this article were in the specified area to study the movement of the tornado that developed on June 25, 2024, as well as its impact on the environment. One of the main tasks of the expedition was to identify the approximate location of the tornado formation.

The team of researchers visiting the Alaverdi Cathedral, had a meeting with His Eminence, Bishop of Alaverdi, Metropolitan David. The damage to the Alaverdi Cathedral and its surroundings was discussed in detail. Important information has been received regarding this issue. The team then continued to survey the above areas.

To solve this problem, the following were used: portable, as well as drone-mounted, photo and film equipment; JPS device; population survey; some materials that were posted on the Internet.

Alaverdi - Cathedral and Monastery is located in the Kakheti region of Akhmeta municipality, on Alazani valley, near the village of Alaverdi, 20 km from Telavi (Fig. 1). The temple is one of the largest church buildings in Georgia. Its height including dome is above 50 meters. The complex includes buildings: Alaverdi St. George Cathedral, defensive wall, chapel, Peikar-Khan's palace, wine cellar and bath.

Fig. 1. Alaverdi - Cathedral and Monastery.

Alaverdi Monastery was founded by Joseph Alaverdeli, one of the Assyrian fathers in the middle of the VI century. At the beginning of the XI century, Kvirike the King of Kakheti built a cathedral (which is known by the name of Alaverdi) at the site of the little church of St. George.

Alaverdi was one of the most outstanding chapels of medieval Georgia. Alaverdoba (September-October) was very popular ecclesiastical and public holiday. Which was celebrated not only by Georgians (from Kakheti, Kiziki, Ertso-Tianeti, Pshav-Khevsureti) but Kists And Dagestan people as well. The market was also held [https://georgiantravelguide.com/en/alaverdi].

Some results of the expedition's research are given below.

Results

Results in Table 1-3 and Fig. 2-8 are presented.

In Fig. 2 and Table 1 information about some locations the tornado distribution area in Kakheti on June 25, 2024. Table 1 also provides information on damage to various objects along the tornado's path.

Fig. 2. Some locations the tornado distribution area in Kakheti on June 25, 2024.

Table 1. Coordinates of locations the tornado distribution area in Kakheti according to Fig. 2.

Point N	Lat, °N	Long, °E	H, m, a.s.l.	Comment
0	42.03236	45.37742	446	Center dome of the Cathedral.
1	42.0356	45.38649	437	Agricultural cold storage farm. A large tree branch was broken and part of the building's roof collapsed.
2	42.03584	45.38761	435	To the direction of the tornado movement.
3	42.03664	45.38904	435	To the direction of the tornado movement.
4	42.03538	45.38543	437	Roof remains found.
5	42.0348	45.38156	439	Road to the cold storage farm (behind the Cathedral).
6	42.03424	45.37951	440	Damaged shed roof.
7	42.03395	45.37731	441	A damaged tree behind the Cathedral.
8	42.03405	45.37462	443	Shop between the cathedral and the village Alaverdi.
9	42.03354	45.38095	440	Farm with badly damaged roof next to the Cathedral.
10	42.03321	45.37783	443	Cemetery. Damaged trees and broken tiles. Next to the Cathedral.
11	42.03328	45.37783	443	Cemetery. A possible place where the cross fell.
12	42.03272	45.31199	466	Farm in the Zemo Alvani. Farmer - Chikhoshvili Khvicha.
13	42.02984	45.30888	466	Approximate location of tornado formation.
14	42.03351	45.32413	458	Damaged house under construction at the end of a farm in Zemo Alvani.
15	42.03317	45.32011	461	A heavily damaged farm roof in the path of a tornado.
16	42.03565	45.31116	467	The temple at Zemo Alvani, near the cemetery, is one of the tornado's travel points.

According to an eyewitness, farmer Kh. Chikhoshvili, it was possible to determine the approximate location of the tornado formation (Fig. 3; point 13 in Fig. 2 and Table 2).

Fig. 3. Approximate location of tornado origin. On the left is our photo, on the right is a still from the video of farmer Khvicha Chikhoshvili.

In particular, as follows from Fig. 2 and Table 2, distance from the approximate location of tornado formation to the center dome of the Cathedral is ≈ 5.7 km. The greatest distance we found from the site of tornado formation to point 3 is approximately 6.67 km. Thus, even without taking into account the tortuosity of the trajectory, the tornado covered a distance of at least 7 km. This fact, according to available data, is quite rare for the continental part of Georgia.

Table 2. Distance from approximate location of tornado formation to surveyed points according to Table 1.

N of points	0	1	2	3	4	5	6	7
Distance, km	5.67	6.45	6.54	6.67	6.36	6.03	5.86	5.67
N of points	8	9	10	11	12	14	15	16
Distance, km	5.45	5.97	5.71	5.71	0.41	1.32	1.00	0.67

Table 3 shows data on the distance from the central dome of the Cathedral to the points under study.

Table 3. Distance from the center dome of the Cathedral to surveyed points according to Table 1.

N of points	1	2	3	4	5	6	7	8	9	10	11
Distance, km	0.83	0.93	1.07	0.74	0.44	0.27	0.18	0.30	0.32	0.10	0.11

Along with the covering of the central dome of the cathedral, the tornado tore off the cross, which was found approximately 0.11 km from this dome on the territory of the cemetery (Fig. 2, Tables 1 and 3).

Other objects in the vicinity of the Cathedral were also damaged. So, for example, distance from the center dome of the Cathedral to agricultural cold storage farm (Point 1) is ≈ 0.83 km, and to farm with badly damaged roof (Point 9) is ≈ 0.32 km.

According to preliminary data, the tornado formed at approximately 5:10 p.m. and disintegrated at approximately 5:24 p.m.

In Fig. 4-8 for clarity, show photographs of some objects damaged by the tornado (farm roofs in the Zemo Alvani, covering of the dome of the Alaverdi Cathedral, badly damaged roof next to the cathedral, agricultural cold storage farm).

Fig. 4. Damaged farm roofs in the Zemo Alvani. (Point 15, Table 1).

Fig. 5. Removal of the covering of the dome of the Alaverdi Cathedral. The time interval between frames is 1 second. Video source: https://www.youtube.com/watch?v=ZFvYlzEhBr4.

Fig. 6. Damaged dome of Alaverdi Cathedral. Photo from drone.

Fig. 7. Farm with badly damaged roof next to the cathedral. (Point 9, Table 1).

Fig. 8. Agricultural cold storage farm. A part of the building's roof collapsed. Photo from drone. (Point 1, Table 1).

Fig. 9. Our group of scientists with His Eminence, Bishop of Alaverdi, Metropolitan David (in the center). From left to right - Nodar Varamashvili, Viktor Chikhladze, Avtandil Amiranashvili, Mikheil Pipia.

Finally, in Fig. 9 shows a photograph of His Eminence, Bishop of Alaverdi, Metropolitan David and the authors of this article against the background of the Alaverdi Cathedral with a damaged dome.

It is important to note that intensive work is currently underway to restore the damaged coverings of the cathedral and other parts of it.

Conclusion

In the near future, we plan more detailed studies of this natural phenomenon. In particular: determining the conditions for the formation of a tornado; determination of the trajectory and speed of movement of a tornado, taking into account radar data on thunderstorm and hail clouds in the study area; estimation of the speed of air flows inside a tornado; clarify the strength of the tornado, etc.

Acknowledgments

The authors thank everyone who assisted in carrying out the study: His Eminence, Bishop of Alaverdi, Metropolitan David; farmer - Chikhoshvili Khvicha; residents of the municipality; all persons and organizations that posted photos and video materials about the tornado in Kakheti on the Internet.

References

[1] Tavartkiladze K., Begalishvili N., Kharchilava J., Mumladze D., Amiranashvili A., Vachnadze J., Shengelia I., Amiranashvili V. Contemporary climate change in Georgia. Regime of some climate parameters and their variability. Monograph, ISBN 99928-885-4-7, Tbilisi, 2006, 177 p., (in Georgian).

[2] Elizbarashvili E.Sh., Elizbarashvili M.E. Stikhiynyye meteorologicheskiye yavleniya na territorii Gruzii. Tbilisi, Zeon, 2012, 104 s., (in Russian).

[3] Elizbarashvili E. Climate of Georgia. Monograph, Institute of Hydrometeorology of GTU, ISBN 978-9941-0-9584-9, Tbilisi, 2017, 360 p., (in Georgian).

[4] Amiranashvili A.G., Chikhladze V.A., Gvasalia G.D., Loladze D.A. Statistical Characteristics of the Daily Max of Wind Speedin Kakheti in 2017-2019. Journal of the Georgian Geophysical Society, e-ISSN: 2667-9973, p-ISSN: 1512-1127, Physics of Solid Earth, Atmosphere, Ocean and Space Plasma, v. 23(1), 2020, pp. 73-86. DOI: https://doi.org/10.48614/ggs2320202655

[5] Amiranashvili A., Chikhladze V., Gvasalia G., Loladze D. Statistical Characteristics of the Daily Max of Wind Speed in Kakheti in the Days with and without Hail Processes in 2017-2019. Int. Sc. Conf. „Modern Problems of Ecology“, Proceedings, ISSN 1512-1976, v. 7, Tbilisi-Telavi, Georgia, 26-28 September, 2020, pp.197-201.

[6] Kartvelishvili L., Tatishvili M., Amiranashvili A., Megrelidze L., Kutaladze N. Weather, Climate and their Change Regularities for the Conditions of Georgia. Monograph, Publishing House “UNIVERSAL”, ISBN: 978-9941-33-465-8, Tbilisi 2023, 406 p., https://doi.org/10.52340/mng.9789941334658

[7] Svanidze G.G., Tsutskiridze Ia. A. (edit.). Opasnie gidrometeorologicheskie protsessi na Kavkaze. L., Gidrometeoizdat, 1980, 288 p., (in Russian).

[8] Varazanashvili O., Tsereteli N., Amiranashvili A., Tsereteli E., Elizbarashvili E., Dolidze J., Qaldani L., Saluqvadze M., Adamia Sh., Arevadze N., Gventcadze A. Vulnerability, Hazards and Multiple Risk Assessment for Georgia. Natural Hazards, Vol. 64, Number 3, 2012, pp. 2021-2056. DOI: 10.1007/s11069-012-0374-3, http://www.springerlink.com/content/9311p18582143662/fulltext.pdf.

[9] AmiranashvilI A.G. Increasing Public Awareness of Different Types of Geophysical Catastrophes, Possibilities of Their Initiation as a Result of Terrorist Activity, Methods of Protection and Fight with Their Negative Consequences. Engaging the Public to Fight Consequences of Terrorism and Disasters. NATO Science for Peace and Security Series E: Human and Societal Dynamics, vol. 120. IOS Press, Amsterdam•Berlin•Tokyo•Washington, DC, ISSN 1874-6276, 2015, pp. 155-164. http://www.nato.int/science; http://www.springer.com; http://www.iospress.nl

[10] Pipia M., Elizbarashvili E., Amiranashvili A., Beglarashvili N. Dangerous Regions of Blizzard in Georgia. Annals of Agrarian Science, ISSN 1512-1887, vol. 17, No 4, 2019, pp. 403 – 408.

[11] Amiranashvili A., Bliadze T., Chikhladze V. Photochemical smog in Tbilisi. Monograph, Trans. of Mikheil Nodia institute of Geophysics, ISSN 1512-1135, vol. 63, Tb., 2012, 160 p., (in Georgian).

[12] Kukhalashvili V.G., Kordzakhia G.I. Gigauri N.G., Surmava A.A., Intskirveli L.N. Numerical Modelling of Dust Propagation in the Atmosphere of Tbilisi City: The Case of Background Eastern

Gentle Breeze. Journal of the Georgian Geophysical Society, ISSN: 1512-1127, Physics of Solid Earth, Atmosphere, Ocean and Space Plasma, v. 23(1), 2020, pp. 46-50.

[13] Saakashvili N.M., Tabidze M.Sh., Tarkhan-Mouravi I.D., Amiranashvili A.G., Melikadze G.I., Chikhladze V.A. To a Question about the Certification of the Health Resort and Tourist Resources of Georgia. "Modern Problems of Using of Health Resort Resources", Collection of Scientific Works of International Conference, Sairme, Georgia, June 10-13, 2010, ISBN 978-9941-0-2529-7, Tbilisi, 2010, pp. 175-180, (in Russian).

[14] Amiranashvili A.G., Japaridze N.D., Kartvelishvili L.G., Khazaradze K.R., Matzarakis A., Povolotskaya N.P., Senik I.A. Tourism Climate Index of in the Some Regions of Georgia and North Caucasus. Journal of the Georgian Geophysical Society, Issue B. Physics of Atmosphere, Ocean and Space Plasma, v. 20B, 2017, pp. 43–64.

[15] Amiranashvili A.G., Kartvelishvili L.G., Megrelidze L.D. Changeability of the Meteorological Parameters Associated with Some Simple Thermal Indices and Tourism Climate Index in Adjara and Kakheti (Georgia). Journal of the Georgian Geophysical Society, ISSN: 1512-1127, Physics of Solid Earth, Atmosphere, Ocean and Space Plasma, v. 21(2), Tbilisi, 2018, pp. 77-94.

[16] Beglarashvili N., Chikhladze V., Janelidze I., Pipia M., Tsintsadze T. Strong Wind on the Territory of Georgia in 2014-2018. Int. Sc. Conf. „Natural Disasters in the 21st Century: Monitoring, Prevention, Mitigation", Proceedings, ISBN 978-9941-491-52-8, Tbilisi, Georgia, December 20-22, 2021, pp. 19-22.

[17] Amiranashvili A., Jamrishvili N., Janelidze I., Pipia M., Tavidashvili Kh. Statistical Analysis of the Daily Wind Speed in Tbilisi in 1971-2016. Int. Conf. of Young Scientists "Modern Problems of Earth Sciences". Proceedings, ISBN 978-9941-36-044-2, Publish House of Iv. Javakhishvili Tbilisi State University, Tbilisi, November 21-22, 2022, pp. 159-163. http://openlibrary.ge/handle/123456789/10250

[18] Beglarashvili N., Jamrishvili N., Janelidze I., Pipia M., Tavidashvili Kh., Tsintsadze T. Some Results of Statistical Analysis of the Daily Wind Speed in Tbilisi in 1971-2020. Int. Sc. Conf. "Geophysical Processes in the Earth and its Envelopes". Proceedings, ISBN 978-9941-36-147-0, Publish House of Iv. Javakhishvili Tbilisi State University, November 16-17, 2023, pp. 151-155. http://www.openlibrary.ge/handle/123456789/10423

[19] Beglarashvili N., Pipia M., Jamrishvili N., Janelidze I. Some Results of the Analysis of Number of Days with Strong Wind in Various Regions of Georgia in 2019-2022. Georgian Geographical Journal, E-ISSN: 2667-9701, Vol.3 (2), 2023, 5 p. DOI: https://doi.org/10.52340/ggj.2023.03.02.05

[20] Varazanashvili O., Gaprindashvili G., Elizbarashvili E., Basilashvili, Ts., Amiranashvili A., Fuchs S. The First Natural Hazard Event Database for the Republic of Georgia (GeNHs). Catalog, 2023, 270 p. http://dspace.gela.org.ge/handle/123456789/10369; DOI: 10.13140/RG.2.2.12474.57286

[21] Elizbarashvili E.Sh., Varazanashvili O.Sh., Amiranashvili A.G., Fuchs F., Basilashvili Ts.Z. Statistical Characteristics of Hurricane Winds over Georgia for the Period 1961–2022. European Geographical Studies, E-ISSN: 2413-7197, 10(1), 2023, pp. 8-18, DOI: 10.13187/egs.2023.1.8, https://egs.cherkasgu.press

[22] Elizbarashvili E., Varazanashvili O., Lagidze L., Pipia M., Chikhladze V. About Strong Winds in Kakheti Region. Int. Sc. Conf. "Geophysical Processes in the Earth and its Envelopes". Proceedings, ISBN 978-9941-36-147-0, Publish House of Iv. Javakhishvili Tbilisi State University, November 16-17, 2023, pp. 156-160, (in Georgian). http://www.openlibrary.ge/handle/123456789/10424

[23] Chikhladze V., Jamrishvili N., Tavidashvili Kh. Tornadoes in Georgia. Int. Sc. Conf. „Natural Disasters in the 21st Century: Monitoring, Prevention, Mitigation", Proceedings, ISBN 978-9941-491-52-8, Tbilisi, Georgia, December 20-22, 2021, pp. 23-26.

[24] Chikhladze V., Amiranashvili A., Gelovani G., Tavidashvili Kh., Laghidze L., Jamrishvili N. Assessment of the Destructive Power of a Tornado on the Territory of the Poti Terminal on September 25, 2021. II International Scientific Conference "Landscape Dimensions of Sustainable Development Science – Carto/GIS – Planning – Governance", Dedicated to the 75th Anniversary of Professor Nikoloz (Niko) Beruchashvili, Proceedings, 12-16 September 2022, Tbilisi, Georgia, Ivane Javakhishvili Tbilisi State University Press, 2022, ISBN 978-9941-36-030-5, pp. 275-281, (in Georgian). http://www.dspace.gela.org.ge/handle/123456789/10120

კახეთში 2024 წლის 25 ივნისს ტორნადოს გავრცელების არეალის ექსპედიციური კვლევის ზოგიერთი შედეგი

ა. ამირანაშვილი, ვ. ჩიხლაძე, მ. ფიფია, ნ. ვარამაშვილი

რეზიუმე

წარმოდგენილია 2024 წლის 25 ივნისს კახეთში ტორნადოს გავრცელების არეალის ექსპედიციური კვლევის ზოგიერთი შედეგი. ალავერდის საკათედრო ტაძარში მეცნიერთა ჯგუფს შეხვედრა ჰქონდა მის მაღალყოვლადუსამღვდელესოებასთან აბბა ალავერდელ მიტროპოლიტ - დავითთან. დაწვრილებით იქნა განხილული ალავერდის ტაძრის დაზიანებები. მიღებული იქნა მნიშვნელოვანი ინფორმაცია ამ საკითხთან დაკავშირებით. შემდგომი კვლევა გაგრძელდა ტაძრის მიმდებარე ტერიტორიაზე და სოფლების ქვემო და ზემო ალვანის მიმართულებით. დადგენილი იქნა ქარბორბალას წარმოშობის სავარაუდო ადგილი, გავრცელების ტრაექტორია და არეალი. შესწავლილი იქნა გავრცელების ტრაექტორიაზე ქარბორბალათი გამოწვეული დაზიანებები. უახლოეს მომავალში იგეგმება ამ ბუნებრივი ფენომენის უფრო დეტალური შესწავლა.

საკვანძო სიტყვები: სტიქიური უბედურება, ქარიშხლი, ტორნადო, გავრცელების არეალი, ობიექტების დაზიანება.

Некоторые результаты экспедиционного исследования ареала распространения торнадо в Кахетии 25 июня 2024 года

А. Амиранашвили, В. Чихладзе, М. Пипиа, Н. Варамашвили

Резюме

Представлены некоторые результаты экспедиционного исследования района распространения смерча в Кахетии 25 июня 2024 года. Группа исследователей, посетившая Алавердский собор, встретилась с Высокопреосвященнейшим епископом Алавердским митрополитом Давидом. Подробно обсуждался ущерб, причиненный собору Алаверди и его окрестностям. По данному вопросу получена важная информация. Дальнейшие исследования были продолжены в районе Алавердского собора и в направлении сел Квемо и Земо Алвани. Определены вероятное место зарождения смерча, траектория и район его распространения. Изучен ущерб, причиняемый смерчем на траектории распространения. В ближайшее время планируются более детальные исследования этого природного явления.

Ключевые слова: стихийные бедствия, ураганные ветры, торнадо, ареал распространения, повреждение объектов.

Journal of the Georgian Geophysical Society, e-ISSN: 2667-9973, p-ISSN: 1512-1127
Physics of Solid Earth, Atmosphere, Ocean and Space Plasma, v. 27(1), 2024, pp. 77 – 90

Variability of the Holiday Climate Index in Tsalka (Georgia)

[1]Avtandil G. Amiranashvili, [2,3] Liana G. Kartvelishvili, [4,5]Andreas Matzarakis

[1]M. Nodia Institute of Geophysics of the I. Javakhishvili Tbilisi State University, Tbilisi, Georgia
[2]Institute of Hydrometeorology of the Georgian Technical University, Tbilisi, Georgia
[3]Georgian National Environmental Agency, Tbilisi, Georgia
[4]Faculty of Environment and Natural Resources, University of Freiburg, Freiburg im Breisgau, Germany
[5]Democritus University of Thrace, Komotini, Greece

ABSTRACT

Data about long-term monthly average values of Holiday Climate Index (HCI) for Tsalka (Georgia) are presented. Detailed analysis of the monthly, seasonal and annual HCIs values over the 60-year period (1956-2015) are carried out. The variability of the HCI in 1986-2015 compared to 1956-1985 was studied, and the trends of the HCI in 1956-2015 were also investigated.

Key Words: *Bioclimate, Tourism Climate Index, Holiday Climate Index.*

Introduction

The formation and successful functioning of the resort and tourism economy of an area largely depends on its geographical location, relief, historical-cultural and natural monuments, vegetation, the presence of natural disasters, weather, climate, etc. [1-5]. At the same time, weather and climate are the two main factors determining the bioclimatic resources of the territory. Accordingly, the study of these resources plays an important role for the organization and development of the resort and tourism industry in the area [6-12].

In recent decades in various studies, including Georgia, many climate indices for tourism have been used [6-17]. However, the most widely known index used both in the past and in the present is the Tourist Climate Index (TCI), proposed by Mieczkowski [18].

In southern Caucasus countries, the monthly TCI was first calculated for Tbilisi (Georgia) [19] and then for many other locations in the Caucasus (Armenia, Azerbaijan, North Caucasus, etc.) [3, 20-26]. The study [27] presents the first TCI calculations for Zimbabwe. In the work [28] evaluated the climate comfort of Argentina as an intangible resource for tourism. The applicability of the tourism climate index for Saudi Arabia in [29] is presented. In [30] assessing climate change impacts on tourism demand in Turkey through the Tourism Climate Index is carried out.

Despite the wide application of the TCI, it has been subject to substantial critiques [31]. The four key deficiencies of the TCI include the following: (1) the subjective rating and weighting system of climatic variables; (2) it neglects the possibility of the overriding influence of physical climatic parameters (e.g., rain, wind); (3) the low temporal resolution of climatic data (i.e., monthly data) has limited relevance for tourist decision-making; and (4) it neglects the varying climatic requirements of major tourism segments and destination types (i.e., beach, urban, winter sports tourism).

To overcome the above limitations of the TCI, the Holiday Climate Index (HCI) was developed to more precisely assess the climatic suitability of tourism destinations. The word "Holiday" was chosen to better reflect what the index was designed for (i.e., leisure tourism), as tourism is much broader by definition ("Tourism is a social, cultural and economic phenomenon which entails the movement of people to countries or places outside their usual environment for personal or business/professional purposes") [32-36]. In the same works, comparisons between the HCI and TCI were made.

A comparison of the Holiday Climate Index and Tourism Climate Index at several locations in Georgia and the North Caucasus in [37-39] are presented. The long-term average HCIs for 12 Kakheti locations (Akhmeta, Dedoplistskaro, Gombori, Gurjaani, Kvareli, Lagodekhi, Omalo, Sagarejo, Shiraki, Telavi, Tsnori and Udabno) in [40] are presented. For 6 stations in this region (Dedoplistskaro, Gurjaani, Kvareli, Lagodekhi,

Sagarejo and Telavi), detailed analyses of the monthly, seasonal and annual HCIs over the 60-year period (1956-2015) were carried out.

It was found that there is a high degree of correlation between the HCI and TCI. However, considering that the TCI is calculated for the so-called "average tourist" (regardless of gender, age, physical condition), the value and category of this index are lower than the HCI values and categories. In general, based on our estimation, the HCI more adequately determines the bioclimatic state of the environment for the development of various types of tourism than does the TCI [37-40].

It should be noted that the scale of various bioclimatic indices (including TCI and HCI) is quite consistent with data on public health in various regions of Georgia [15, 41,42], as well as on the spread of the COVID-19 virus in Tbilisi [43].

Great importance is attached to studying the impact of climate change on TCI and HCI.

In study [9] noted that the TCI and HCI are good indicators of the environmental conditions for leisure activities in the Canary Islands. Using the Regional Climate Model, it is shown that by 2030-2059 and 2070-2099, tourism performance is expected to improve significantly in the winter and off-season but deteriorate in the summer months, including October, in the southeast, which is where hotels are currently located.

The aim of the study [44] is to assess the future HCI performances of urban and beach destinations in the greater Mediterranean region. For this purpose, HCI scores for the reference (1971-2000) and future (2021-2050, 2070-2099) periods were computed. HCI: The urban results showed that the Canary Islands have suitable conditions for tourism during almost all four seasons and all periods, which will have certain implications when other core Mediterranean competitors lose their relative climatic attractiveness. The HCI:Beach results for the summer season showed that Las Canteras, Alicate, Pampelonne, Myrtos, Golden Sands and Edremit all pose very good to excellent conditions without any Humidex risks for the extreme future scenario (2070-2099).

The study [45] provides the first application of a tourism climate index in the tropical southwest Indian Ocean, applying the recently developed Holiday Climate Index (HCI) for Réunion Island. The suitability of this index is evaluated for the case of this French department, with a particular focus on air conditioning availability in tourism accommodation establishments as this index excludes night-time thermal comfort. Both iterations of the HCI (HCI_{Beach} and HCI_{Urban}) are computed with meteorological data from Roland Garros Airport for the period 1991–2020, exploring monthly, annual, and seasonal climatic suitability. Mean monthly HCI scores reveal considerable seasonality in climatic suitability for tourism on the island with scores ranging from 89.3 (Excellent) to 36.9 (Marginal) for the HCI_{Beach} and 85.0 (Excellent) to 27.5 (Unacceptable) for the HCI_{Urban}, with more favourable scores calculated for July and August, displaying a clear austral winter peak seasonal classification. Over the 30-year period, there is no statically significant change in mean annual climatic suitability, and at a monthly scale, only one month of the year for each index displays statistically significant trends. These results are important in informing tourism strategies for the island to maximise visitor satisfaction through targeting advertising more deliberately for peak touristic climate suitability during the winter months.

The purpose of study [46] was to investigate the status of urban tourism climate in West Azerbaijan province using Holiday Climate Index (HCI). At first, daily meteorological data of 8 major cities in the province were collected for a ten years period (2008-2017) and after data processing and database preparation, the HCI values were calculated daily and monthly. The results showed that Mahabad with 197 days has the highest number of comfortable days in this province. Khoy with 192 days, Salmas with 182 days, Urmia and Piranshahr with 181 days, Sardasht with 171 days, Takab with 164 days and Maku with 155 days are next. in these days, there are ideal conditions for recreation and tourism. May and September are also the best months for tourism activities in West Azerbaijan province.

In [11] the tourism climate comfort of Longji Terraced Fields from 2002 to 2022 is discussed. The results show that the current Holiday Climate Index and Modified Climate Index for Tourism are not suitable for evaluating the Longji Terraces. Adjustments were made to these indices to account for the high annual precipitation and relative humidity of Longsheng. Combining extensive questionnaire surveys, it was found that the improved evaluation model better reflects tourists' perceptions of climate comfort. Analysis indicates that when the modified model value is above 70, tourist satisfaction exceeds 80%. The most comfortable tourism periods for the Longji Terraces are August, September, and October, while the least comfortable periods are January, February, and March. This study helps to understand the seasonal variations in tourism climate comfort at Longji Terraced Fields and provides a scientific basis for local tourism industry responses to climate change, thereby increasing tourism revenue.

The aim of study [47] is to assess the future HCI performance of urban and beach destinations in the greater Mediterranean region. For this purpose, HCI scores for the reference (1971–2000) and future (2021–

2050, 2070–2099) periods were computed with the use of two latest greenhouse gas concentration trajectories, RCP 4.5 and 8.5, based on the Middle East North Africa (MENA) Coordinated Regional Downscaling Experiment (CORDEX) domain and data. The outputs were adjusted to a 500 m resolution via the use of lapse rate corrections that extrapolate the climate model topography against a resampled digital elevation model. All periodic results were seasonally aggregated and visualized on a (web) geographical information system (GIS). The web version of the GIS also allowed for a basic climate service where any user can search her/his place of interest overlaid with index ratings. Exposure levels are revealed at the macro scale while sensitivity is discussed through a validation of the climatic outputs against visitation data for one of Mediterranean's leading destinations, Antaly.

The study [48] derived the Holiday Climate Index (HCI: Coast, HCI: Urban, and HCI: Combined) in the Mediterranean coastal provinces of Türkiye from 1976 to 2020. Utilizing the derived indices, the effects of climate-related holiday comfort on the number of tourist arrivals as well as on overnight stays between 1976 and 2020 were examined by panel data analysis. The study examined how comfort patterns could change during the period 2026–2050 under the pessimistic RCP8.5 scenario. It was detected that the comfort level significantly and positively affects the number of arrivals and overnight stays of tourists. Besides, comfort levels were found to deteriorate in the period 2026–2050 compared to the reference period, 1976–2020. As the comfort conditions get worse, the number of tourist arrivals and overnight stays is expected to decline in the future.

In [49] a study was conducted to analyze the holiday climate index (HCI) for Sri Lanka's urban and beach destinations. The analysis covered historical years (2010–2018) and forecasted climatic scenarios (2021–2050 and 2071–2100), and the results were presented as colored maps to highlight the importance of HCI scores. Visual analysis showed some correlation between HCI scores and tourist arrivals, but the result of the overall correlation analysis was not significant. However, a country-specific correlation analysis revealed interesting findings, indicating that the changing climate can be considered among other factors that impact tourist arrivals. The research proposes that authorities assess the outcomes of the study and conduct further research to develop adaptive plans for Sri Lanka's future tourism industry. The study also investigated potential scenarios for beach and urban destinations under two climate scenarios (RCP 4.5 and RCP 8.5) for the near and far future, presenting the findings to tourism industry stakeholders for any necessary policy changes.

In study [36] to investigate the TCI and HCI index to determine nature tourism in the Khamir-Qeshm mangrove forests from 1996 to 2021. The results of TCI revealed that the best tourism season is autumn late and winter in December, January, and February while the most unfavorable climatic conditions are June, July, August, September, and October. Based on the results of HCI, the most favorable tourism season is related to winter and especially March month, while the status of this index is acceptable from June to October. In general, the results of TCI and HCI indicate that autumn to the end of winter is the best time in terms of tourism climate, and spring to summer late, has the most unfavorable conditions for visitor's presence due to the extreme heat, high humidity, and sultry climate of the area. The statistical analysis of TCI and HCI also indicates that there is a significant and direct relationship between these two indicators with climatic variables and with the increase of the final coefficient, the climatic conditions of the area will be more favorable for tourists' presence. Considering the increasing tourism industry and nature tourism development in Khamir-Qeshm mangrove forests, proper planning in accordance with the favorable conditions of the tourism climate can protect this area, provide suitable infrastructure and facilities for tourists, and will also help create conditions to understand the comfortable feeling and tourist's satisfaction.

Study [50] presents an assessment of climate suitability for outdoor leisure activities in Romania using the Holliday Climate Index (HCI) for the near future (2021–2040), focusing on unfavorable and good climate conditions. The analysis employs data from an ensemble of model simulations in the context of RCP4.5 and RCP8.5 climate change scenarios. The results indicate that the number of days with low weather suitability is decreasing in almost the entire country, especially during the warm season, while during the winter and spring, extended regions may be characterized by a higher number of days favorable for outdoor activities than during the current climate. An estimation of the impact of climate change on tourism flux in Romania is further carried out, suggesting that the increasing attractivity of climate conditions may lead to an increased number of tourist overnights in the near future, and this will be more pronounced in rural destinations.

Assessing the impact of dust events on the Holiday Climate Index in the Taklimakan Desert region in [51] is presented.

Detailed information on the variability of the monthly values of the Holiday Climate Index in Tbilisi in 1956-2015 is presented in [52]. It also presents data on the interval forecasts of HCI variability in Tbilisi for the next few decades.

In the work [38] is performed a detailed analysis of monthly, seasonal and annual HCI values during a 60-year period (1956-2015) for 13 mountainous locations in Georgia (Bakhmaro, Bakuriani, Borjomi, Goderdzi, Gudauri, Khaishi, Khulo, Lentekhi, Mestia, Pasanauri, Shovi, Stepantsminda, and Tianeti) and compared HCIs and TCIs of monthly values for three points in Georgia (Goderdzi, Khulo and Mestia) based on data from 1961 to 2010. The variability data of the HCI in 1986-2015 compared to those in 1956-1985 and the trends of the HCI in 1956-2015 are also presented. Using Mestia as an example, the expected changes in the monthly, seasonal and annual HCIs of 2041-2070 and 2071-2100 were assessed. Some results of this work were used in [5, 53].

Finally, in the work [54] an analysis of data on the long-term average values of the Holiday Climate Index (HCI) for 8 settlements in the Kvemo Kartli region of Georgia (Bolnisi, Gardabani, Dmanisi, Tetri Tskaro, Marneuli, Tsalka, Manglisi, Rustavi) is presented. The intra-annual distribution of HCI values was studied; correlations between individual stations were determined based on average monthly and seasonal HCI values; it was found that the regression equations for the intra-annual variation of average monthly HCI values for all points of Kvemo Kartli have the form of a ninth-order polynomial; categories of average monthly and seasonal HCI values in the specified settlements of Kvemo Kartli were determined; a comparison was made of the statistical characteristics of average monthly HCI values in 8 points of Kvemo Kartli with the indicated characteristics in Bolnisi, Gardabani, Marneuli, Rustavi (height of stations above sea level $H < 1$ km) and in Dmanisi, Tetri Tskaro, Tsalka, Manglisi ($H > 1$ km), and a corresponding analysis of the repeatability of HCI categories was conducted. It is shown that the bioclimatic conditions in Kvemo Kartli are favourable for the development of the resort and tourism industry for all months of the year. A visual map of the distribution of mean monthly HCI categories on the territory of Kvemo Kartli has been constructed.

This work is a continuation of the study [54]. Analysis results of investigations of variability of the Holiday Climate Index (HCI) in Tsalka in 1956-2015 are presented below.

Study area

Tsalka (41.60 N°, 44.08 E°, 1458 m, a.s.l.) is a town and municipality center in southern Georgia's Kvemo Kartli region.

The district had a population of 2326. There are important historical monuments in Tsalka: Kldekari Fortress (ninth century) and the church of St. George in Dashbashi (tenth-eleventh centuries). Tsalka Canyon (formerly Dashbashi Canyon) and its new bridge are also interesting tourist attractions.

Tsalka Canyon in Georgia is a deep mountain gorge situated 100 kilometers west of Tbilisi in Tsalka Municipality. Long popular with visitors, the canyon has become even more alluring since a touristic center opened on the site in the summer of 2021, providing plenty of options for comfort and adventure in a picturesque setting.The canyon, measuring 7 kilometers long and 300 meters deep, was formed on a volcanic plateau through the process of erosion. This natural wonder is defined by steep slopes covered in lush vegetation, at the bottom of which flows the rapid waters of the Khrami River (Fig. 1). Yet the major attraction of Tsalka Canyon is its spectacular cluster of cascading waterfalls (Fig. 2).

In the summertime, their emerald waters glisten among the lavish green foliage, while in winter the waterfalls freeze, creating a frosty fairytale landscape.Visitors can easily travel from Tbilisi to Dashbashi Canyon (Tsalka Canyon) on a 2-hour drive one way. Once you reach the canyon’s entrance you must park your car and walk downhill along a well-marked mountain path that winds for 1.5 kilometers to the falls. The most challenging part of the trek is the steep climb back, but guests should also be prepared to walk across the stone-covered banks of the Khrami River. Most people need about 1-1.5 hours to complete the round-trip Dashbashi Canyon hike.In August 2021, a new complex opened at Tsalka Canyon with the aim of developing the nature reserve into an attractive touristic area.

The complex includes a 240-meter-long glass bridge right above the canyon, with a diamond-shaped cafe bar in the middle. There is also a visitor center, a high-quality hotel complex with cottages, an open garden restaurant, swimming pools, bridges, camping sites and a 500-meter paved road to the canyon river.A trip to Tsalka Canyon makes an ideal getaway from Tbilisi and can also be a stopping point on a more extensive journey. Near the canyon lies the picturesque Tsalka Lake, a favourite destination of Georgian fishermen. You can also hike to the ruins of the 9th-century Kldekari Fortress, and although little is left of this once-powerful citadel, the trek to it is rather charming. Another option is to combine a visit to Tsalka Canyon with a trip to Poka Nunnery of Saint Nino, situated on the shores of Paravani Lake [https://www.advantour.com/georgia/tsalka-canyon.htm]

Tsalka Canyon is a rewarding outdoor destination that will deepen your appreciation of Georgia's natural beauty [https://en.wikipedia.org/wiki/Tsalka].

Fig. 1. Tsalka Canyon [https://www.advantour.com/georgia/tsalka-canyon.htm; https://www.tripadvisor.com/AttractionProductReview-g294195-d17566244-Trip_to_The_Diamond_Bridge_and_Dashbashi_Canyon-Tbilisi.html]

Fig. 2. Dashbashi waterfall, situated at the bottom of Tsalka Canyon. [https://en.wikipedia.org/wiki/Tsalka_Canyon#/media/File:Dashbashi_24.jpg]

Material and methods

For the monthly mean values of HCI calculation data of National Environmental Agency of Georgia from 1956 to 2015 were used: T_{max} - maximum air temperature, °C; RH – air relative humidity, %; P - precipitation, mm; CC – total cloud cover, degree; W wind speed, m/s (Table 1 and 2). HCI values and their categories were determined in accordance with the methodology described in the works [31, 37-39].

In the work analysis of data is carried out with the use of the standard statistical analysis methods. The following designations will be used below: Mean – average values; Min – minimal values; Max - maximal values; Range - variational scope; St Dev - standard deviation; σ_m – standard error; C_v, % – coefficient of variation (C_v = 100·St Dev/Average); 95%(+/-) - 95% confidence interval of mean; I)1956÷1985 – mean value of meteorological parameters and HCI in 1956-1985, first period; II)1986÷2015 - second period; t - Student criterion; α - the level of significance; Diff.(II-I) – difference between mean values of meteorological parameters and HCI in second and first periods were determined with use of Student criterion (α≤0.15); R - coefficient of linear correlation (α≤0.15); Δ_1 = 100· Diff.(II-I)/Mean(1956-2015) - relative variability of the difference between the mean values of the HCI in two periods of time relative to the mean value for the entire observation period, %; Δ_2 = 100·[HCI(2015) – HCI(1956)]/Mean(1956-2015) - relative variability of the difference between the HCI values in 2015 and 1956, determined by linear regression equations, in relation to the mean value for the entire observation period, %; a and b - coefficients of the linear equation of the trend of HCI values (HCI = a·year/month + b).

Table 1. Monthly values of meteorological parameters for HCI calculation in Tsalka during the cold season in three period of time.

Variable	Period	Jan	Feb	Mar	Oct	Nov	Dec	Cold	Year
T_{max}, °C	1956-2015	1.8	2.3	5.8	13.7	8.2	3.9	6.0	12.2
	II)1986-2015	2.1	2.7	6.4	14.1	8.3	3.9	6.3	12.6
	I)1956-1985	1.5	1.9	5.1	13.3	8.1	3.8	5.6	11.8
	Diff.(II-I)	0.6	0.9	1.3	0.8	0.2	0.1	0.6	0.8
	t	0.86	1.28	2.17	1.55	0.34	0.15	1.94	3.56
	α	No	No	0.03	0.13	No	No	0.06	<0.01
RH, %	1956-2015	73.9	74.6	75.2	79.6	77.0	74.6	75.8	76.8
	II)1986-2015	73.0	73.2	72.5	80.2	76.5	73.8	74.9	76.0
	I)1956-1985	74.9	76.0	77.9	78.9	77.6	75.5	76.8	77.6
	Diff.(II-I)	-1.9	-2.8	-5.4	1.3	-1.1	-1.7	-1.9	-1.6
	t	1.05	1.96	3.62	1.03	0.71	1.09	2.46	2.21
	α	No	0.05	<0.01	No	No	No	0.02	0.03
P, mm	1956-2015	21.5	28.1	38.9	49.8	33.5	22.7	32.4	57.0
	II)1986-2015	19.6	28.3	37.4	53.0	34.7	23.6	32.8	55.3
	I)1956-1985	23.4	27.9	40.3	46.6	32.3	21.7	32.0	58.7
	Diff.(II-I)	-3.7	0.4	-2.9	6.4	2.5	1.9	0.8	-3.4
	t	0.98	0.10	0.56	0.93	0.44	0.50	0.34	1.38
	α	No	No	No	No	No	No	No	No
CC	1956-2015	6.0	6.3	6.8	6.5	6.3	6.0	6.3	6.5
	II)1986-2015	6.2	6.5	6.8	7.0	6.3	6.3	6.5	6.7
	I)1956-1985	5.7	6.2	6.8	5.9	6.2	5.7	6.1	6.3
	Diff.(II-I)	0.5	0.4	0.0	1.0	0.1	0.6	0.4	0.4
	t	2.02	1.43	0.03	3.78	0.36	2.02	3.98	4.91
	α	0.05	0.15	No	<0.01	No	0.05	<0.01	<0.01
W, m/s	1956-2015	1.7	1.6	1.5	1.1	1.3	1.6	1.5	1.3
	II)1986-2015	1.4	1.2	1.3	0.8	1.0	1.2	1.2	1.1
	I)1956-1985	2.0	1.9	1.8	1.4	1.6	1.9	1.7	1.5
	Diff.(II-I)	-0.6	-0.6	-0.5	-0.5	-0.5	-0.6	-0.6	-0.5
	t	3.65	3.24	3.94	6.42	4.17	5.76	6.84	7.17
	α	<0.01	<0.01	<0.01	<0.01	<0.01	<0.01	<0.01	<0.01

In Tables 1,2 data on monthly values of meteorological parameters for HCI calculation in Tsalka during three period of time are presented. In particular, as follows from these tables, in 1956-2015 the average monthly values of these meteorological elements vary within the following limits: T_{max} - 1.8 °C (Jan) - 22.4 °C (Jul, Aug); RH - 73.9% (Jan) - 79.6% (Oct); P - 21.5 mm (Jan) - 116.8 mm (May); CC - 6.0 degree (Jan, Dec) - 7.2 degree (May); W - 1.0 m/s (Jul, Aug) - 1.7 m/s (Jan).

Table 2. Monthly values of meteorological parameters for HCI calculation in Tsalka during the warm season in three period of time.

Variable	Period	Apr	May	Jun	Jul	Aug	Sep	Warm	Year
T_{max}, °C	1956-2015	11.8	16.1	19.7	22.4	22.4	18.6	18.5	12.2
	II)1986-2015	12.1	16.2	20.2	22.9	23.2	19.2	19.0	12.6
	I)1956-1985	11.6	16.0	19.1	21.9	21.6	18.0	18.1	11.8
	Diff.(II-I)	0.5	0.2	1.1	1.0	1.6	1.2	0.9	0.8
	t	0.84	0.48	3.19	2.71	3.57	2.87	4.10	3.56
	α	No	No	<0.01	0.01	<0.01	<0.01	<0.01	<0.01
RH, %	1956-2015	76.1	78.7	78.5	77.5	77.4	79.0	77.9	76.8
	II)1986-2015	75.0	77.8	77.8	77.6	77.0	78.1	77.2	76.0
	I)1956-1985	77.2	79.5	79.2	77.3	77.8	79.9	78.5	77.6
	Diff.(II-I)	-2.2	-1.7	-1.3	0.3	-0.7	-1.8	-1.2	-1.6
	t	1.48	1.24	0.89	0.18	0.48	1.64	1.18	2.21
	α	0.14	No	No	No	No	0.11	No	0.03
P, mm	1956-2015	73.0	116.8	115.6	64.9	65.4	53.5	81.5	57.0
	II)1986-2015	75.8	108.5	122.7	56.2	59.5	43.7	77.7	55.3
	I)1956-1985	70.1	125.1	108.5	73.7	71.2	63.2	85.3	58.7
	Diff.(II-I)	5.7	-16.7	14.2	-17.5	-11.7	-19.5	-7.6	-3.4
	t	0.71	1.35	1.28	2.29	1.22	2.30	1.67	1.38
	α	No	No	No	0.03	No	0.03	0.10	No
CC	1956-2015	7.1	7.2	6.6	6.6	6.5	6.4	6.7	6.5
	II)1986-2015	7.2	7.3	6.8	6.8	6.7	6.5	6.9	6.7
	I)1956-1985	6.9	7.0	6.3	6.3	6.4	6.2	6.5	6.3
	Diff.(II-I)	0.3	0.2	0.4	0.6	0.3	0.3	0.4	0.4
	t	1.41	1.16	2.03	2.62	1.25	1.03	3.17	4.91
	α	0.15	No	0.05	0.01	No	No	<0.01	<0.01
W, m/s	1956-2015	1.3	1.2	1.2	1.0	1.0	1.1	1.1	1.3
	II)1986-2015	1.1	1.0	1.0	0.8	0.8	0.9	1.0	1.1
	I)1956-1985	1.6	1.3	1.4	1.2	1.2	1.3	1.3	1.5
	Diff.(II-I)	-0.5	-0.3	-0.4	-0.4	-0.4	-0.3	-0.4	-0.5
	t	4.29	2.41	3.80	3.88	5.31	4.12	5.56	7.17
	α	<0.01	<0.01	<0.01	<0.01	<0.01	<0.01	<0.01	<0.01

In 1986-2015, compared to 1956-1985, significant variability in the average monthly values of these meteorological parameters occurred as follows. T_{max} - growth in March and from June to October with a range of variability from 0.8 °C (Oct) to 1.6 °C (Aug); RH - decrease from February to April and in September with a variability range from -5.4% (Mar) to -1.8% (Sep); P - decrease only in September (-19.5 mm) and July (-17.5 mm); CC - growth in all months except March, May, August, September and November with a variability range from 0.3 degree (Apr) to 1.0 degree (Oct); W, m/s - decrease in all months of the year with a variability range from - 0.6 m/s (Jan, Feb, Dec) to -0.3 m/s (May, Sep). Thus, during the time period under study, the greatest variability among the studied meteorological parameters was observed for wind speed (all months of the year), the least - for precipitation (two months).

Results of analysis of studies of the variability of the Holiday Climate Index in Tsalka in 1956-2015 against the backdrop of climate change are presented below.

Results and discussion

The results in Fig. 3-6 and Tables 3,4 are presented. Fig. 3,4 and Tables 3,4 present data on the statistical characteristics and changeability of monthly and seasonal values of HCI in Tsalka in 1956-2015.

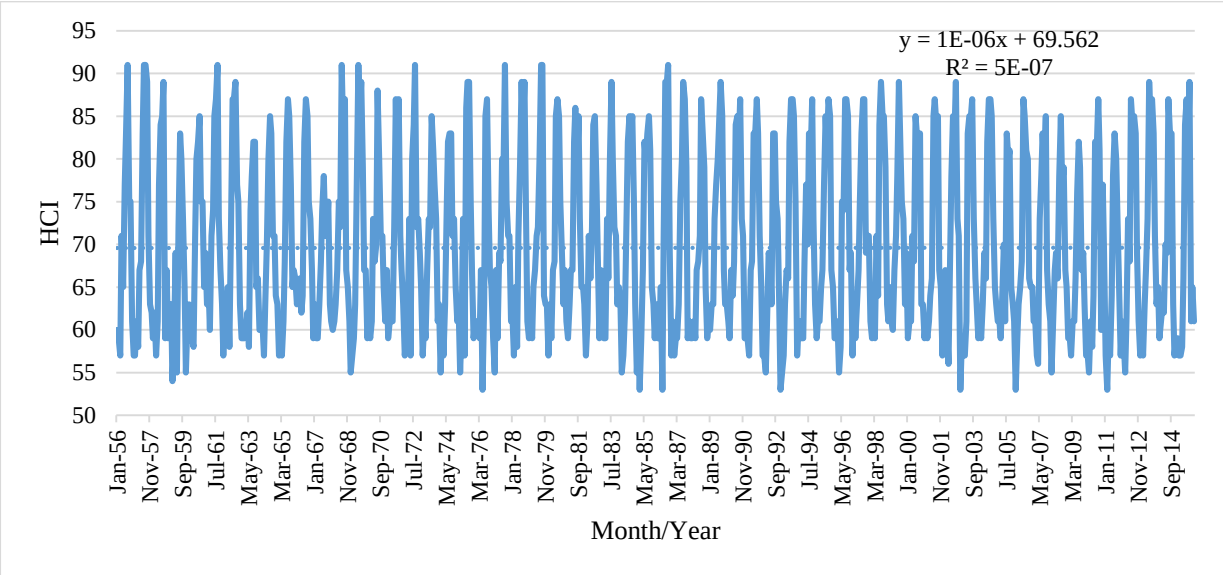

Fig. 3. Variability of monthly values of HCI in Tsalka in 1956-2015.

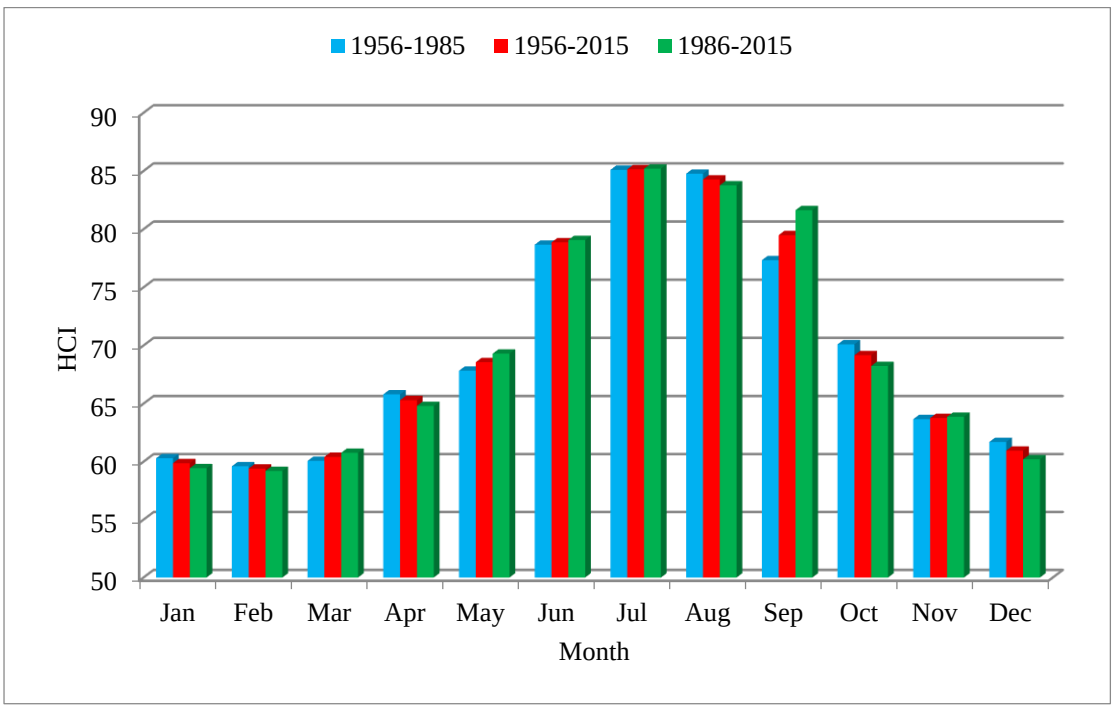

Fig. 4. Monthly values of HCI in Tsalka in three period of time.

In the period from 1956 to 2015 (Fig. 3,4 Tables 3, 4) monthly HCI values varied from 53.0 (“Acceptable”, Jan, Feb, May, Dec) to 91.0 (“Ideal”, Sep). The mean monthly HCI values for the entire observation period varied from 59.4 (“Acceptable”, Feb) to 85.2 (“Excellent”, Jul). Maximal value of Range for monthly values of HCI is 32.0 (Sep), Minimal - 12.0 (Mar).

Table 3. Statistical characteristics of HCI in Tsalka during the cold season (1956-2015).

Parameter	Jan	Feb	Mar	Oct	Nov	Dec	Cold	Year
Mean	59.9	59.4	60.4	69.2	63.8	61.0	62.3	69.6
Min	53.0	53.0	55.0	59.0	55.0	53.0	58.7	65.6
Max	67.0	67.0	67.0	79.0	77.0	69.0	65.5	72.3
Range	14.0	14.0	12.0	20.0	22.0	16.0	6.8	6.8
St Dev	2.8	3.0	2.8	4.2	3.9	3.5	1.6	1.6
σ_m	0.37	0.39	0.36	0.55	0.51	0.46	0.21	0.20
C_v (%)	4.7	5.0	4.6	6.1	6.1	5.8	2.6	2.2
95%(+/-)	0.7	0.8	0.7	1.1	1.0	0.9	0.4	0.4
II)1986÷2015	59.4	59.2	60.8	68.2	63.9	60.2	62.0	69.6
I)1956÷1985	60.3	59.6	60.1	70.1	63.7	61.7	62.6	69.6
Diff.(II-I)	-0.9	-0.4	0.7	-1.9	0.2	-1.5	-0.6	0.0
t	-1.19	-0.52	0.98	-1.73	0.20	-1.68	-1.50	0.11
α(t)	No	No	No	0.09	No	0.10	0.14	No
R	0.17	0.20	0.16	0.27	0.06	0.12	0.20	0.03
Δ_1, %	-1.4	-0.7	1.2	-2.7	0.3	-2.5	-1.0	0.1
α(R)	No	0.13	No	0.03	No	No	0.13	No
a	-0.0277	-0.0334	0.0257	-0.0663	0.0143	-0.0233	-0.0184	-0.0023
b	114.9	125.7	9.4	200.8	35.3	107.1	98.9	74.1
Δ_2, %	-2.7	-3.3	2.5	-5.7	1.3	-2.3	-1.7	-0.2

Table 4. Statistical characteristics of HCI in Tsalka during the warm season (1956-2015).

Parameter	Apr	May	Jun	Jul	Aug	Sep	Warm	Year
Mean	65.3	68.6	78.9	85.2	84.3	79.5	76.9	69.6
Min	56.0	53.0	61.0	78.0	71.0	59.0	70.8	65.6
Max	73.0	83.0	91.0	91.0	91.0	91.0	81.5	72.3
Range	17.0	30.0	30.0	13.0	20.0	32.0	10.7	6.8
St Dev	4.8	6.3	6.6	2.9	4.2	6.8	2.5	1.6
σ_m	0.63	0.82	0.85	0.38	0.55	0.88	0.33	0.20
C_v (%)	7.4	9.2	8.3	3.4	5.0	8.5	3.3	2.2
95%(+/-)	1.2	1.6	1.7	0.7	1.1	1.7	0.6	0.4
II)1986÷2015	64.8	69.3	79.1	85.2	83.8	81.6	77.3	69.6
I)1956÷1985	65.8	67.8	78.7	85.1	84.8	77.3	76.6	69.6
Diff.(II-I)	-1.0	1.5	0.4	0.1	-1.0	4.3	0.7	0.0
t	-0.80	0.90	0.23	0.13	-0.91	2.58	1.10	0.11
α(t)	No	No	No	No	No	0.01	No	No
R	0.12	0.10	0.06	0.04	0.24	0.32	0.10	0.03
Δ_1, %	-1.5	2.1	0.5	0.1	-1.2	5.4	0.9	0.1
α(R)	No	No	No	No	0.06	0.01	No	No
a	-0.0331	0.0375	0.0208	-0.0061	-0.059	0.1232	0.0139	-0.0023
b	131.1	-5.8	37.6	97.2	201.4	-165.1	49.4	74.1
Δ_2, %	-3.0	3.2	1.6	-0.4	-4.1	9.1	1.1	-0.2

The trend of monthly HCI values for all observational data is generally insignificant positive (Fig. 3). A significant linear positive trend in HCI values in certain months of the year was observed in September; negative – in February, August, October and in the cold half of the year. A significant increase in average monthly and seasonal HCI values in the second period of time compared to the first was observed in September,

a decrease – in October, December and in the cold half of the year. The maximum absolute value of $\Delta_1 = 5.4\%$ (Sep) and $\Delta_2 = 20.2\%$ (Oct). The values of the coefficient of variation vary from 3.4% (Jul) to 9.2% (May). Thus, the variability of the HCI values in Tsalka during the study period is generally insignificant (Tables 3, 4).

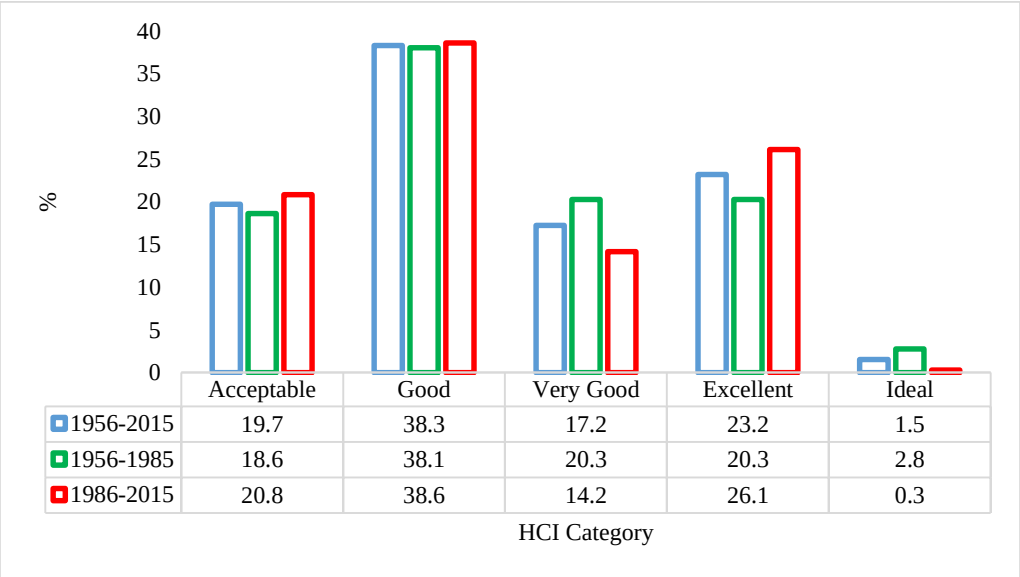

Fig. 5. Repetition of category of monthly values of HCI in Tsalka in three periods of time.

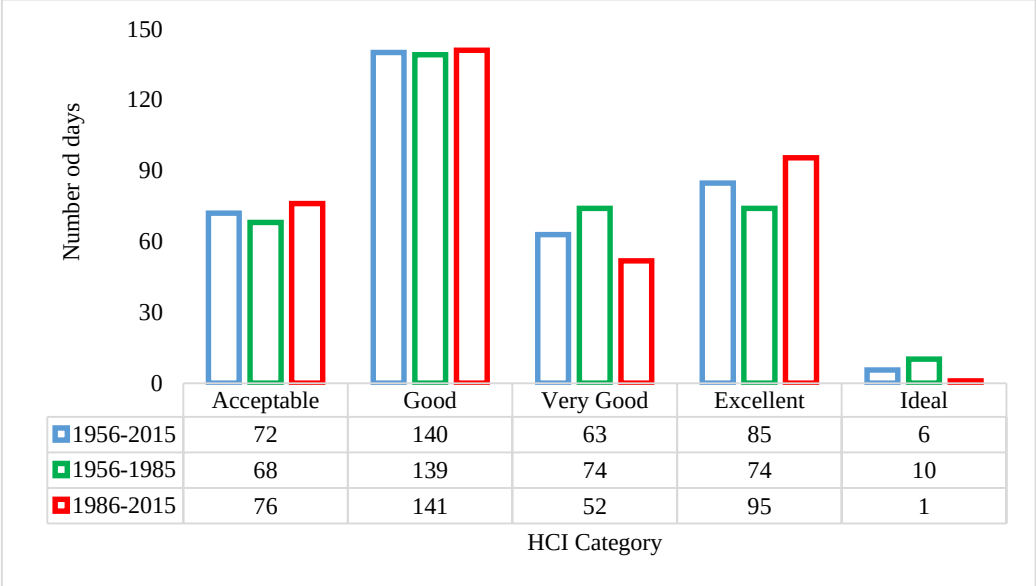

Fig. 6. Number of days in year with different category of HCI in Tsalka in three periods of time.

In the period from 1956 to 2015 the highest repeatability of HCI values (Fig. 5,6) was in the "Good" category (38.3% of cases, 140 days per year), the lowest - in the "Ideal" category (1.5% of cases, 6 days per year). In the second period (1986-2015) compared to the first (1956-1985) in Tsalka, climate change did not lead to a change in HCI categories. At the same time, the frequency of occurrence of the HCI "Acceptable" category increased from 18.6% to 20.8% (respectively, 68 and 76 days a year), the "Good" category increased very slightly - from 38.1% to 38.6% (respectively, 139 and 141 days a year), the "Very Good" category decreased from 20.3% to 14.1% (74 and 52 days a year, respectively), the "Excellent" category increased from

20.3% to 26.1% of cases (respectively 74 and 95 days a year), the “Ideal” category decreased from 2.8% to 0.3% (10 and 1 days a year, respectively). In general, in Tsalka practically all year round there are favorable bioclimatic conditions for recreation and tourism.

Conclusion

In the future, we plan to continue similar studies for other regions of Georgia (mapping the territory of Georgia by HCI values, studying their long-term trends, forecasting of HCI variability due to climate change). Research will also continue on the impact of various simple and complex bioclimatic indices, including HCI, on the peoples health.

References

[1] Vadachkoria M.K., Ushveridze G.A., Jaliashvili V.G. Health Resorts of the Georgian SSR.//Book: "Sabchota Sakartvelo" Publishers, Tbilisi, 1987, 383 p., (in Georgia, English and Russian).

[2] Kartvelishvili L., Matzarakis A., Amiranashvili A., Kutaladze N. Assessment of Touristical-Recreation Potential of Georgia on Background Regional Climate Change. //In the book: Proc. of IIst Int. Scientific-Practical Conference “Tourism: Economics and Business”, June 4-5, Batumi, Georgia, 2011, pp. 250-252.

[3] Kartvelishvili L., Amiranashvili A., Megrelidze L., Kurdashvili L. Turistul Rekreaciuli Resursebis Shefaseba Klimatis Cvlilebebis Fonze. Book: Publish House "Mtsignobari”, ISBN 978-9941-485-01-5, Tbilisi, 2019, 161 p., (in Georgian). http://217.147.235.82/bitstream/1234/293074/1/turistulRekreaciuli ResursebisShefasebaKlimatisCvlilebebisFonze.pdf.

[4] Lanchava O. A., Iliashi N., Radu S., Tsikarishvili K., Lezhava Z., Amiranashvili A., Chikhladze V., Asanidze L. Potential practical potential of Tskaltubo (Western Georgia) "White Cave". GEORGIAN SCIENTISTS, E-ISSN: 2667-9760, Vol. 3, N 1, 2021, 15 p., (in Georgian). Retrieved from https://journals.4 science.ge/index.php/GS/article/view/285

[5] Kartvelishvili L., Tatishvili M., Amiranashvili A., Megrelidze L., Kutaladze N. Weather, Climate and their Change Regularities for the Conditions of Georgia. Monograph: Publishing House “UNIVERSAL”, Tbilisi, 2023, 406 p., https://doi.org/10.52340/mng.9789941334658

[6] Matzarakis A. Weather - and Climate-Related Information for Tourism. Tourism and Hospitality Planning & Development, August, vol. 3, No. 2, 2006, pp. 99–115.

[7] Amiranashvili A.G., Chikhladze V.A., Saakashvili N.M., Tabidze M.Sh., Tarkhan-Mouravi I.D. Bioclimatic Characteristics of Recreational Zones – Important Component of the Passport of the Health Resort – Tourist Potential of Georgia. Trans. of the Institute of Hydrometeorology at the Georgian Technical University, vol. 117, ISSN 1512-0902, 2011, pp. 89-92.

[8] Matzarakis A., Cheval S., Lin T.-P., Potchter, O. Challenges in Applied Human Biometeorology. Atmosphere, 12, 296, 2021. https://doi.org/10.3390/atmos12030296

[9] Carrillo J., González A., Pérez J. C., Expósito F. J., Díaz, J. P. Impact of Climate Change on the Future of Tourism Areas in the Canary Islands. //In the book: EGU General Assembly 2021, online, 19–30 Apr 2021, EGU21-11981, https://doi.org/10.5194/egusphere-egu21-11981, 2021.

[10] Rutty M., Steiger R., O. Demiroglu O.C., Perkins D.R. Tourism Climatology: Past, Present, and Future. Int. Journ. of. Biometeorology. Published online: 08 January 2021. https://doi.org/10.1007/s00484-020-02070-0

[11] Hu L., Guo X., Yan P., Li X. The Construction and Application of a Model for Evaluating Tourism Climate Suitability in Terraced Agricultural Cultural Heritage Sites: A Case Study of Longji Terraced Fields in China. Atmosphere, 15(7), 2024, 756. https://doi.org/10.3390/atmos15070756

[12] Pan S.-L., Wu L., Morrison A.M. A review of studies on tourism and climate change from 2007 to 2021. International Journal of Contemporary Hospitality Management, Vol. 36 No. 5, 2024, pp. 1512-1533. https://doi.org/10.1108/IJCHM-11-2022-1397

[13] Amiranashvili A.G., Kartvelishvili L. G. Long-Term Variations of Air Effective Temperature in Tbilisi. Trans. of the Institute of Hydrometeorology, vol. 115, ISSN 1512-0902, Tbilisi, 2008, pp. 214–219, (in Russian).

[14] Amiranashvili A.G, Bolashvili N.R., Chikhladze V.A., Japaridze N.D., Khazaradze K.R., Khazaradze R.R., Lezhava Z.L., Tsikarishvili K.D. Some New Data about the Bioclimatic Characteristics of the Village of Mukhuri (Western Georgia). Journal of the Georgian Geophysical Society, Issue B. Physics of Atmosphere, Ocean and Space Plasma, v.18B, Tbilisi, 2015, pp. 107-115.

[15] Amiranashvili A.G., Japaridze N.D., Khazaradze K.R. On the Connection of Monthly Mean of Some Simple Thermal Indices and Tourism Climate Index with the Mortality of the Population of Tbilisi City Apropos of Cardiovascular Diseases. Journal of the Georgian Geophysical Society, ISSN: 1512-1127, Physics of Solid Earth, Atmosphere, Ocean and Space Plasma, v. 21(1), Tbilisi, 2018, pp.48-62. http://www.jl.tsu.ge/index.php/GGS/article/view/2489

[16] Amiranashvili A., Japaridze N., Kartvelishvili L., Megrelidze L., Khazaradze K. Statistical Characteristics of the Monthly Mean Values of Air Effective Temperature on Missenard in the Autonomous Republic of Adjara and Kakheti (Georgia). Transactions of Mikheil Nodia Institute of Geophysics, ISSN 1512-1135, vol. LXIX, 2018, pp. 118-138, (in Russian).

[17] Amiranashvili A., Japaridze N., Kartvelishvili L., Khazaradze K., Revishvili A. Changeability the Monthly Mean Values of Air Effective Temperature on Missenard in Batumi in 1956-2015. Journal of the Georgian Geophysical Society, e-ISSN: 2667-9973, p-ISSN: 1512-1127, Physics of Solid Earth, Atmosphere, Ocean and Space Plasma, v. 25(2), 2022, pp. 49–58. DOI: https://doi.org/10.48614/ggs2520225960

[18] Mieczkowski Z. The Tourism Climate Index: A Method for Evaluating World Climates for Tourism. The Canadian Geographer, N 29, 1985, pp. 220-233.

[19] Amiranashvili A., Matzarakis A., Kartvelishvili L. Tourism Climate Index in Tbilisi. Trans. of the Institute of Hydrometeorology, ISSN 1512-0902, Tbilisi, vol. 115, 2008, pp. 27 - 30.

[20] Amiranashvili, A., Chargazia, Kh., Matzarakis, A. Comparative Characteristics of the Tourism Climate Index in the South Caucasus Countries Capitals (Baku, Tbilisi, Yerevan). Journal of the Georgian Geophysical Society, ISSN: 1512-1127, Issue (B). Physics of Atmosphere, Ocean, and Space Plasma, vol.17B, 2014, pp. 14-25.

[21] Amiranashvili A., Chargazia Kh., Matzarakis A., Kartvelishvili L. Tourism Climate Index in the Coastal and Mountain Locality of Adjara, Georgia.//In the book: Int. Sc. Conf. "Sustainable Mountain Regions: Make Them Work". Proceedings, Borovets, Bulgaria, ISBN 978-954-411-220-2, 14-16 May,2015, pp. 238-244, http://geography.bg/MountainRegions_Sofia2015

[22] Rybak O. O., Rybak E. A. Application of Climatic Indices for Evaluation of Regional Differences in Tourist Attractiveness. Nauchnyy zhurnal KubGAU, №121(07), 2016, 24 p. http://ej.kubagro.ru/2016/07/pdf/16.pdf

[23] Amiranashvili A.G., Japaridze N.D., Kartvelishvili L.G., Khazaradze K.R., Matzarakis A., Povolotskaya N.P., Senik I.A. Tourism Climate Index of in the Some Regions of Georgia and North Caucasus. Journal of the Georgian Geophysical Society, ISSN: 1512-1127, Issue (B). Physics of Atmosphere, Ocean, and Space Plasma, vol.20B, 2017, pp. 43-64.

[24] Amiranashvili A.G., Japaridze N.D., Kartvelishvili L.G., Khazaradze K.R., Kurdashvili L.R. Tourism Climate Index in Kutaisi (Georgia).//In the book: Int. Sc. Conf. "Modern Problems of Ecology", Proceedings, ISSN 1512-1976, v. 6, Kutaisi, Georgia, 21-22 September, 2018, pp. 227-230.

[25] Amiranashvili A.G., Kartvelishvili L.G., Matzarakis A., Megrelidze L.D. The Statistical Characteristics of Tourism Climate Index in Kakheti (Georgia). Journal of the Georgian Geophysical Society, ISSN: 1512-1127, Physics of Solid Earth, Atmosphere, Ocean and Space Plasma, v. 21(2), Tbilisi, 2018, pp. 95-112.

[26] Amiranashvili A., Kartvelishvili L. Statistical Characteristics of the Monthly Mean Values of Tourism Climate Index in Mestia (Georgia) in 1961-2010. Journal of the Georgian Geophysical Society, ISSN: 1512-1127, Physics of Solid Earth, Atmosphere, Ocean and Space Plasma, v. 22(2), 2019, pp. 68–79.

[27] Mushawemhuka W.J., Fitchett J.M., Hoogendoorn G. Towards Quantifying Climate Suitability for Zimbabwean Nature-Based Tourism. South African Geographical Journal, 2020. DOI: 10.1080/03736245.2020.1835703

[28] Tanana, A. B. et al. Confort climático en la Argentina: un recurso intangible para el turismo. Cuadernos Geográficos 60(3), 2021, pp. 52-72.

[29] Faraj T.K., Tarawneh Q.Y., Oroud I.M. The applicability of the tourism climate index in a hot arid environment: Saudi Arabia as a case study. Int. J. Environ. Sci. Technol. 20, 2023, pp. 3849–3860. https://doi.org/10.1007/s13762-022-04228-2

[30] Aygün Oğur A., Baycan T. Assessing climate change impacts on tourism demand in Turkey. Environ Dev Sustain 25, 2023, pp. 2905–2935. https://doi.org/10.1007/s10668-022-02135-7

[31] Scott D., Rutty M., Amelung B., Tang M. An Inter-Comparison of the Holiday Climate Index (HCI) and the Tourism Climate Index (TCI) in Europe. Atmosphere 7, 80, 2016, 17 p. doi:10.3390/atmos7060080www.

[32] Javan K. Comparison of Holiday Climate Index (HCI) and Tourism Climate Index (TCI) in Urmia. Physical Geography Research Quarteli. vol. 49, iss. 3, 2017, pp. 423-439.

[33] Hejazizadeh Z., Karbalaee A., Hosseini S.A., Tabatabaei S.A. Comparison of the Holiday Climate Index (HCI) and the Tourism Climate Index (TCI) in Desert Regions and Makran Coasts of Iran. Arab. J. Geosci. 12, 803, 2019, https://doi.org/10.1007/s12517-019-4997-5

[34] Rutty M., Scott D., Matthews L., Burrowes R., Trotman A., Mahon R., Charles A. An Inter-Comparison of the Holiday Climate Index (HCI: Beach) and the Tourism Climate Index (TCI) to Explain Canadian Tourism Arrivals to the Caribbean. Atmosphere, 11, 412, 2020.

[35] Yu D. D., Rutty M., Scott D., Li S. Comparison of the Holiday Climate Index: Beach and the Tourism Climate Index Across Coastal Destinations in China. International Journal of Biometeorology, 2020. https://doi.org/10.1007/s00484-020-01979-w, 8 p.

[36] Sobhani P., Danehkar A. Investigating tourism climate conditions in Iran's mangrove forests using Tourism Comfort Climate Index (TCI) and Holiday Climate Index (HCI). Journal of Natural Environment, 75(Special Issue Coastal and Marine Environment), 2023, pp.29-45. DOI: 10.22059/JNE.2022.351668.2494

[37] Amiranashvili A., Kartvelishvili L., Matzarakis A. Comparison of the Holiday Climate Index (HCI) and the Tourism Climate Index (TCI) in Tbilisi. In the book: Int. Sc. Conf. "Modern Problems of Ecology", Proc., ISSN 1512-1976, v. 7, Tbilisi-Telavi, Georgia, 26-28 September, 2020, pp. 424-427.

[38] Amiranashvili A.G., Kartvelishvili L.G., Kutaladze N.B., Megrelidze L.D., Tatishvili M.R. Holiday Climate Index in Some Mountainous Regions of Georgia. Journal of the Georgian Geophysical Society, e-ISSN: 2667-9973, p-ISSN: 1512-1127, Physics of Solid Earth, Atmosphere, Ocean and Space Plasma, v. 24(2), 2021, pp. 92 – 117. DOI: https://doi.org/10.48614/ggs2420213327

[39] Amiranashvili A., Povolotskaya N., Senik I. Comparative Analysis of the Tourism Climate Index and the Holiday Climate Index in the North Caucasus. Transactions of Mikheil Nodia Institute of Geophysics, ISSN 1512-1135, vol. LXXIII, 2021, pp. 96-113, (in Russian).

[40] Amiranashvili A.G., Kartvelishvili L.G. Holiday Climate Index in Kakheti (Georgia). Journal of the Georgian Geophysical Society, e-ISSN: 2667-9973, p-ISSN: 1512-1127, Physics of Solid Earth, Atmosphere, Ocean and Space Plasma, v. 24(1), 2021, pp. 44-62.

[41] Amiranashvili A., Bliadze T., Chikhladze V. Photochemical smog in Tbilisi.//Monograph: Trans. of Mikheil Nodia institute of Geophysics, ISSN 1512-1135, vol. 63, 2012, 160 p., (in Georgian). http://www.dspace.gela.org.ge/bitstream/123456789/636/3/ფოტოქიმიური%20სმოგი%20თბილისში_წიგნი_2012_Ge.pdf

[42] Amiranashvili A.G., Japaridze N.D., Khazaradze K.R. On the Connection of Monthly Mean of Some Simple Thermal Indices and Tourism Climate Index with the Mortality of the Population of Tbilisi City Apropos of Cardiovascular Diseases. Journal of the Georgian Geophysical Society, ISSN: 1512-1127, Physics of Solid Earth, Atmosphere, Ocean and Space Plasma, v. 21(1), Tbilisi, 2018, pp.48-62. http://www.jl.tsu.ge/index.php/GGS/article/view/2489

[43] Amiranashvili A., Japaridze N., Kartvelishvili L., Khazaradze K., Revishvili A. Preliminary Results of a Study on the Impact of Some Simple Thermal Indices on the Spread of COVID-19 in Tbilisi. Journal of the Georgian Geophysical Society, e-ISSN: 2667-9973, p-ISSN: 1512-1127, Physics of Solid Earth, Atmosphere, Ocean and Space Plasma, v. 25(2), 2022, pp. 59–68. DOI: https://doi.org/10.48614/ggs2520225961

[44] Araci S.F. S., Demiroglu O. C., Pacal A., Hall C. M., Kurnaz, M. L. Future Holiday Climate Index (HCI) Performances of Urban and Beach Destinations in the Mediterranean. In the book: EGU General Assembly 2021, online, 19–30 Apr 2021, EGU21-13217, https://doi.org/10.5194/egusphere-egu21-13217, 2021.

[45] Prinsloo A.S., Fitchett J.M. Quantifying climatic suitability for tourism in Southwest Indian Ocean Tropical Islands: Applying the Holiday Climate Index to Réunion Island. Int J Biometeorol, 2024. https://doi.org/10.1007/s00484-024-02700-x

[46] Hemmati S., Taghiloo A. Determine the Suitable Time for Tourism in West Azerbaijan Province Using Holiday Climate Index (HCI). Geography and Human Relationships, 2024. DOI: 10.22034/GAHR.2024.433059.2017

[47] Demiroglu O.C., Saygili-Araci F.S., Pacal A., Hall C.M.,M. Levent Kurnaz M.L. Future Holiday Climate Index (HCI) Performance of Urban and Beach Destinations in the Mediterranean. Atmosphere, 11, 911, 2020. doi:10.3390/atmos11090911

[48] Bilgin B., Acar S., Demirala, Z., An N., Turp M. T., Kurnaz M. L. A synthetic approach to the Holiday Climate Index for the Mediterranean Coast of Türkiye. International Journal of Biometeorology, 2024, pp. 1-15. https://doi.org/10.1007/s00484-024-02704-7

[49] Samarasinghe J.T., Wickramarachchi C.P., Makumbura R.K., Meddage P., Gunathilake M.B., Muttil N., Rathnayake U. Performances of holiday climate index (HCI) for urban and beach destinations in Sri Lanka under changing climate. Climate, 11(3), 2023, p. 48. https://doi.org/10.3390/cli11030048
[50] Velea L., Bojariu R., Irimescu A., Craciunescu V., Puiu S., Gallo A. Climate Suitability for Tourism in Romania Based on HCI: Urban Climate Index in the Near-Future Climate. Atmosphere, 14(6), 2023, 1020. https://doi.org/10.3390/atmos14061020
[51] Xu X., Liu X., Yang X., Liu L., Guan J. Assessing the impact of dust events on the Holiday Climate Index in the Taklimakan Desert region. Int. J. Biometeorol., 68, 2024, pp. 1073–1079. https://doi.org/10.1007/s00484-024-02645-1
[52] Amiranashvili A., Kartvelishvili L., Matzarakis A. Changeability of the Holiday Climate Index (HCI) in Tbilisi. Transactions of Mikheil Nodia Institute of Geophysics, ISSN 1512-1135, vol. LXXII, 2020, pp. 131-139.
[53] Fourth National Communication of Georgia. Under the United Nations Framework Convention on Climate Change. (2021)//Book: Tbilisi. pp. 333-339. https://unfccc.int/sites/default/files/resource/4%20Final%20Report%20-%20English%202020%2030.03_0.pdf
[54] Amiranashvili A., Bolashvili N., Kartvelishvili L., Liparteliani G., Tsirgvava G. Holiday Climate Index in Kvemo Kartli (Georgia). Georgian Geographical Journal, E-ISSN: 2667-9701, 24(1), 2024, pp. 35-46. https://doi.org/10.52340/ggj.2024.04.01.05

წალკაში (საქართველო) დასვენების კლიმატის ინდექსის ცვალებადობა

ა. ამირანაშვილი, ლ. ქართველიშვილი, ა. მატზარაკისი

რეზიუმე

წარმოდგენილია წალკისთვის (საქართველო) დასვენების კლიმატის ინდექსის (HCI) მრავალწლიანი საშუალო თვიური მნიშვნელობების მონაცემები. ჩატარდა ყოველთვიური, სეზონური და წლიური HCI-ის მნიშვნელობების დეტალური ანალიზი 60 წლის განმავლობაში (1956-2015). შესწავლილია HCI-ის ცვალებადობა 1986-2015 წლებში 1956-1985 წლებთან შედარებით და შესწავლილი იქნა HCI-ის ტენდენციები 1956-2015 წლებში.

საკვანძო სიტყვები: ბიოკლიმატი, ტურიზმის კლიმატური ინდექსი, დასვენების კლიმატური ინდექსი.

Изменчивость климатического индекса отдыха в Цалке (Грузия)

А. Амиранашвили, Л. Картвелишвили, А. Матзаракис

Резюме

Представлены данные о многолетних среднемесячных значениях климатического индекса отдыха (HCI) для Цалки (Грузия). Проведен детальный анализ месячных, сезонных и годовых значений HCI за 60-летний период (1956-2015 гг.). Изучена изменчивость HCI в 1986-2015 гг. по сравнению с 1956-1985 гг., а также исследованы тенденции HCI в 1956-2015 гг.

Ключевые слова: Биоклимат, климатический индекс туризма, климатический индекс отдыха.

Journal of the Georgian Geophysical Society, e-ISSN: 2667-9973, p-ISSN: 1512-1127
Physics of Solid Earth, Atmosphere, Ocean and Space Plasma, v. 27(1), 2024, pp. 91 - 103

The Importance of Electric Field in Formation of Sporadic E (Es) at the Equatorial Region

Giorgi T. Dalakishvili, Goderdzi G. Didebulidze, Maya M. Todua, Lekso A. Toriashvili

Ilia State University, Space Research Center, G. Tsereteli str.3a, 0162 Tbilisi, Georgia.
didebulidze@iliauni.edu.ge

ABSTRACT

It has been shown analytically and by appropriate numerical methods that the formation and localization of sporadic E (Es) in the equatorial area can be determined by the height profiles of the ion vertical drift velocity and its divergence. In this case, the existence of a minimum negative value (maximum convergence rate) in the divergence profile, when ions converge vertically into the Es layer, is significantly determined by both the neutral wind velocity and the zonal and vertical components of the electric field.

In the equatorial region, with a constant westward electric field, the maximum vertical convergence rate of ions is in the region of the height where the ion-neutral collisional (ν_{in}) and ion cyclotron (Ω_i) frequencies are equal. In case of the constant upwards or downwards electric field, this rate is located at approximately 0.9H (where H is a neutral scale) above or below the region where $\nu_{in} = \Omega_i$, respectively. The vertical convergence of the ions developed in these regions and the formation of the Es layer can take place against the background of their upward or downward drift. It localizis in the node of this drift velocity, or in the regions where this velocity disappears. Such predicted formation and behavior of Es layers are demonstrated by numerical methods.

The effect of the zonal and vertical components of the electric field, as well as the wind velocity determined by the HWM14 data, on the processes of ion convergence/divergence development is shown. In these cases, the ion convergence/divergence process induced by the electric field can affect both the formation and disruption (depletion) of the Es layer formed by neutral wind, as well as can also form an additional layer.

Key words: *lower thermosphere, electric field, sporadic E (Es), ion vertical drift velocity, numerical methods.*

1. Introduction

Sporadic E(Es) are observed in the lower thermosphere of globe including the equatorial regions [1, 2]. The Es layers observed in equatorial regions are not always localized in the region of zonal neutral wind polarization change [3-5], as defined by the windshear theory [6-9]. This indicates that there is an additional mechanism of convergence of ions in the Es type layer in the equatorial region, which can be caused by the presence of an electric field [3, 10].

The vertical ion drift (EB drift) caused by the electric field of equatorial electrojet origin [11, 12] penetrate the equatorial ionosphere E and F regions is important for studying the behavior of ions/electrons in these regions of the ionosphere. Therefore, the electric field can influence the formation and localization of Es layers in the lower thermosphere [13, 14].

The presented studies will show that the electric field in the equatorial lower thermosphere can cause the existence of a minimum negative value in the divergence of ions vertical drift velocity necessary to develop ions vertical convergence [13, 14]. This condition can be fulfilled even when the electric field is constant and leads to the development of the process of vertical convergence of ion/electrons into a narrow layer (convergence instability) and thus the formation of a high density Es layer is possible [15, 16].

By theoretical and appropriate numerical methods, the formation and localization of Es layers in the height regions of about 90-150 km of the equatorial lower thermosphere will be shown. Along

with the electric field, the presence of the neutral wind will be considered. The horizontal wind is determined by the HWM14 data [17, 18].

2. Theoretical background of sporadic E(Es) formation at the equatorial region.

The condition of ion vertical convergence into narrow thin layer and formation Es layer can be obtain by solving the continuity equation of ions in the analytical approach, which $N_i(z,t)$ in analogy Dalakishvili et al. [13] and Didebulidze et al. [15] has the following form:

$$N_i(z,t) \approx N_{om} \exp\left\{-\left(\frac{2D}{H_{ic}^2} + div\mathbf{w}_{iv}\right)(t-t_o) - \left(\frac{z-[z_{om}+\mathrm{w}_{iv}(t-t_o)]}{H_{ic}}\right)^2\right\} \quad (1)$$

Here the small variations of ions drift velocity $\mathbf{w}_{iv}(0,0,\mathrm{w}_{iv})$ and its vertical changes $\partial \mathrm{w}_{iv}/\partial z$ during time $t - t_o << H_{ic}^2/2D$ are assumed. H_{ic} is the characteristic scale height of ions which at some initial time $t = t_o$ determines the main ion/electron layer thickness ($2H_{ic}$) and the height region $z - z_{om} = \pm H_{ic}$, where their density decreases e-times. $H_{ic}^2/2D$ is the characteristic time of the ion density decrease by their diffusion ($\propto D$).

Equation (1) of ion/electron $N_e(z,t)$ density (assuming quasineutrality $N_i = N_e$) describes the evolution of their Gaussian type distribution, which at the initial time $t = t_o$, has maximal density (peak density) N_{om} at height $z = z_{om}$ (initial peak height). The value of $(div\mathbf{w}_{iv})\min < 0$ (or $(-div\mathbf{w}_{iv})\max > 0$) is characteristic to ion/electron density increase rate and the value of $(div\mathbf{w}_{iv})\max > 0$ to its depletion rate.

In analogy with Dalakishvili et al. [13] and Didebulidze et al. [15], when occurs the conditions:

$$(div\mathbf{w}_{iv})\min < -\frac{2D}{H_{ic}^2} \quad (2)$$

then the equation (1) shows a tendency of formation of high density Es type layer of ion/electron ($\frac{N_m(t>t_o)}{N_{om}} > 1$). The peak height of this layer $z = z_{om} + \mathrm{w}_{iv}(t-t_o)$ moves upward ($\mathrm{w}_{iv} > 0$) or downward ($\mathrm{w}_{iv} < 0$) by ions vertical drift velocity w_{iv} and it could be localized at the height region with $\mathrm{w}_{iv} = 0$ or $\mathrm{w}_{iv} \to 0$. According to the equation (2), at the region with maximal ion vertical drift velocity divergence $(div\mathbf{w}_{iv})\max > 0$ the ion/electron density depletion ($\frac{N_m(t>t_o)}{N_{om}} < 1$) occurs.

We take a right-handed set of coordinates (*x*, *y*, *z*) with *x* directed to the magnetic north, y to the west and *z* vertically upward.

The effect of electric field $\mathbf{E}(E_x, E_y, E_z)$ and neutral wind velocity $\mathbf{V}_n(V_{xn}, V_{yn}, V_{zn})$ on ions motion is included in its vertical drift velocity w_{iv}, which at equatorial region (with *I*=0 and $E_x = 0$), have the following form [13, 19]:

$$\mathrm{w}_i = \mathrm{w}_{iv} - \frac{D_i}{N_i}\frac{\partial N_i}{\partial z}, \quad (3)$$

where

$$w_{iv} = -C_v \frac{E_y}{B} - C_h\left(V_y - \frac{E_z}{B}\right) \tag{4}$$

$$C_v = \frac{1}{\kappa^2 + 1} \quad , \tag{5}$$

$$C_h = \frac{\kappa}{\kappa^2 + 1} \quad , \tag{6}$$

$$D_i = \frac{\kappa^2}{\kappa^2 + 1}\frac{k_B T_i}{m_i \nu_{in}} . \tag{7}$$

The quation (3) in case of absence of ions diffusion is the same as given by Abdu et al. [19]. This equation shows an importance of electric field zonal (E_y) and vertical (E_z) components in addition with zonal neutral wind (V_y) in ions vertical drift velocity. Here we assume that the ions diffusion also can influence on ions vertical drift and their layered structure in the lower thermosphere.

An analogy between the vertical drift velocities of ions at equatorial (I=0) and mid-latitudes (e.g., I>30°) described by equation (1) [13] shows that the conditions of their into Es-type layer vertical convergence $(-div\mathbf{w}_{iv})\max > 0$ or initial layer divergence/desruption $(div\mathbf{w}_{iv})\max > 0$ in accordance with equations (3-7) can be described by the following equation:

$$-div\mathbf{w}_{iv} = C_v \frac{1}{B}\frac{\partial E_y}{\partial z} + C_v' \frac{E_y}{B} + C_h\left(\frac{\partial V_y}{\partial z} - \frac{1}{B}\frac{\partial E_z}{\partial z}\right) + C_h'\left(V_y - \frac{E_z}{B}\right) \quad , \tag{8}$$

where

$$C_v' = \frac{\partial C_v}{\partial z}, \tag{9}$$

$$C_h' = \frac{\partial C_h}{\partial z} . \tag{10}$$

Equation (8) shows that both in the equatorial area and at mid-latitudes [13,15] the conditions of vertical convergence ($(-div\mathbf{w}_{iv})\max > 0$) and divergence ($(div\mathbf{w}_{iv})\max > 0$) of ions are significantly determined by the height profiles of $C_v(z)$ and $C_h(z)$ factors, equations (5) and (6), and their vertical change $C_{vo}'(z)$ and $C_{ho}'(z)$, equations (9) and (10).

Thus, the factors $C_{v0}(z)$, $C_{h0}(z)$, $C_{vo}'(z)$ and $C_{ho}'(z)$ are important for studying the influence of the zonal wind velocity V_y, electric field (E_y, E_z) magnitude and direction, as well as their vertical change ($\frac{\partial V_y}{\partial z}$, $\frac{\partial E_y}{\partial z}$, $\frac{\partial E_z}{\partial z}$), on the process of convergence of ions/electrons into an Es-type layer in the equatorial region, equation (4). It is somewhat similar to studying the influence of the magnitude, direction and their vertical shear ($\frac{\partial V_x}{\partial z}$, $\frac{\partial V_y}{\partial z}$) of meridional V_x and zonal wind velocity V_y at mid-latitudes with factors $\sin I \cos I \cdot C_v$, $\cos I \cdot C_h$, $\sin I \cos I \cdot C_v'$ and $\cos I \cdot C_h'$ on the vertical convergence of ions/electrons into an Es-type layer [13, 15].

In Fig. 1 the height profiles of ion convergence/divergence rate $(-div\mathbf{w}_{iv})\max > 0$ factors a) $C_v(z)$ and $C_h(z)$, b) $C_v'(z)$ and $C_h'(z)$ at equatorial regions (I=0), are given.

Fig. 1 shows that the factor $C_v^{'}(z)$ has a maximum value at an altitude of about 121 km, which corresponds to the region at equatorial and mid-latitudes, where $\kappa = 1$ ie $\nu_{in} = \Omega_i$. In the absence of equatorial zonal wind and vertical electric field ($V_y = 0$, $E_z = 0$) in this height region, the condition $(div\, w_{iv})\min = (\frac{\partial w_{iv}}{\partial z})\min < 0$ of vertical convergence of ions occurs for the westward constant electric field ($E_y = constant > 0$), and the condition $(div\, w_{iv})\max = (\frac{\partial w_{iv}}{\partial z})\max > 0$ of their divergence takes place for the eastward electric field ($E_y < 0$), see equation (9) . In these cases, the formation of the Es layer and the depletion of ions are expected respectively, see equation (2).

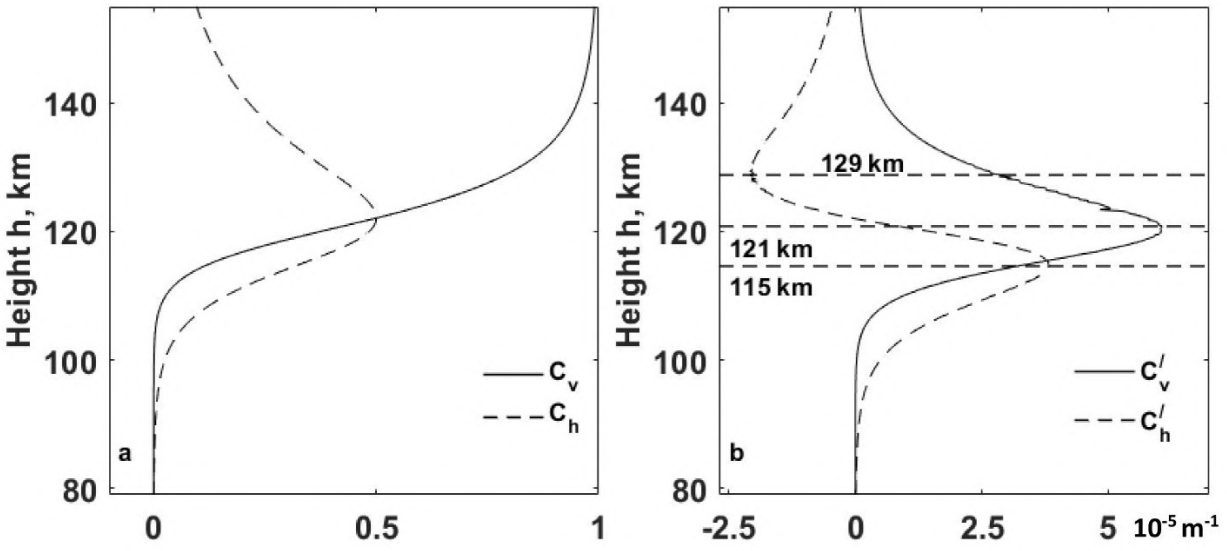

Fig. 1. The height profiles of ion convergence/divergence rate $-div\mathbf{w}_{iv}$ factors a) $C_v(z)$ and $C_0(z)$, b) $C_v^{'}(z)$ and $C_h^{'}(z)$ at equatorial region (*I*=0).

Fig. 1 also shows that similarly the mid-latitude [15]$_{C_v}$ factor has a maximum positive value approximately 0.9H below the altitude corresponding to the condition $\nu_{in} = \Omega_i$ (*h*=115km) and a minimum negative value above 0.9H (*h*= 129km).

In this case, on the vertical drift velocity of ions in the equatorial region, equation (4), the combined action ($V_y - \frac{E_z}{B}$) of the zonal wind (V_y) and the vertical electric field (E_z), it is possible to form an Es type layer even when the magnitude of $V_y - \frac{E_z}{B}$ is constant. When $V_y - \frac{E_z}{B} = \text{constant} > 0$ and $E_y = 0$, then the convergence processes of ions develop against the background of drift below them, and the formation of the Es layer is expected in the lower height *h*<115 km regions. In this case ($V_y - \frac{E_z}{B} = \text{constant} > 0$) in the regions of upper heights around *h* = 129 km ($(div\, w_{iv})\max > 0$) the depletion of the ion/electrons is expected.

When $V_y - \frac{E_z}{B} = \text{constant} < 0$ and $E_y = 0$, then the inverse behavior of ions/electrons is expected: in the height regions of about *h*=129 km occurs $(div\, w_{iv})\min < 0$ and the formation of Es layer is

expected, and in the lower heights about h=115 km where $(div\,w_{iv})\max > 0$ the charged particles depletion is expected.

Thus, the zonal E_y electric field can form the Es layer independently of the neutral wind, and that of the by the vertical electric field E_z, is possible in the case when the neutral wind is relatively weak ($V_y << -\frac{E_z}{B}$).

We will demonstrate these and other cases of ion behavior and Es layer formation that can be predicted by the suggested theory numerically in the next section. Hereafter the vertical coordinate z represents the residual between some actual h and initial heights h_o ($z = h - h_o$).

3. Results and discussion

To investigate the behavior of the height profile of ion/electron density $N_e(z,t)$ (assuming quasi-neutrality $N_e = N_i(Fe^+)$) under the influence of the electric field $\mathbf{E}(0, E_y, E_z)$ and horizontal wind with velocity $\mathbf{V}_n(V_{xn}, V_{yn}, 0)$ we solve the continuity equation of ions numerically [15, 20-22], taking into account the ions vertical drift velocity w_i for equatorial, equations (3-7), region. We use the initial conditions of ion/electron distributions in accordance with the analytical approach, equation (1), of the solution of ions continuity equation.

In this stage of study, we consider the nighttime condition, and the ion/electron production and loss rates are neglected. In the presented simulation, the neutral particle densities of the lower thermosphere are used from the NRLMSISE-00 model [23], for the equatorial (7°± 2°N, 45° ± 2° E; I=0± 2°) region. Further, we will consider the existence of the horizontal wind velocity $\mathbf{V}_n(V_{xn}, V_{yn}, 0)$, of which meridional V_{xn} and zonal V_{yn} components height profiles are determined by the HWM14 data [17,18].

To consider the importance of electric field $\mathbf{E}(0, E_y, E_z)$ in formation of a sporadic E we demonstrate the possibility of its formation even in case when zonal E_y or/and vertical E_z components of the electric field are homogeneous and the horizontal wind is absent. We will use the zonal and vertical electric field values $E_y = \pm 0.4 mV/m$ and $E_z = \pm 2 mV/m$, which are about those used by [5, 19]. For the initial ion/electron layer peak height (h_{om}), we consider the upper $h_{om} = 120\ km$ and the lower $h_{om} = 105\ km$ cases. The height of the upper peak is relatively close to the maximum/minimum regions of convergence $C_v'(z)$ and $C_h'(z)$ factors (121 km, 115 km, 129 km), while the location of the lower peak $h_{om} = 105\ km$ is close to the regions of the often observed location of Es layers (about 102-104 km) [24, 25].

In Fig. 2 the behavior of ion/electron density $N_e(z,t)/N_{om}$ at equatorial region with I=0 (7 ° N; 45 ° E) for initial layer peak height (panels a,b,c,d) at $h_{om} = 120\,km$ and (panels e, f, g, h) $h_{om} = 105\,km$, under an influence (panels a and e) westward $E_y = 0.4 mV/m$, (b and f) eastward $E_y = -0.4 mV/m$, (c and g) upward $E_z = 2 mV/m$ and (d and h) downward $E_z = -2 mV/m$ electric field in case of absence horizontal wind ($V_{yn} = 0$) are demonstrated.

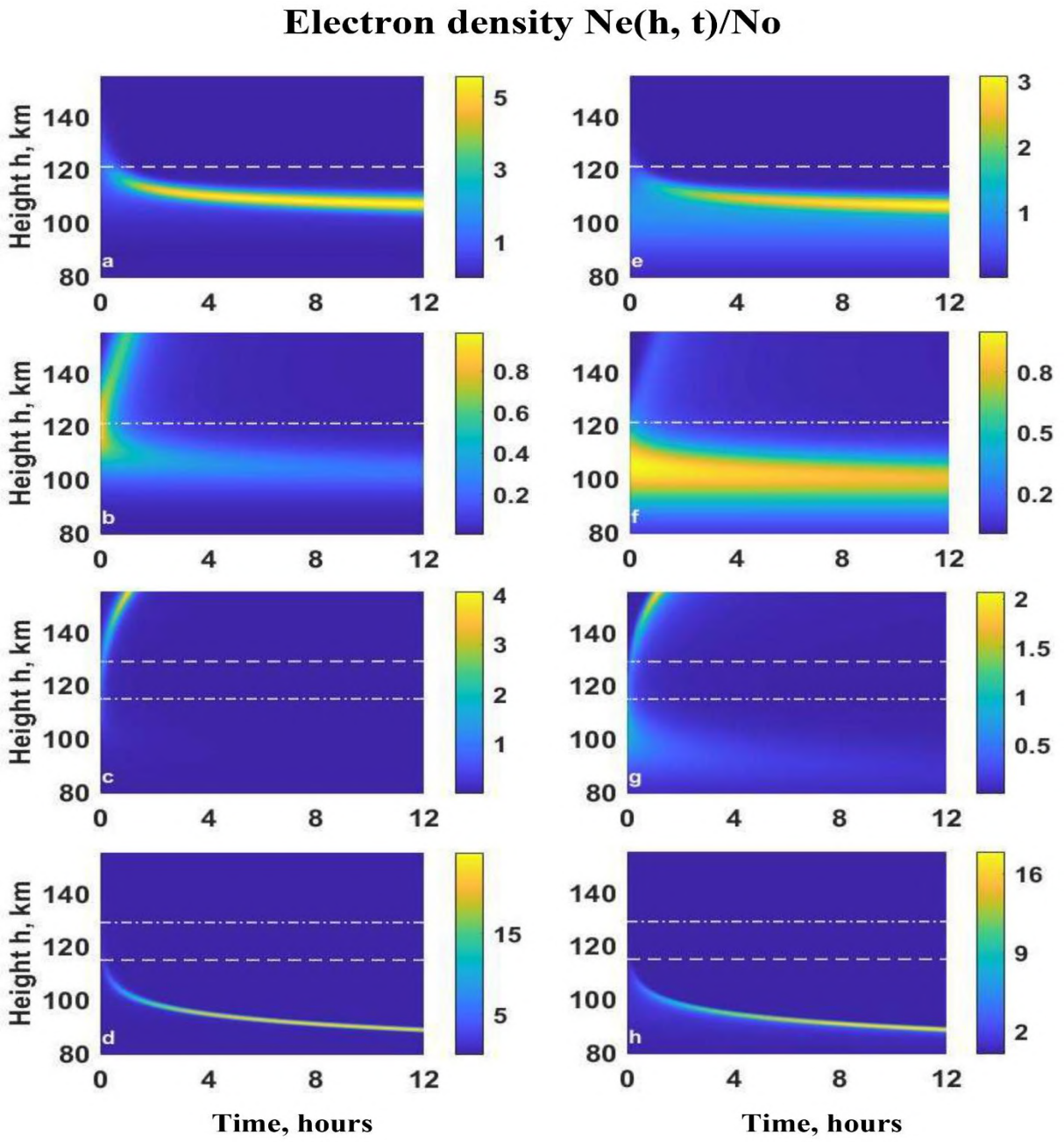

Fig. 2. The behavior of ion/electron density $N_e(z,t)/N_{om}$ at the equatorial region I=0 (7 º N; 45 º E) for the initial peak heights of the layer at $h_{om}=120\,km$ (panels a,b,c,d) and $h_{om}=105\,km$ (panels e, f, g, h), under an influence of westward $E_y=0.4\,mV/m$ (panels a and e), eastward $E_y=-0.4\,mV/m$ (b and f), upward $E_z=2\,mV/m$ (c and g) and downward $E_z=-2\,mV/m$ (d and h) electric fields, in case of absence of the horizontal wind ($V_{yn}=0$=0) . The dashed and dashed-dotted lines correspond to the heights of development of ion convergence ($(div\mathbf{w}_{iv})\min<0$) and divergence ($(div\mathbf{w}_{iv})\max>0$), respectively.

(Fig. 2a), $N_{em}/N_{om}>1.5$ (Fig. 2c) and $N_{em}/N_{om}>25$ (Fig. 2d) exceeds their magnitudes $N_{em}/N_{om}\geq 3$ (Fig. 2e), $N_{em}/N_{om}\approx 1$ (Fig. 2g) and $N_{em}/N_{om}>16$ (Fig. 2h) for the lower location $h_{om}=105\,km$ of the initial peak.

Fig. 2 shows that in the absence of wind $V_{yn}=0$ the westward $E_y>0$ (panels a and e), upward $E_z>0$ (panels c, d) and downward $E_z<0$ (panels g and h) electric fields can form a high density Es layer, even when it is homogeneous: $N_{em}/N_{om}>5$ (Fig. 2a), $N_{em}/N_{om}>1.5$ (Fig. 2c), $N_{em}/N_{om}>25$ (Fig. 2d), $N_{em}/N_{om}\geq 3$ (Fig. 2e), $N_{em}/N_{om}\approx 1$ (Fig. 2g) and $N_{em}/N_{om}>16$ (Fig. 2h). In these cases, the Es layer is formed in presence of conditions of vertical convergence of ions $(div\mathbf{w}_{iv})\min<0\propto(C_v')\max>0$ and $(div\mathbf{w}_{iv})\min<0\propto(C_h')\max>0$, equations (4-10) (see Fig. 1b as well), at height about *h*=121 km (panels a and e), *h*=131 km (panels c and g) and *h*=115 km (panels d and h), respectively. Here, the Es type layer is formed during the downward $-C_v\frac{E_y}{B}<0$ (panels a and e), $-C_h\frac{E_z}{B}<0$ (panels d and h) and upward $-C_h\frac{E_z}{B}>0$ (panels c and g) drift of ions. They are respectively localized below (*h*<121km and *h*<115km) and above (*h*>129km) the height regions of ions convergence development where $w_{iv}\to 0$.

The densities of the Es layer formed in these cases are higher when the peak height of the initial layer of ions is located near the region of its convergence development. For example, in the case of the westward electric field $E_y>0$ (Figures 2a and 2e), as well as for $E_z>0$ (Fig. 2d and 2h) at the upper location of the ion/electron peak $h_{om}=120\ km$, their density $N_{em}/N_{om}>5$

Fig. 2 also shows that for the eastward electric field $E_y<0$ (panels b and f), at the height regions around 121 km a divergence condition $\left(-\frac{\partial w_{iv}}{\partial z}\right)\max\propto(C_v')\max>0$ occurs and accordingly the initial layer is depleted/destructed ($N_e/N_{om}<<1$). The role of the eastward electric field in the destruction of the observed Es layers is noted by [26].

Here it is also important to note that, in the case of a vertically downward field $E_z<0$ (Fig. 2d and 2h), the divergence of ions developed in the 129 km height region increases their flow to the lower *h*<129 km regions. At the same time, the convergence developed at 115 km leads to the formation of a relatively high density Es layer with $N_{em}/N_{om}>25$ and $N_{em}/N_{om}>1.5$, than it was in the direction above the field $E_z>0$ (Fig. 2c and 2g), as well as in its westward direction $E_y>0$ (Fig. 2a and 2e). It is also important to note that the influence of ion diffusion on their convergence, equations (4)-(6), and therefore on the density of the Es layer, is noticeable for the upper heights of the lower thermosphere. In our case (see Fig. 2c and 2g) for the upward electric field $E_z>0$ the Es layer formed at *h*>129 km is less dense and lasts for a shorter time (about $t-t_o<2\ h$) than when it is formed in the lower regions (see Fig. 2 a, 2d, 2e and 2h).

Thus, in the equatorial lower thermosphere, the Es layer can be formed both westward $E_y>0$ (Fig. 2a and 2e), and upward $E_z>0$ (Fig. 2c and 2g) or downward $E_z<0$ of the homogeneous electric field (Fig. 2d and 2h), which, according to equations (4), (5) and (6), is due to the presence of the minimum negative value of divergence of the vertical drift velocity $\mathbf{w}_{iv}$ of ions $(div\mathbf{w}_{iv})\min<0$ (or $\left(-\frac{\partial w_{iv}}{\partial z}\right)\max\propto(C_v')\max,(C_h')\max>0$) (see Fig. 1b), equation (10). In these cases ($E_y=0$ or $E_z=0$ and $V_{yn}=0$) there is no ion drift velocity node $w_{iv}=0$, equation (4), and the formed Es type layer is localized in the regions where $w_{iv}\to 0$.

The behavior of ions in the lower thermosphere is influenced by both the electric field and the neutral wind, equation (4). In order to distinguish the share/part of the influence of the electric field (see Fig. 2) together with its neutral wind in the vertical convergence of ions and, accordingly, in the formation of sporadic E, we consider its formation both in the case of wind only (**E**=0 and **V**≠0) and during their simultaneous presence (**V**≠0 and **E**≠0) at equatorial latitudes.

We estimate in ions qontituity equation the vertical ion drift velocity w_{iv} and its divergence $div\mathbf{w}_{iv o}$ for nighttime ($t-t_o \le 12\,h$) height profiles in the lower thermosphere at equatorial *I*=0 (7 ^{o} N; 45 ^{o} E) regions, using neutral wind velocity HWM14 data.

Fig. 3a and 3b show that the vertical drift velocity of ions w_{iv}, caused by the zonal wind determined by HWM14 data, and its divergence $div\mathbf{w}_{iv}$ in certain regions of the lower thermosphere at 90-160 km height fulfill the condition of vertical convergence of ions $(div\mathbf{w}_{iv})\min < 0$, equation (2). The presence of this condition is noticeable for at least $t - t_o \le 3h$, and accordingly the vertical convergence of ions develops and high-density Es layers are formed both at the top of the initial layer peak $h_{om} = 120\,km$ (panel c) and at the bottom $h_{om} = 105\,km$ location (panel d). In these cases, the Es layers are localized in the ion drift velocity nodes $w_{iv} = 0$ (for example, at *h*=140-150km altitudes), as well as towards the bottom of the lower thermosphere, where $w_{iv} \to 0$ (panels c and d). We estimate in ions qontituity equation the vertical ion drift velocity w_{iv} and its divergence $div\mathbf{w}_{iv}$ for nighttime ($t-t_o \le 12\,h$) height profiles in the lower thermosphere at equatorial *I*=0 (7 ^{o} N; 45 ^{o} E) regions, using neutral wind velocity HWM14 data.

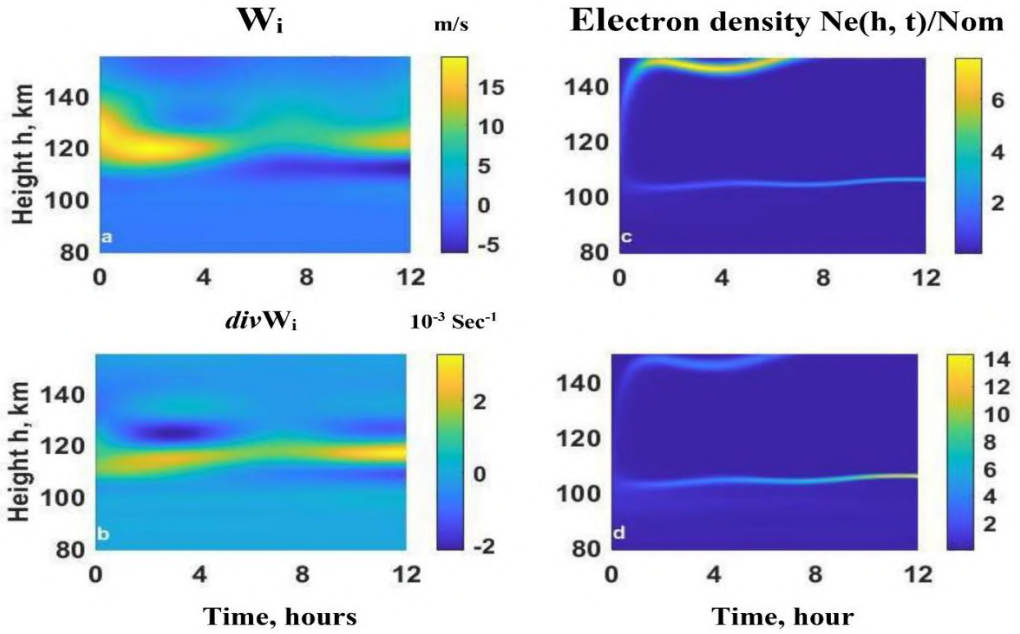

Fig. 3. The behavior of the ion/electron vertical drift velocity Wiv determined by the HWM14 data (day 102) of zonal wind velocity (panel a) and its divergence div Wiv (panel b) and correspondingly numerically estimated ion/electron density $N_e(z,t)/N_{om}$ at the equatorial region with *I*=0 (7 ^{o} N; 45 ^{o} E) for the initial peak height $h_{om} = 120\,km$ (panel c) and $h_{om} = 105\,km$ (panel d).

Fig. 3a and 3b show that the vertical drift velocity of ions w_{iv}, caused by the zonal wind determined by HWM14 data, and its divergence $div\mathbf{w}_{iv}$ in certain regions of the lower thermosphere at 90-160 km height fulfill the condition of vertical convergence of ions $(div\mathbf{w}_{iv})\min < 0$, equation (2). The presence of this condition is noticeable for at least $t - t_o \le 3h$, and accordingly the vertical convergence of ions develops and high-density Es layers are formed both at the top of the initial layer peak $h_{om} = 120\,km$ (panel c) and at the bottom $h_{om} = 105\,km$ location (panel d). In these cases, the Es layers are localized in the ion drift velocity nodes $w_{iv} = 0$ (for example, at *h*=140-150km altitudes), as well as towards the bottom of the lower thermosphere, where $w_{iv} \to 0$ (panels c and d).

The formation of the lower Es layer takes place continuously from the convergence region (about 100-105 km) against the background of the drift of ions below (Fig. 3a) and for these times they are localizing in the vicinity of *h*=100 km (Fig. 3c and 3d). It is important to note that for the ion/electron initial layer peak height ($h_{om}=105\,km$) is located below divergence height region (about 115 km) and close to the lower convergence region (around 110-100km), the upper layer is no longer formed and charge particles mainly accumulating in the lower Es layer ($N_{em}/N_{om}\geq 12$), where $w_{iv}\to 0$

Thus, with the presented theoretical model by use the HWM14 data, it is possible to form Es layers at the equatorial regions. In these cases (Fig. 3c and 3d), despite the different behavior of the formed Es layers than it was under the influence of the electric field (Fig. 2), the development of the vertical convergence of ions and the formation and localization of the Es layer can be determined by the profiles of the vertical drift of ions and its divergence, equations (2), (4) and (9).

We further show the significant influence of the electric field and the neutral wind combined effect on the ions drift velocity and their vertical convergence, by consideration the Es layers formation and behavior for the wind and field parameters discussed above (Fig. 2).

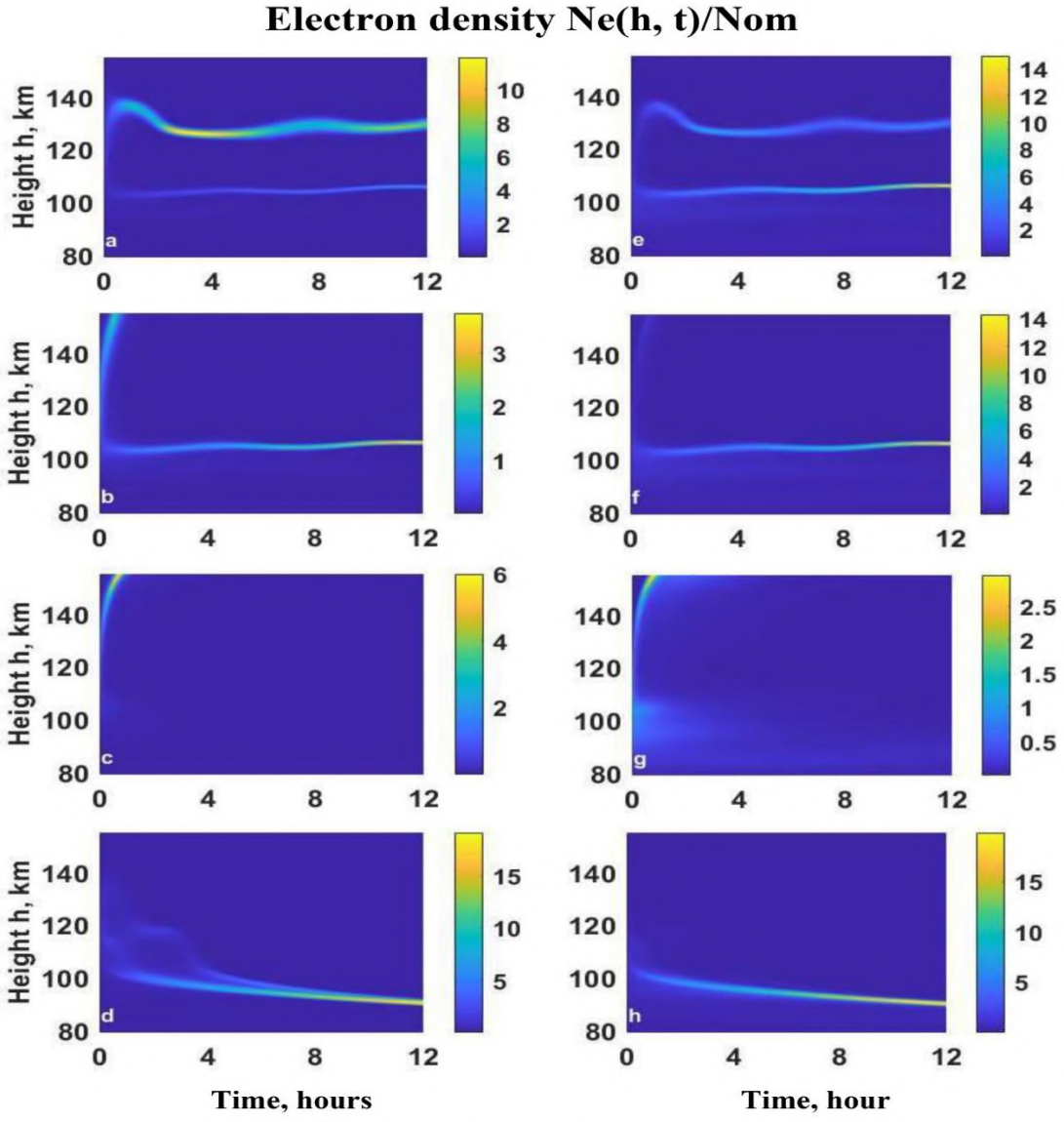

Fig. 4. That of the given in Fig. 2 in case of presence horizontal wind with velocity (V_{yn}) determined by the HWM14 used in Fig. 3.

Fig. 4 shows that sporadic E formation is possible due to the combined action of the electric field and neutral wind on the behavior of the ions, and it is possible both for the upper ($h_{om} = 120\,km$) (panels a-d) and lower ($h_{om} = 105\,km$) locations (panels e-h) of their initial layer peak. Here, sporadic E can be formed by two sub-Es layers, (e.g., see panels a, b, e and f), which were not formed only in zonal electric field (see Fig. 2a, 2b, 2e and 2f) or only in neutral wind (see Fig. 5a and 5b). Here, the behavior of the lower Es layer formed at about *h*=104 km corresponds to the behavior of the wind-induced Es layer (Figures 3c and 3d), while the upper one formed at about 130-140 km is determined by the combined action of both the westward electric field and the westward/eastward wind.

Fig. 4c, 4d, 4g and 4h also show that for the considered vertical electric field (2 mV/m) the neutral wind has little influence on the localization region of the upper (140-150 km altitude) and lower (about 90 km) Es layers formed during 1-3 hours (see Fig. 2, 4a and 4b). Here, the neutral wind somewhat changes the concentration of the formed Es layers.

Fig. 4 c and g also show that in the considered case, the Es layer (see Fig. 4c and 4d) formed by the zonal wind at about 104 km is destroyed when the ions drift upwards caused by the vertically directed electric field.

Thus, in the equatorial region, both the zonal and vertical components of the electric field together with the zonal component of the neutral wind have an impact on the vertical convergence of ions, equations (4) and (9), and therefore on the formation and behavior of Es layers. We consider the same in the simultaneous presence of the zonal and vertical components of the electric field and the neutral zonal wind in this region. In this case, the vertical drift of ions caused by the electric field (**E**) and the wind, equation (4), and therefore the convergence/divergence rate, equation (9), are determined by the total effect of these parameters and the development of the cases discussed above.

Thus, with the presented theoretical model, we have shown that under the influence of the horizontal neutral wind, homogeneous electric field, and also their combined action on the behavior of ions/electrons, it is possible to form sporadic E(Es) in the lower thermosphere of equatorial regions (see Figures 2-4). The obtained sporadic E multilayer structure, the influence of the electric field on it, the lowering and localization of Es layers towards the lower height *h*<110km regions, as well as the relatively low density of these layers towards the upper *h*>120-130km regions are observed phenomena [27-29].

4. Conclusions

The formation of sporadic E (Es) in the equatorial region by the electric field, zonal wind, as well as their joint action on the ions vertical convergence, was studied theoretically and by appropriate numerical methods.

1. It was shown that the formation and localization of sporadic E (Es) at the equatorial region, in analogy to the mid-latitudes [13], can be determined by the height profiles of the ion vertical drift velocity $\mathbf{w}_{i\mathrm{v}}$ and its divergence $div\mathbf{w}_{i\mathrm{v}} = \frac{\partial \mathrm{w}_{i\mathrm{v}}}{\partial z}$. In this case, the presence of a minimal negative value of $(div\mathbf{w}_{i\mathrm{v}})\min < 0$ (maximal convergence rate $(-div\mathbf{w}_{i\mathrm{v}})\max > 0$) in the divergence profile, during which the ions converge vertically into the Es layer, equations (1) and (2), is significantly determined by the zonal velocity of neutral wind V_{yn}, as well as by the zonal Ey and vertical Ez components of the electric field, equation (4).

The theoretically predicted formation and localization of Es layer in the regions with $\mathrm{w}_{i\mathrm{v}} = 0$ or $\mathrm{w}_{i\mathrm{v}} \to 0$, equation (1), as well as ion/electron depletion, when the condition $(div\mathbf{w}_{i\mathrm{v}})\max > 0$ occurs, are demonstrated by numerical methods (see Fig. 2 and 3).

2. It is shown that when neutral wind is absent, then in the equatorial region the westward electric field Ey>0, as well as the upward $\mathrm{E}_z > 0$ and downward Ez<0 fields can form an Es type layer

(see Fig. 2 and 3), even when the field is homogeneous. For the westward $E_y = const\tan t > 0$ ($E_z = 0$) field, the region of convergence development with $(-div\mathbf{w}_{ivo})\max \propto (C'_{vo})\max > 0$, equation (2), corresponds to the height (about *h*=121km), where $\nu_{in} = \Omega_i$ (Fig. 1b). For the upward $E_z = const\tan t > 0$ ($E_y = 0$) and downward electric field the region of development of ions vertical convergence with $(-div\mathbf{w}_{iv I})\max \propto (-C'_{ho})\max > 0$ is usually above or below by about 0.9H from the region where $\nu_{in} = \Omega_i$

In the same cases, an upward $E_z > 0$ or downward $E_z < 0$ Ez<0 electric fields can cause destruction/depletion of the layer at the heights which are 0.9H below (about *h*=115km) and above (about *h*=129 km), respectively, from the region with condition $\nu_{in} = \Omega_i$.

3. For the eastward $E_y = const\tan t > 0$ ($E_z - 0$, $V_{yn} = 0$) electric field in the height region where $\nu_{in} = \Omega_i$ (*h*=121km, Fig. 1) the condition $(div\mathbf{w}_{ivo})\max > 0$ occurs, the divergence process develops and the initial layer is depleted (disrupted). A similar ion divergence condition occurs for downward electric field $E_z < 0$ in the area of about 129 km height, while for $E_z > 0$ the process of ion depletion develops at about 115 km height and the initial layer is disrupted.

4.In the equatorial region (e.g., *I*=0; 7° N, 45° E) only the zonal wind can form the Es layers. Accordingly, the regions of their formation development ($(div\mathbf{w}_{ivo})\min < 0$, $(div\mathbf{w}_{iv I})\min < 0$) and localization ($w_{ivo} = 0$ or $w_{iv0} \to 0$; $w_{iv I} = 0$ or $w_{iv I} \to 0$) (Fig. 4), are defined by the magnitude, direction and vertical shear of wind velocity, equations (8). This is demonstrated for the HWM14 typical data (Figure 4).

5. In the presence of an electric field (with E_y or/and E_z components) and zonal wind in the equatorial region (e.g., I=0, 7 ° N, 45 ° E), the ions drift velocity ($\mathbf{w}_{ivo}$) and their vertical convergence/divergence condition ($(div\mathbf{w}_{ivo})\min < 0 / (div\mathbf{w}_{ivo})\max > 0$) include both the field and the neutrals factors. Their total effect is manifested in convergence, as well as during the development of divergent processes. The expression of their joint action is the appearance of an additional Es layer, the changes in their localization regions ($w_{ivo} = 0$ or $w_{iv0} \to 0$) and densities, as well as their destruction (depletion) (see Fig. 2), unlike the case with only neutral wind (see Fig. 4).

Acknowledgements: This study is supported by the Shota Rustaveli National Science Foundation of Georgia, Grant no. FR-21-22825.

References

[1] Whitehead J. D. J. Atmos. Terr. Phys., v.51, 1989, pp. 401-424.
[2] Mathews J.D. J. Atmos. Sol.-Terr. Phys., v.60, 1998, pp. 413-435.
[3] Abdu M. A., MacDougall J. W., Batista et al. J. Geophys. Res., v. 108(A6), 2003, p.1254.
[4] Moro J., Resende L. C. A., Denardini C. M. et al., J. Geophys. Res.: Space Phys., v. 122, 2017, pp.12,517–12,533. https://doi. org/10.1002/2017JA024734.
[5] Resende L. C. A., Shi J. K., Denardini C. M. et al., J. Geophys. Res.: Space Phys., v.125, 2020, pp. e2019JA027519. https://doi.org/ 10.1029/2019JA027519
[6] Haldoupis C., Pancheva D. J. Geophys. Res., v.107, 2002, doi:10.1029/2001JA000212.
[7] Haldoupis C. Space Sci. Rev., v.168, 2012, pp. 441–461, DOI 10.1007/s11214-011-9786-8.
[8] Jacobi Ch., Kandieva K., Arras Ch. Adv. Radio Sci., v. 20, 2023, pp. 85–92, https://doi.org/10.5194/ars-20-85-2023.
[9] Oikonomou C., Haralambous H., Leontiou T. et al. Adv. Space Res. v.69, 2022, pp. 96–110.
[10] Nygrén T., Jalonen L., Oksman J., Turunen T. J. Atmos. Terr. Phys. v.46(4), 1984, pp. 373-381.
[11] Haerendel G., Eccles J.V., Cakir S.C. J. Geophys. Res. v. 97, 1994, pp. 1209–1223.
[12] Alken P., Maus S. J. Atmos.Sol.-Terr. Phys., v. 72, 2010, pp. 319-326.

[13] Dalakishvili G., Didebulidze G., Todua M. J. Atmos. Sol.-Terr. Phys., v. 209, 2020, pp. 105403.
[14] Qiu L., Yamazaki Y., Yu T., Miyoshi Y., ZuoX. J. Geophy. Res.: Space Phys., v. 128, 2023, pp. e2023JA031508. https://doi. org/10.1029/2023JA031508
[15] Didebulidze G., Dalakishvili G., Todua M., Atmosphere, v. 11, 2020, pp. 653. doi:10.3390/atmos11060653.
[16] Didebulidze G., Dalakishvili G., Todua M., Toriashvili L. Atmosphere, v. 14, 2023, Issue 6, 1008. https://doi.org/10.3390/atmos14061008.
[17] Drob D. P., Emmert J.T., Meriwether J.W. et al. J. Geophys. Res., v.113, 2008, A12304, doi:10.1029/2008JA013668.
[18] Drob D. P., Emmert J.T., Meriwether J.W. et al. Earth Space Sci., v.2, 2015, pp. 301–319.
[19] Abdu M.A., de Souza J.R., Batista I.S. et al. J. Atmos. Sol.-Terr. Phys., v.115-116, 2014, pp. 95–105.
[20] Du Fort E. C., Frankel S.P. MTAC, v.7, 1953, pp. 135-152.
[21] Lanser D., Verwer G. J. J. Com.Appl. Math., v.111, 1999, pp. 201-216.
[22] Hundsdorfer W., Verwer G.J. Springer-Verlag Berlin Heidelberg, pp. 325-417.
[23] Picone J. M., Hedin A.E., Drob D.P., Aikin A.C. J. Geophys. Res., v. 107(A12), 2002, pp.1468. doi.org/10.1029/2002JA009,430.
[24] Garcia-Fernandez M., Tsuda T. Earth Planets Space, v. 58, 2006, pp. 33–36.
[25] Qiu L., Yu T., Yan X. et al. J. Geophys. Res. Space Phys., v.126, 2021, pp. e2021JA029454.
[26] Arras et al. Earth, Plan. Space, 74:163, 2022. https://doi.org/10.1186/s40623-022-01718-y.
[27] Wakabayashi M., Ono T. Ann. Geophys., v, 23, 2005, pp. 2347–2355.
[28] Bishop R. L. et al. J. Geophys. Res., v.110, 2005, (A04309), doi:10.1029/2004JA010686.
[29] Yuan T., Wang J., Cai X. et al. J. Geophys. Res. Space Phys., v. 119, 2014, pp. 5985–5999.

ელექტრული ველის მნიშვნელობა ეკვატორულ არეში სპორადული E (Es) ფენის ფორმირებაში

გ. დალაქიშვილი, გ. დიდებულიძე, მ. თოდუა, ლ, ტორიაშვილი

რეზიუმე

ანალიზურად და შესაბამისი რიცხვითი მეთოდებით ნაჩვენებია, რომ ეკვატორულ არეში სპორადული E (Es) ფორმირება და ლოკალიზაცია შესაძლებელია განისაზღვროს იონების ვერტიკალური დრეიფის სიჩქარის და მისი დივერგენციის სიმაღლის პროფილებით. ამ შემთხვევაში, დივერგენციის პროფილში მინიმალური უარყოფითი მნიშვნელობის (მაქსიმალური კონვერგენციის სისწრაფის) არსებობა, რომლის დროსაც იონები ვერტიკალურად კონვერგირდებიან Es ფენად, მნიშვნელოვნადაა განსაზღვრული, როგორც ნეიტრალური ქარით, ასევე ელექტრული ველის ზონალური და ვერტიკალური კომპონენტებით. ეკვატორულ არეში მუდმივი დასავლეთის ელექტრული ველისას იონების მაქსიმალური ვერტიკალური კონვერგენციის სისწრაფე იონ-ნეიტრალების დაჯახების (ν_{in}) და იონების ციკლოტრონული სიხშირის (Ω_i) ტოლობის სიმაღლის რეგიონშია. მხოლოდ ზემოთ ან ქვემოთ მიმართული მუდმივი ელექტრული ველის შემთხვევაში კი ის მდებარეობს $\nu_{in} = \Omega_i$ რეგიონიდან შესაბამისად დაახლოებით 0.9H ნეიტრალების შკალით ზემოთ ან ქვემოთ, შესაბამისად.ამ რეგიონებში განვითარებული იონების ვერტიკალური კონვერგენცია და Es-ტიპის ფენის ფორმირება შესაძლებელია მიმდინარეობდეს მათი ზემოთ ან ქვემოთ დრეიფის ფონზე. ის ლოკალიზდება ამ დრეიფის სიჩქარის ნოდაში, ან რეგიონებში სადაც ეს სიჩქარე ქრება. Es-ტიპის ფენების ამგვარი ნაწინასწარმეტყველევი ფორმირება და დინამიკა დემონსტრირებულია რიცხვითი მეთოდებით.

ნაჩვენებია, როგორც ელექტრული ველის ზონალური და ვერტიკალური კომპონენტების, ასევე HWM14 მონაცემებით განსაზღვრული ქარის სიჩქარის ეფექტი იონების კონვერგენცია/დივერგენციის განვითარების პროცესებზე. ამ შემთხვევებში ელექტრული ველით გამოწვეულ იონების კონვერგენცია/დივერგენციის პროცესს შეუძლია გავლენა იქონიოს ქარით Es-ტიპის ფენის როგორც ფორმირებასა და დაშლაზე (გამოფიტვაზე), ასევე შეუძლია წარმოქმნას დამატებითი ფენა.

საკვანძო სიტყვები: ქვედა თერმოსფერო, ელექტრული ველი, სპორადული E (Es), იონის ვერტიკალური დრიფტის სიჩქარე, რიცხვითი მეთოდები.

Значение электрического поля в формировании спорадических E (Es) в экваториальной области

Г. Далакишвили, Г. Дидебулидзе, М. Тодуа, Л. Ториашвили

Резюме

Аналитически и соответствующими численными методами показано, что образование и локализация спорадических E (Es) в экваториальной области может определяться высотными профилями скорости вертикального дрейфа ионов и ее дивергенцией. При этом существование минимального отрицательного значения (максимальной скорости сходимости) в профиле расходимости, когда ионы сходятся вертикально в слой Es, существенно определяется как скоростью нейтрального ветра, так и зональной и вертикальной составляющими электрического поля.

В экваториальной области при постоянном западном электрическом поле максимальная скорость вертикальной конвергенции ионов приходится на область высот, где ионно-нейтральная столкновительная (ν_{in}) и ионно-циклотронная (Ω_i) частоты равны. В случае постоянного восходящего или нисходящего электрического поля эта скорость находится примерно на 0.9H (где H – нейтральная шкала) выше или ниже области где $\nu_{in} = \Omega_i$, соответственно. Вертикальная конвергенция ионов, развивающихся в этих областях, и образование слоя Es могут происходить на фоне их дрейфа вверх или вниз. Она локализуется в узле этой скорости дрейфа или в областях исчезновения этой скорости. Такое предсказанное формирование и поведение слоев Es демонстрируется численными методами.

Показано влияние зональной и вертикальной составляющих электрического поля, а также скорости ветра, определенной по данным HWM14, на процессы развития конвергенции/расхождения ионов. В этих случаях процесс сближения/расхождения ионов, индуцированный электрическим полем, может влиять как на образование, так и на разрушение (истощение) слоя Es, образованного нейтральным ветром, а также может образовывать дополнительный слой.

Ключевые слова: нижняя термосфера, электрическое поле, спорадическое E (Es), скорость вертикального дрейфа ионов, численные методы.

Journal of the Georgian Geophysical Society, e-ISSN: 2667-9973, p-ISSN: 1512-1127
Physics of Solid Earth, Atmosphere, Ocean and Space Plasma, v.27(1), 2024, pp. 104 - 104

TENGIZ TSINTSADZE
Obituary

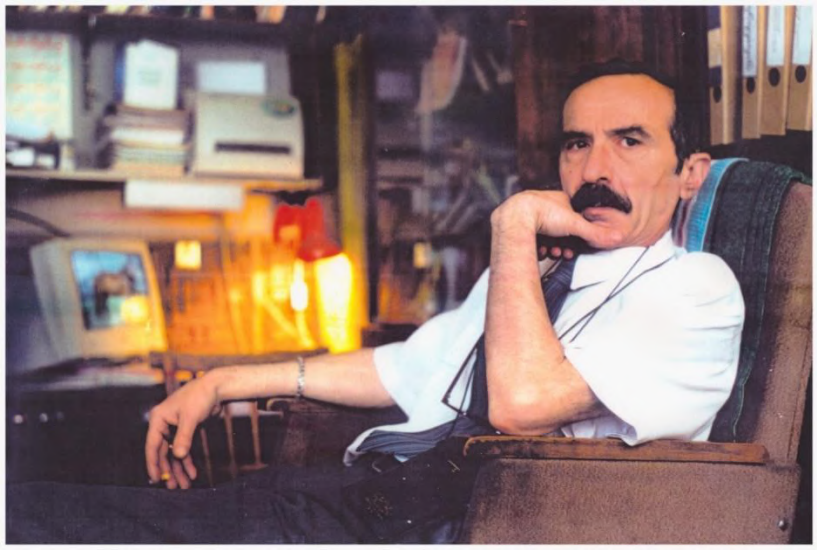

Hydrometeorological science suffered a great loss. The famous Georgian hydrologist, academician of the Academy of Engineering Sciences of Georgia, Knight of the Order of Honor, Doctor of Technical Sciences, Director of the Institute of Hydrometeorology of the GeorgianTechnical University

Tengiz Tsintsadze died.

Tengiz Tsintsadze was born on January 21, 1949 in the city of Ozurgeti. In 1978, he graduated from the Faculty of Geography-Geology of Tbilisi State University, majoring in terrestrial hydrology. After successfully graduating from the University, Mr. Tengiz started working as an engineer-hydrologist at the Institute of Hydrometeorology of the Georgian Academy of Sciences. During 1982-1987 He was the head of the field experimental base, since 1987 - the Deputy Director of the Institute in the scientific and industrial field, and since 2008 he has been the Director of the Institute.

During his work at the field experimental base, he collected very interesting experimental material that was the basis for his Candidate's Thesis, which he successfully defended in 1985 on the topic - "Hydrological method for determining the effectiveness of artificially increasing river runoff by actively influencing hydrometeorological processes". It was a new word in the field of precipitation artificial regulation.

Mr. Tengiz Tsintsadze has published about 100 scientific works, including monographs. He contributed greatly to the editing, publication and promotion of the Institute's works and proceedings. Among them are such fundamental publications as "Climatic and Agroclimatic Atlas of Georgia", "Cadastre of Snow Avalanches", "Ecological Monitoring", "Climate of Georgia", "Agrometeorology" and others. He devoted a lot of time to the personnel policy of the Institute. He promoted the qualification and promotion of young scientists.

Tengiz Tsintsadze was awarded the Order of Merit, the Gold Medal of the Georgian Technical University and other awards for his fruitful scientific and research activities.

The famous scientist, an exemplary citizen, an honest, noble, decent person distinguished by human qualities has left us. How strange life is...from now on we have to refer to it as an exile and say goodbye to it. May the native land resting on the heart of Mr. Tengiz be light.

Institute of Hydrometeorology
GeorgianTechnical University

Information for contributors

Papers intended for the Journal should be submitted in two copies to the Editor-in-Chief. Papers from countries that have a member on the Editorial Board should normally be submitted through that member. The address will be found on the inside front cover.

1. Papers should be written in the concise form. Occasionally long papers, particularly those of a review nature (not exceeding 16 printed pages), will be accepted. Short reports should be written in the most concise form not exceeding 6 printed pages. It is desirable to submit a copy of paper on a diskette.
2. A brief, concise abstract in English is required at the beginning of all papers in Russian and in Georgian at the end of them.
3. Line drawings should include all relevant details. All lettering, graph lines and points on graphs should be sufficiently large and bold to permit reproduction when the diagram has been reduced to a size suitable for inclusion in the Journal.
4. Each figure must be provided with an adequate caption.
5. Figure Captions and table headings should be provided on a separate sheet.
6. Page should be 20 x 28 cm. Large or long tables should be typed on continuing sheets.
7. References should be given in the standard form to be found in this Journal.
8. All copy (including tables, references and figure captions) must be double spaced with wide margins, and all pages must be numbered consecutively.
9. Both System of units in GGS and SI are permitted in manuscript
10. Each manuscript should include the components, which should be presented in the order following as follows:
    Title, name, affiliation and complete postal address of each author and dateline.
    The text should be divided into sections, each with a separate heading or numbered consecutively.
    Acknowledgements. Appendix. Reference.
11. The editors will supply the date of receipt of the manuscript.

CONTENTS - სარჩევი

საქართველოს გეოფიზიკური საზოგადოების ჟურნალი

მყარი დედამიწის, ატმოსფეროს, ოკეანისა და კოსმოსური პლაზმის ფიზიკა

ტომი 27, № 1

ჟურნალი იბეჭდება საქართველოს გეოფიზიკური საზოგადოების პრეზიდიუმის დადგენილების საფუძველზე

ტირაჟი 20 ცალი

JOURNAL OF THE GEORGIAN GEOPHYSICAL SOCIETY

Physics of Solid Earth, Atmosphere, Ocean and Space Plasma

Vol. 27, № 1

Printed by the decision of the Georgian Geophysical Society Board

Circulation 20 copies

ЖУРНАЛ ГРУЗИНСКОГО ГЕОФИЗИЧЕСКОГО ОБЩЕСТВА

Физика Твердой Земли, Атмосферы, Океана и Космической Плазмы

Том 27, № 1

Журнал печатается по постановлению президиума Грузинского геофизического общества

Тираж 20 экз

Tbilisi-თბილისი-Тбилиси
2024